# Seasonal variations in triple oxygen isotope ratios of precipitation in the western and central United States

**P. G. Aron[1], S. Li[2], J. R. Brooks[3], J. M. Welker[4, 5, 6], and N. E. Levin[1]**

[1] Department of Earth and Environmental Sciences, University of Michigan, Ann Arbor, MI, USA. [2] Institute of Geochemistry, School of Earth and Space Sciences, Peking University, CN. [3] Pacific Ecological Systems Division, Center for Public Health and Environmental Assessment, Office of Research and Development, U.S. Environmental Protection Agency, Corvallis, OR, USA. [4] Department of Biological Sciences, University of Alaska, Anchorage, AK, USA. [5] Ecology and Genetics Research Unit, University of Oulu, Finland. [6] University of the Arctic (UArctic), Rovaniemi, Finland

Corresponding author: Phoebe Aron (paron@umich.edu)

**Key Points:**

- Precipitation $\delta'^{18}O$-$\delta'^{17}O$ slopes often differ from the 0.528 reference value
- Precipitation $\Delta'^{17}O$ values are typically higher in the winter and lower in the summer
- Different controls on $\Delta'^{17}O$ and $\delta^{18}O$ mean that $\Delta'^{17}O$ provides new information for paleoclimate reconstructions

This is the author manuscript accepted for publication and has undergone full peer review but has not been through the copyediting, typesetting, pagination and proofreading process, which may lead to differences between this version and the Version of Record. Please cite this article as doi: 10.1029/2022PA004458.

**Abstract**

Triple oxygen isotope ratios ($\Delta'^{17}O$) offer new opportunities to improve reconstructions of past climate by quantifying evaporation, relative humidity, and diagenesis in geologic archives. However, the utility of $\Delta'^{17}O$ in paleoclimate applications is hampered by a limited understanding of how precipitation $\Delta'^{17}O$ values vary across time and space. To improve applications of $\Delta'^{17}O$, we present $\delta^{18}O$, d-excess, and $\Delta'^{17}O$ data from 26 precipitation sites in the western and central United States and three streams from the Willamette River Basin in western Oregon. In this dataset, we find that precipitation $\Delta'^{17}O$ tracks evaporation but appears insensitive to many controls that govern variation in $\delta^{18}O$, including Rayleigh distillation, elevation, latitude, longitude, and local precipitation amount. Seasonality has a large effect on $\Delta'^{17}O$ variation in the dataset and we observe higher seasonally amount-weighted average precipitation $\Delta'^{17}O$ values in the winter (40 ± 15 per meg (± standard deviation)) than in the summer (18 ± 18 per meg). This seasonal precipitation $\Delta'^{17}O$ variability likely arises from a combination of sub-cloud evaporation, atmospheric mixing, moisture recycling, sublimation, and/or relative humidity, but the dataset is not well suited to quantitatively assess isotopic variability associated with each of these processes. The seasonal $\Delta'^{17}O$ pattern, which is absent in d-excess and opposite in sign from $\delta^{18}O$, appears in other datasets globally; it showcases the influence of seasonality on $\Delta'^{17}O$ values of precipitation and highlights the need for further systematic studies to understand variation in $\Delta'^{17}O$ values of precipitation.

## 1. Introduction

Ratios of oxygen isotopes ($^{18}O/^{16}O$, or $\delta^{18}O$) are often used to reconstruct past environmental and climatic conditions (e.g., Koch, 1998; Liu et al., 2017; Rowley, 2007; Zachos, 2001). However, interpreting $\delta^{18}O$ data from geologic archives can be challenging as it is often difficult to attribute $\delta^{18}O$ variation to specific fractionating processes (e.g., Rech et al., 2019; Thompson et al., 2000; Wostbrock and Sharp, 2021). This challenge can be particularly problematic in terrestrial paleoclimate archives that often integrate information about temperature, seasonality, vegetation cover, evaporation, the amount and isotopic composition of local precipitation, atmospheric and oceanic conditions, and biological physiology (e.g., Breecker et al., 2009; Bryant and Froelich, 1995; Kelson et al., 2020; Kohn, 1996; Quade et al., 2007).

Differentiating among these $\delta^{18}O$ controls is a critical component to improving reconstructions of past climate.

Recent advances in characterizing distributions of $^{17}O$, the third and least abundant stable isotope of oxygen, demonstrate potential for using $^{17}O/^{16}O$ ratios ($\delta^{17}O$) to help constrain interpretations of $\delta^{18}O$ records (see recent reviews by Galewsky et al. 2016; Aron et al. 2021a; Surma et al. 2021; Passey and Levin, 2021). The power of $\delta^{17}O$ measurements comes from assessing how their distributions vary from expected relationships with $\delta^{18}O$ values. When used in studies of the hydrosphere (past and present), the $\Delta'^{17}O$ parameter is defined as the deviation from a reference relationship between $\delta'^{18}O$ and $\delta'^{17}O$ (Barkan and Luz, 2007):

$$\Delta'^{17}O = \delta'^{17}O - 0.528*\delta'^{18}O \qquad (1)$$

where $\delta = (R_{sample}/R_{standard} - 1)$, R is the ratio of heavy-to-light isotopes, and $\delta'$ is the logarithmic version of $\delta$ ($\delta' = \ln(\delta + 1)$; Miller, 2002). The slope of the $\delta'^{18}O$–$\delta'^{17}O$ reference relationship ($\lambda_{ref}$), 0.528, was initially thought to approximate the global relationship through meteoric water $\delta'^{18}O$ and $\delta'^{17}O$ (Luz and Barkan, 2010; Meijer and Li, 1998), but recent studies indicate this value is biased high by polar waters (Aron et al., 2021a; Miller, 2018; Sharp et al., 2018). Still, we continue to use 0.528 in the definition of $\Delta'^{17}O$ to maintain consistency with previous work; this value also has a mechanistic significance as it is nearly identical to the $\delta'^{18}O$–$\delta'^{17}O$ slope during Rayleigh distillation (Luz and Barkan, 2010).

The last several years have produced a spate of studies that showcase the utility of high-precision $\Delta'^{17}O$ analysis for reconstructing past environments. This work has shown how $\Delta'^{17}O$ data from sediments and fossils can be used to account for the effects of evaporation to reconstruct the $\delta^{18}O$ values of meteoric waters (e.g., Passey and Ji, 2019), identify shifts in paleohydrology (e.g., Evans et al., 2018; Gázquez et al., 2020), serve as a proxy for paleo-humidity (Alexandre et al., 2018; Gázquez et al., 2018; Sha et al., 2020; Lehmann et al. 2022), refine paleoaltimetry estimates (Chamberlain et al., 2021; Ibarra et al., 2021, Kelson et al., 2022), and detect diagenesis (Gehler et al., 2011; Levin et al., 2014; Sengupta and Pack, 2018; Wostbrock et al., 2020). In each of these examples, $\Delta'^{17}O$ brings information beyond what can be determined with the analysis of

$\delta^{18}O$ alone and helps expand the utility of oxygen isotopes for reconstructing climate, hydrology, and elevation in ancient systems.

The $\Delta'^{17}O$ sensitivity to evaporation is well documented in geologic materials and waters (Aron et al., 2021a; Beverly et al., 2021; Evans et al., 2018; Gázquez et al., 2018, 2020; Herwartz et al., 2017; Ibarra et al., 2021; Li et al., 2017; Passey et al., 2014; Passey and Ji, 2019; Surma et al., 2015, 2018; Voigt et al., 2021). Understanding the $\Delta'^{17}O$ variation in meteoric waters that are relatively unevaporated – these are the waters responsible for the majority of recharge to terrestrial water reservoirs (e.g. lakes, rivers, groundwater, soil water) and are assumed to reflect primarily equilibrium fractionation processes – is critical to these studies, but it is not well defined. Until recently, average meteoric water was thought to have a $\Delta'^{17}O$ value of ~ 33 per meg (Luz and Barkan, 2010) and this value was used as a benchmark in some paleoclimate applications (e.g., Passey and Ji, 2019; Ibarra et al. 2021). However, recent compilations of water $\delta^{18}O$ and $\delta^{17}O$ data show that $\Delta'^{17}O$ values of meteoric water are regionally variable and that many non-polar waters yield $\Delta'^{17}O$ values less than 33 per meg (Aron et al., 2021a; He et al., 2021; Miller, 2018; Sharp et al., 2018). Still, uncertainty around an average $\Delta'^{17}O$ value of meteoric water exists because so many surface water $\Delta'^{17}O$ datasets focus on waters that experienced extensive evaporation (e.g., Aron et al., 2021a; Bershaw et al., 2020) and all existing precipitation $\Delta'^{17}O$ datasets are from single sites (Affolter et al., 2015; Beverly et al., 2021; Gázquez et al., 2017; Gimenez et al., 2021; He et al., 2021; Landais et al., 2010; Surma et al., 2018; Tian et al., 2021; Tian and Wang, 2019; Uechi and Uemura, 2019).

Here we present precipitation $\delta^{18}O$, d-excess, and $\Delta'^{17}O$ data from 26 sites in the western and central United States and stream $\delta^{18}O$, d-excess, and $\Delta'^{17}O$ data from the Willamette River Basin in western Oregon. The distribution of sample sites and collection times make this dataset ill-suited for spatial or temporal analysis, but we use the dataset to evaluate variation in precipitation $\Delta'^{17}O$ values in the North America, compare stream and precipitation $\Delta'^{17}O$ values, and begin to determine the range of amount-weighted precipitation $\Delta'^{17}O$ values in North America.

## 2. Isotope systematics

The utility of triple oxygen isotope ratios in paleoclimate and hydrologic applications relies on characterizing differences in the linear relationships between $\delta'^{18}O$ and $\delta'^{17}O$ during equilibrium and kinetic fractionation. This approach is similar to the framework used to infer climatic and hydrologic information from $\delta^{18}O$ and $\delta^{2}H$ values in which most meteoric waters plot on a line with a slope of 8, reflecting equilibrium fractionation (Craig, 1961; Dansgaard 1964; Horita and Wesolowski, 1994; Majoube, 1971), and processes involving kinetic fractionation with a lower slope (~ 2.5 to 8; Gonfiantini et al., 2018; Brady and Hodell, 2021). Analogous to $\Delta'^{17}O$, d-excess quantifies the deviation from a reference relationship (Dansgaard, 1964), where

$$\text{d-excess} = \delta^{2}H - 8*\delta^{18}O. \quad (2)$$

The d-excess parameter provides information on non-equilibrium processes and has been used extensively to characterize evaporation during evapotranspiration, moisture transport and precipitation (see Gat 1996; Galewsky et al. 2016; Bowen et al 2019). The magnitude of d-excess is controlled mainly by relative humidity during kinetic fractionation (Craig and Gordon, 1965) and by temperature during equilibrium fractionation (Majoube, 1971).

Following similar principles as d-excess, $\Delta'^{17}O$ values of water track hydrological processes because there are distinct $\delta'^{18}O$–$\delta'^{17}O$ relationships for equilibrium and kinetic fractionation. The $\delta'^{18}O$–$\delta'^{17}O$ slope is higher (0.529) during equilibrium fractionation (Barkan and Luz, 2005; Young et al., 2002) and lower during kinetic fractionation (0.5185 to 0.5188) (Barkan and Luz, 2007; Hellmann and Harvey, 2020). Distinctions between the reference slope (0.528) and slopes associated with fractionation mean that $\Delta'^{17}O$ is more sensitive to processes involving kinetic fractionation (e.g., diffusive effects during evaporation) than equilibrium fractionation and most rainout processes because these fractionation slopes are very close to the reference slope. Given a minimal sensitivity of $\Delta'^{17}O$ to temperature, the combined use of $\Delta'^{17}O$ and d-excess holds promise for characterizing variations in moisture source relative humidity and temperature (e.g., Uechi and Uemera 2019) and for constraining rain re-evaporation (e.g., Landais et al. 2010). When evaporation drives isotopic fractionation, d-excess and $\Delta'^{17}O$ co-vary linearly (e.g., Landais et al. 2010; Li et al. 2017; Surma et al. 2018). In other circumstances, the lack of a relationship between d-excess and $\Delta'^{17}O$ has been used to identify processes such as mixing and recycling (e.g., Landais et al. 2010; Voigt et al. 2021). Studies of precipitation, vapor, and lakes show that the combination of d-excess and $\Delta'^{17}O$ make a powerful tool for understanding hydrological and meteorological processes (e.g., Landais et al. 2012b; Galewsky et al. 2016; Pierchala et al. 2022). It can be difficult to generate d-excess records in the geologic record, as

$\delta^{18}O$ and $\delta^{2}H$ are rarely preserved in the same material (e.g., Evans et al. 2018), but $\Delta'^{17}O$ records represent an opportunity to track evaporation in ancient waters (lakes, body waters, rivers, soils etc.). Constraints on the $\Delta'^{17}O$ values of the starting water that feeds these water bodies are critical for this approach.

## 3. Materials and Methods

### *3.1 Sample collection*

Precipitation and stream samples included in this study were selected for triple oxygen isotope analysis from two pre-existing sample sets. First, we selected 109 weekly precipitation samples from the USNIP dataset (Welker, 2012) collected in 1997 (n = 19) and 2006 (n = 90) from 22 sites mostly in the western and central United States (Figures 1 and 2, Table S1). Samples were selected to explore the impacts of geography and season on $\Delta'^{17}O$ variation in summer (June to August) and winter (December to February) months (Figure 2a). This dataset provides an initial view of $\Delta'^{17}O$ values of seasonal and annual amount-weighted precipitation in the western and central United States but is too spatially coarse to directly compare site-to-site or sample-to-sample data, characterize relationships between $\Delta'^{17}O$ values with local conditions, or evaluate local $\Delta'^{17}O$ variations during synoptic events.

Second, we analyzed $\delta^{18}O$ and $\delta^{17}O$ values of 24 weekly precipitation samples from Corvallis, Oregon and 18 stream samples from the surrounding Willamette River Basin (Table S1; Brooks et al., 2012) to explore seasonal $\Delta'^{17}O$ variability and compare $\Delta'^{17}O$ values between streams and precipitation. The precipitation samples from Corvallis include one sample per month from February 2009 to December 2010. Stream samples were collected three times per year in 2009 and 2010 to capture spring snowmelt, low summer flow, and winter storms. Stream samples were collected from three small streams in an east-west transect across the Willamette River Basin that vary in distance from the Pacific Ocean and thus vary in precipitation rainout effects. The western most stream was a small stream within the Luckiamute River watershed, an eastward-facing basin that drains the Coast Range (n = 6, 121 meters above sea level (masl)) and flows into the western side of the Willamette Valley. The other two small streams were located within North Santiam River watershed, a westward-facing basin that drains the Cascade Mountains (n = 12) and flows into the eastern side of the Willamette Valley. The two North Santiam stream sites varied in elevation (838 masl and 197 masl, n = 6 each).

*3.2 Isotopic analysis*

*3.2.1 $\delta^{18}O$ and $\delta^{17}O$ measurements*

Triple oxygen isotope ratios of waters were analyzed using the cobalt(III) fluoride method developed by Baker et al. (2002) and Barkan and Luz (2005). Measurements were made on a Thermo Scientific MAT 253 isotope ratio mass spectrometer (IRMS) at Johns Hopkins University in 2012–2014, using methods described in Passey et al. (2014) and Li et al. (2017, 2015). All $\delta^{18}$O and $\delta^{17}$O values were normalized to the VSMOW-SLAP scale using the approach described by Schoenemann et al. (2013), using measurements of VSMOW2 and SLAP2 analyzed concurrently with unknowns. As such, values of $\delta^{18}$O were defined as 0‰ for VSMOW2 and −55.5‰ for SLAP2, $\Delta'^{17}$O was assumed to be 0‰ for both VSMOW2 and SLAP2, $\lambda_{ref}$ was defined as 0.528, and $\delta^{17}$O was 0‰ for VSMOW2 and −29.6986‰ for SLAP2. We monitored analytical performance by regularly analyzing $\delta^{18}$O and $\delta^{17}$O values of USGS 45, 46, 47, and 48 reference waters and determined that analytical precision (root-mean-square-error) of USGS waters was better than 0.2‰ for $\delta^{17}$O, 0.3‰ for $\delta^{18}$O, and 7 per meg for $\Delta'^{17}$O. See Table S2 for reports of raw and normalized data for standards and unknowns.

*3.2.2 $\delta^{18}O$ and $\delta^{2}H$ data*

The $\delta^{18}$O and $\delta^{2}$H data reported in this study are considered part of the primary dataset, but were previously published in Brooks et al. (2012) and Welker . (2012). USNIP precipitation samples were analyzed at the University of Alaska Anchorage Stable Isotope Lab with a TCEA unit attached to a Thermo Finnigan IRMS (Welker, 2012). Analytical precision of the measurements at the University of Alaska Anchorage (UAA) are 0.2‰ for $\delta^{18}$O and 0.5‰ for $\delta^{2}$H. Stream samples from the Willamette River Basin and precipitation samples from Corvallis, OR were analyzed on a Laser Absorption Water-Vapor Isotope Spectrometer (Los Gatos Research (LGR) Model 908-0004) at the Integrated Stable Isotope Research Facility at the Western Ecology Division of the Environmental Protection Agency (EPA), Corvallis, OR (Brooks et al., 2012).

Analytical precision of $\delta^{18}O$ and $\delta^{2}H$ values from the EPA measurements are 0.2 and 0.5‰, respectively (Brooks et al., 2012). All $\delta^{18}O$ and $\delta^{2}H$ data from UAA and the EPA research facility are reported relative to VSMOW.

*3.2.3 Data quality checks and caveats*

Precipitation and stream samples were stored for up to 15 years before triple oxygen isotope analysis, so it is important to evaluate sample quality. At EPA, precipitation and stream samples were stored upside-down in 20 ml glass scintillation vials with polycone caps. USNIP samples were stored at UAA in 40 ml screw cap Nalgene bottles at 4 ˚C. These common storage techniques typically preserve the isotopic composition of water samples, but it is important to confirm that isotopic ratios did not drift during storage.

First, to confirm that isotopic ratios did not drift and to evaluate analytical accuracy, we compared the $\delta^{18}O$ values measured at Johns Hopkins University with those measured at the EPA research facility or UAA. More than 98% of the $\delta^{18}O$ values measured at Johns Hopkins University are identical (within $\delta^{18}O$ analytical precision) of those analyzed at EPA or UAA (Figure S1). Two precipitation samples have $\delta^{18}O$ values that differ by more than 4‰. We can find no clear analytical explanation for such different $\delta^{18}O$ values. Isotope data from these outliers are reported in Table S1 but are excluded from subsequent analysis.

Second, because the goal of this study is to explore the variability of $\Delta'^{17}O$ across the western and central United States, we ensured that our dataset is representative of isotopic compositions in this region. To confirm this, we compared the $\delta^{18}O$ and d-excess values from our dataset with previously published data from the western and central United States (Figure S2) accessed from the University of Utah water isotope database (waterisotopesdb.org; Putman and Bowen, 2019). Both the range and patterns of $\delta^{18}O$ and d-excess values from our dataset are statistically indistinguishable from previously published observations (Welch Two Sample t-test p values > 0.05), so we conclude that our dataset is representative of isotopic variability across the western and central United States.

Third, we confirmed the accuracy and precision of our $\Delta'^{17}O$ measurements by comparing $\Delta'^{17}O$ values of USGS reference waters measured at Johns Hopkins University with other reported values of the same waters (Table S3). Values of $\Delta'^{17}O$ of USGS reference waters reported in this study are statistically indistinguishable from those reported by Aron et al. (2021a) and Berman et al. (2013), so we are confident that the $\Delta'^{17}O$ data reported in this study are accurate and precise.

In total, we analyzed $\delta^{18}O$ and $\delta^{17}O$ from 151 water samples. Excluding the two precipitation samples with very different (more than 4‰) $\delta^{18}O$ values between Johns Hopkins University and EPA or UAA, the final dataset contains 149 samples (18 stream and 131 precipitation samples).

### *3.3 Meteorological data*

Weekly precipitation amount data were collected at each USNIP site as part of the North American Deposition Program (NADP; http://nadp.slh.wisc.edu/) and at the EPA Western Ecology Division climate station in Corvallis, OR (Brooks et al., 2012). The EPA climate station also recorded temperature and relative humidity. Temperature and relative humidity were not recorded as part of the NADP network, so these data were filled in from nearby National Weather Service meteorological stations from the MesoWest database (https://mesowest.utah.edu/).

### *3.4 Theoretical Modeling*

Simple Rayleigh distillation and evaporation modeling was conducted to compare theoretical $\Delta'^{17}O$, $\delta^{18}O$, and d-excess values during Rayleigh distillation and pan evaporation with observed precipitation $\Delta'^{17}O$, $\delta^{18}O$, and d-excess data. Theoretical values were calculated using supplementary script 4 from Aron et al. (2021a) and average meteorological conditions from coastal and near-coastal sites in this study (Olympic National Park, Alsea Guard Ranger Station, H.J. Andrews Experimental Forest, and Corvallis, OR) as the initial conditions for calculations.

## **4. Results**

### *4.1 General results*

Site information, meteorological data, and isotope data are reported in Table S1. Raw isotope data are reported in Table S2. Values of $\delta^{18}O$ ranged from −25.2 to 4.5‰, $\delta^{17}O$ ranged from −13.6 to 2.2‰, $\delta^{2}H$ ranged from −192.9 to 12.3‰, d-excess ranged from −59.1 to 17.8‰, and $\Delta'^{17}O$ ranged from −54 to 71 per meg. As expected, $\delta'^{17}O$ and $\delta'^{18}O$ were strongly correlated ($R^2 > 0.9999$), following a line with a slope 0.5255 ± 0.0002 and intercept −0.002 ± 0.002

(uncertainty on the reported slopes and intercepts is the standard error) that is slightly shallower than the triple oxygen isotope reference line ($\delta'^{17}O = 0.528*\delta'^{18}O$; Luz and Barkan, 2010) (Figure 3a). Values of $\delta^{18}O$ and $\delta^2H$ were also well correlated ($R^2 = 0.96$) with most points on or slightly below the $\delta^{18}O$–$\delta^2H$ Global Meteoric Water Line (Craig, 1961). The regression line through observed $\delta^{18}O$ and $\delta^2H$ values had a slope of 7.2 ± 0.1 and intercept of −1.0 ± 1.3 (Figure 3b).

*4.2 Precipitation*

Annual amount-weighted average precipitation $\Delta'^{17}O$ was 31 per meg. Among the precipitation samples, the best-fit linear regression lines were $\delta'^{17}O = 0.5255 \pm 0.0002 * \delta'^{18}O - 0.002 \pm 0.0002$ and $\delta^2H = 7.2 \pm 0.1 * \delta^{18}O - 1.4 \pm 1.4$. Precipitation $\Delta'^{17}O$ values were strongly negatively correlated with $\delta'^{18}O$ (Pearson's $r = -0.72$, $p < 0.05$, Figure 4a) and strongly positively correlated with d-excess ($r = 0.63$, $p < 0.05$, Figure 4c). The negative correlation between precipitation d-excess and $\delta^{18}O$ ($r = -0.48$, $p < 0.05$, Figure 4b) was weaker than that between $\Delta'^{17}O$ and $\delta^{18}O$; much of this negative correlation for d-excess and $\delta^{18}O$ was related to a handful of samples with low (< 0‰) d-excess values (Figure S3). Excluding low d-excess samples, precipitation d-excess and $\delta^{18}O$ were only weakly correlated ($r = -0.29$, $p < 0.05$, Figure 4e) while $\Delta'^{17}O$ and $\delta'^{18}O$ remained strongly negatively correlated ($r = -0.64$, $p < 0.05$, Figure 4d). Similarly, correlations between $\delta^{18}O$, $\Delta'^{17}O$, and d-excess and local meteorological conditions such as precipitation amount (r = −0.20, 0.34, and 0.28, respectively), temperature (r = 0.83, −0.69, −0.31, respectively), and relative humidity (r = −0.45, 0.49, 0.17, respectively) were generally stronger for $\delta^{18}O$ and $\Delta'^{17}O$ than for d-excess (Figure 5, Figure S4). We used meteorological quarters to consider seasonal patterns, where winter was defined as the months of December-January-February and summer is June-July-August (Table S1). Most precipitation samples in the dataset were collected during winter or summer so we focused our comparison on these seasons.

The most pronounced pattern among the precipitation data was seasonal $\delta^{18}O$ and $\Delta'^{17}O$ variability (Figures 4–6). Across all the years of sample collection and most sites, seasonal amount-weighted precipitation $\Delta'^{17}O$ averages were higher in the winter (40 ± 15 per meg), lower in the summer (18 ± 18 per meg), and statistically distinct ($p < 0.05$, Figure 4). The seasonal pattern of precipitation $\delta^{18}O$ was opposite, with lower amount-weighted $\delta^{18}O$ in the winter (−13.0 ± 5.9‰) than the summer (−7.0 ± 2.9‰). Average seasonal amount-weighted summer and winter d-excess values were nearly indistinguishable (7.0 ± 12.4‰ and 10.7 ± 4.6‰, respectively). These seasonal $\delta^{18}O$ and $\Delta'^{17}O$ patterns were consistent across almost every site but were slightly less pronounced along the Pacific coast and in the Willamette River Basin where the isotopic composition of rain was presumably more closely tied to oceanic moisture source conditions than sites located in the continental interior (Figure 6). Regression lines for $\delta'^{18}O$-$\delta'^{17}O$ and $\delta^{18}O$-$\delta^{2}H$ also varied seasonally, with steeper slopes and higher intercepts in the winter than in the summer (Figure S5). This dataset does not show clear spatial patterns in precipitation $\Delta'^{17}O$ values. Correlations were weak between precipitation $\delta^{18}O$, $\Delta'^{17}O$, and d-excess with elevation (r = −0.21, 0.02, 0.13, respectively), latitude (r = −0.24, 0.05, −0.16, respectively), and longitude (r = 0.01, −0.11, 0.07, respectively; Figure 5). However, a seasonal difference was found across the Cascade Range, with less seasonal $\delta^{18}O$ and $\Delta'^{17}O$ variability at sites west of the Cascades (OR02, Corvallis, OR10) and pronounced seasonal distinctions at sites east of the Cascades (OR18, Figures 6, S6). This longitudinal pattern was absent or even slightly reversed for d-excess, which had slightly larger differences (generally > 6.5‰) between summer and winter values at sites west of the Cascades and smaller seasonal differences (generally < 5‰) at sites east of the Cascades (Figure 6c). Overall, $\Delta'^{17}O$ was generally more variable at inland sites than those closer to the Pacific Coast, but proximity to the coast is not a reliable predictor of $\Delta'^{17}O$ variability (Figures 5 and 6). Theoretical modeling further confirms that isotopic signals of west-to-east rainout across the western and central United States are not clearly captured in observed precipitation $\Delta'^{17}O$, $\delta^{18}O$, and d-excess data (Figure 7). Still, the small size of this dataset limited exploration of trends in isotopic variation between sampling years or events, within sites, or at a greater spatial resolution.

*4.3 Streams*

The isotopic compositions of streams (n = 18) in the Willamette River Basin ranged from −13.0 to −8.4‰ for $\delta^{18}O$, −6.9 to −4.7‰ for $\delta^{17}O$, −89.5 to −59.9‰ for $\delta^{2}H$, 7.6 to 15.5‰ for d-excess, and 21 to 37 per meg for $\Delta'^{17}O$. Average $\Delta'^{17}O$ and $\delta^{18}O$ values for the Luckiamute and North Santiam Rivers (30 ± 6 per meg and −10.4 ± 1.7‰, respectively) were statistically indistinguishable from the annual amount-weighted average value of precipitation in Corvallis (29 ± 9 per meg and −7.8 ± 2.6‰). The best-fit linear regressions through the stream samples were

$\delta'^{17}O = 0.5272 \pm 0.0008 * \delta'^{81}O + 0.022 \pm 0.008$ and $\delta^2H = 7.52 \pm 0.2 * \delta^{18}O + 6.4 \pm 2.5$ (Figure 3).

Average d-excess and $\Delta'^{17}O$ values were slightly higher (12.6‰ and 32 per meg, respectively) in the North Santiam streams than for the stream within the Luckiamute River Basin (11.1‰ and 27 per meg, respectively). However, site-specific isotopic compositions were statistically indistinguishable from each other (p values > 0.05) and there were no clear trends between stream $\Delta'^{17}O$ or d-excess along a longitudinal transect (r = 0.31 and 0.44, respectively). Stream $\delta^{18}O$, $\Delta'^{17}O$, and d-excess values exhibited no seasonal pattern (Figure 4). Stream $\delta^{18}O$ variation was strongly negatively correlated with elevation (r = −0.99), with lower $\delta^{18}O$ values (−13.0 to −12.4‰) from the high elevation stream on the North Santiam River and higher $\delta^{18}O$ values (−10.0 to −8.4‰) from the stream in the Luckiamute watershed and the low elevation stream in the North Santiam basin.

## 5. Discussion

### *5.1 $\Delta'^{17}O$ observations in context of prior studies*

In many ways, the observations presented here confirm trends observed of $\Delta'^{17}O$, $\delta'^{18}O$, $\delta^2H$, and d-excess data from precipitation and streams in other mid- and low-latitude regions (e.g., Bershaw et al., 2020; Marchetti and Marchetti, 2019). This growing body of work shows similarities among seasonal distinctions, isotopic relationships between precipitation and stream water, and the precipitation $\delta'^{18}O$–$\delta'^{17}O$ regression slope (Figure 4). We also do not observe relationships between either precipitation or stream $\Delta'^{17}O$ values and elevation, precipitation amount, latitude, longitude, or local meteorological conditions (Figure 5), which is consistent with previous work (e.g., Aron et al., 2021a). It is possible that spatial $\Delta'^{17}O$ relationships exist, they just are not evident in this dataset largely due to the distribution of samples (i.e., samples were collected from different sites at different times and record different precipitation events). Additional work to investigate spatial $\Delta'^{17}O$ trends is still needed. Despite this limitation, the new data presented here and the existing body of work make clear two important points: seasonal distinctions in $\Delta'^{17}O$ values of precipitation are evident and they are consistent across a variety of geographic and climate regions (see discussion in Section 5.3).

Our observation that the $\Delta'^{17}O$ values of stream water in the northwestern U.S. are seasonally invariant and generally less variable than those of precipitation is also consistent with previous studies (Figures 3 and 4). The relatively narrow range of stream $\Delta'^{17}O$ values occurs because streams, especially in regions where water supplies are dominated by snowmelt and groundwater-fed recharge, typically integrate annual conditions and reflect the annual amount-weighted average isotopic composition of precipitation (Dutton et al., 2005; Kendall and Coplen, 2001). Streams can have very low $\Delta'^{17}O$ values ($< \sim -20$ per meg) and a larger $\Delta'^{17}O$ range than that of precipitation, but these values typically occur in arid regions where slow-flowing streams experience a high degree of evaporation (e.g., Surma et al., 2015; Voigt et al., 2021).

The precipitation $\delta'^{18}O$–$\delta'^{17}O$ regression slope (0.5255) in this dataset is lower than the reference value (0.528; Luz and Barkan, 2010) but is also consistent with previous precipitation observations (Table S4). This highlights two important points. First, nearly every precipitation $\delta'^{18}O$–$\delta'^{17}O$ slope is less than 0.528. Second, on seasonal timescales, nearly every previous study of precipitation and water vapor has reported higher $\delta'^{18}O$–$\delta'^{17}O$ regression slopes in the winter and lower $\delta'^{18}O$–$\delta'^{17}O$ regression slopes in the summer (Affolter et al., 2015; Gimenez et al., 2021; He et al., 2021; Surma et al., 2021; Tian et al., 2018; Tian and Wang, 2019; Uechi and Uemura, 2019). This seasonal pattern leads to higher $\Delta'^{17}O$ values in the winter and lower $\Delta'^{17}O$ values in the summer (Figure 4a). This suggests that 1) the $\delta'^{18}O$-$\delta'^{17}O$ relationship of most precipitation samples differs from the reference relationship and 2) that precipitation $\delta'^{18}O$ and $\delta'^{17}O$ values record more than just Rayleigh distillation. Considering that 0.529 is the theoretical $\delta'^{18}O$–$\delta'^{17}O$ slope for equilibrium fractionation, 0.518 is the theoretical slope for kinetic fractionation, and Rayleigh distillation produces slopes of 0.528, the consistent observation that precipitation $\delta'^{18}O$–$\delta'^{17}O$ slopes are less than 0.528 suggests that $\delta'^{18}O$–$\delta'^{17}O$ relationships hold information about both Rayleigh and non-Rayleigh related processes (Aron et al., 2021a; Luz and Barkan, 2010).

*5.2 Controls on precipitation $\Delta'^{17}O$ in the western and central United States*

The consistency among this dataset and other triple oxygen isotope studies of precipitation (i.e. precipitation $\delta'^{18}O$–$\delta'^{17}O$ slopes < 0.528, seasonal distinctions in precipitation $\Delta'^{17}O$) suggests systematic controls on $\Delta'^{17}O$, but the fractionating processes responsible for this variation have yet to be conclusively identified. In the next sections, we explore the processes and conditions that may be responsible for the relationships we observe among $\delta^{18}O$, d-excess, and $\Delta'^{17}O$ values in the western and central United States.

*5.2.1 Evaporation*

Surface and sub-cloud evaporation are the most well studied processes in the triple oxygen isotope literature. This is likely because the magnitude of $\Delta'^{17}O$ variability due to evaporation is often much greater than the analytical precision of $\Delta'^{17}O$ measurements, evaporation can be hard to identify with $\delta^{18}O$ alone, isotopic models of evaporation are well established, and the co-variation of $\delta^{18}O$, $\Delta'^{17}O$, and d-excess during evaporation is relatively easy to identify. This co-variation includes a negative correlation between $\delta^{18}O$ and $\Delta'^{17}O$ or d-excess, a positive correlation between d-excess and $\Delta'^{17}O$, and d-excess-$\Delta'^{17}O$ slope from ~ 0.7 to 2 per meg ‰$^{-1}$ (e.g., Barkan and Luz, 2007; Landais et al., 2010; Li et al., 2017; Luz and Barkan, 2010).

We observe two signals of sub-cloud evaporation in our precipitation dataset. First, a clear signal of evaporation was found among a small (n = 13) subset of summer precipitation samples that have positive $\delta^{18}O$ values, negative $\Delta'^{17}O$ values, negative d-excess values, a strong positive correlation between $\Delta'^{17}O$ and d-excess (r = 0.82), and a d-excess–$\Delta'^{17}O$ slope of 0.7 ± 0.2 per meg ‰$^{-1}$ (Figures 4a-4c and Figure S3). Such low (< ~ −10‰) d-excess values are unusual for precipitation, but are occasionally observed in western and central United States precipitation (Figure S2) due to sub-cloud evaporation (e.g., Marchetti and Marchetti, 2019). Evaporation might also have occurred after samples accumulated in the rain collection bucket as these summer precipitation events were small in amount, but this is unlikely because NADP has verified that collection devices essentially eliminate evaporative water loss (Lynch et al., 1996). Second, a weaker signal of evaporation occurred among all the summer rain samples. This evaporation was inferred from seasonal $\delta'^{18}O$–$\delta'^{17}O$ and $\delta^{18}O$–$\delta^{2}H$ regression lines (Figure S5). A strong positive correlation (r = 0.75) and positive slope (1.1 per meg ‰$^{-1}$) between summer $\Delta'^{17}O$ and d-excess and a slight positive correlation between summer $\Delta'^{17}O$ values and local relative humidity (r = 0.19) support this interpretation (Gimenez et al., 2021; Landais et al., 2010). These signals are most likely related to sub-cloud evaporation during small summer storms (e.g., Benjamin et al., 2004; Eastoe and Dettman, 2016; Friedman et al., 2002; Marchetti and Marchetti, 2019). Theoretical evaporation modeling (Figure 7) confirms this and shows that evaporation may explain the isotope ratios of a handful of precipitation samples in this dataset, but was not the single controlling mechanism that drives the variation in $\Delta'^{17}O$ values in this study.

*5.2.2 Relative humidity*

Previous work has shown that precipitation $\Delta'^{17}O$ can reflect variations of relative humidity above oceanic moisture sources, along moisture trajectories, and/or at local sample collection sites (e.g., Landais et al., 2012b; Surma et al., 2021; Uechi and Uemura, 2019), but a clear relative humidity-$\Delta'^{17}O$ relationship is not observed in this dataset. Similarly, precipitation d-excess value and local relative humidity are weakly correlated ($r = 0.17$) in this dataset. The absence of a relationship between $\Delta'^{17}O$ and relative humidity may be related to terrestrial water cycling and the interior continental position of many of the sample sites (Fiorella et al., 2018) and/or composite weekly precipitation samples are not clearly linked to site-specific average weekly relative humidity values.

*5.2.3 Rainout*

Much like d-excess, $\Delta'^{17}O$ is generally insensitive to rainout and Rayleigh distillation because these fractionating processes result in $\delta'^{18}O$–$\delta'^{17}O$ slopes that are nearly identical to the slope of the reference line (0.528, Equation 1). As a result, $\delta'^{18}O$ and $\delta'^{17}O$ variation during rainout occurs along a line that is offset from but essentially parallel to the reference line and $\Delta'^{17}O$ values remain nearly constant (Aron et al., 2021a; Luz and Barkan, 2010). In our dataset, regardless of season weak annual correlations between $\Delta'^{17}O$ and local precipitation amount ($r = 0.34$, Figure 5d), elevation ($r = 0.02$, Figure 5a), latitude ($r = 0.05$, Figure 5b), and longitude ($r = -0.11$, Figure 5c) indicate that rainout played a small role in the observed $\Delta'^{17}O$ variability. Simple modeling of $\Delta'^{17}O$, $\delta^{18}O$, and d-excess during Rayleigh distillation (Figure 7) further demonstrates this point.

*5.2.4 Sublimation, stratospheric intrusions, and supersaturation*

These controls are combined because although they all influence precipitation $\Delta'^{17}O$ values (e.g., Schoenemann et al., 2014; Surma et al., 2021; Winkler et al., 2012), they likely play a small role in the observed variation. First, sublimation increases $\Delta'^{17}O$ and d-excess values if precipitation condenses from sublimated vapor (Surma et al., 2021), but the lack of seasonal trends in d-excess values (Figure 4) means that sublimation is unlikely to be responsible for the high winter $\Delta'^{17}O$ values that we observe. Second, stratospheric intrusions could increase precipitation $\Delta'^{17}O$ values without affecting d-excess values by bringing water vapor with exceptionally high (> 1,000 per meg) $\Delta'^{17}O$ values into the troposphere (Franz and Röckmann, 2005; Lin et al., 2013; Winkler et al., 2012). However, this is unlikely because 1) stratospheric air is extremely dry and likely contributes very little to near-surface water cycles, 2) the high winter tropopause above North America generally limits stratospheric downdrafts, and 3) near-surface ozone levels, which increase during stratospheric intrusions, were low during the time periods when precipitation samples were collected (Cooper et al., 2012; Lin et al., 2015; Miller, 2013). Lastly, precipitation $\Delta'^{17}O$ variability has been linked to supersaturation (e.g., Landais et al., 2012b; Schoenemann et al., 2014). We consider this an unlikely explanation for our observations because the magnitude of supersaturation needed for observable fractionation is most common in polar regions where temperatures are very low (< ~ −20˚C). Further, supersaturation decreases $\Delta'^{17}O$ values, which is opposite of the wintertime trends that we observe.

### *5.3 Seasonal variability of precipitation $\Delta'^{17}O$*

Seasonal distinctions in precipitation $\Delta'^{17}O$ values are the most pronounced pattern in our dataset; we observe higher $\Delta'^{17}O$ values in the winter and lower $\Delta'^{17}O$ values in the summer (Figures 4, 5, and 6). Similar seasonal distinctions have also been observed in tropical precipitation in north central Africa (Landais et al., 2010) and eastern Singapore (He et al., 2021), mid-latitude precipitation in northwestern Switzerland (Affolter et al., 2015), southern Japan (Uechi and Uemura, 2019), central United States (Tian et al., 2018), and northern Spain (Gimenez et al., 2021), and polar precipitation in Greenland (Landais et al., 2012b) and East Antarctica (Landais et al., 2012a; Pang et al., 2019; Schoenemann and Steig, 2016; Touzeau et al., 2016). Seasonal $\Delta'^{17}O$ variation has also been observed in tap water from the United States (Li et al., 2015) and atmospheric water vapor from central Europe (Surma et al., 2021).

Although seasonal $\Delta'^{17}O$ variation has been observed across a wide range of climates and water types around the globe, explanations of this pattern vary widely. Seasonal precipitation $\Delta'^{17}O$ variation is often explained by a switch from processes with a greater influence of kinetic fractionation in the summer and to those dominated by equilibrium fractionation in the winter (e.g., Affolter et al., 2015; Landais et al., 2012a; Tian et al., 2018), but these explanations are not linked to climate conditions or hydrologic processes. In some instances the seasonal $\Delta'^{17}$O pattern is directly related to the relative humidity at remote moisture sources (e.g., Landais et al., 2012b; Uechi and Uemura, 2019), while in other cases seasonal $\Delta'^{17}$O variation is independent of relative humidity at either moisture source regions or sample collection sites (e.g., He et al., 2021; Li et al., 2015). In the tropics and mid-latitudes, seasonal $\Delta'^{17}$O variation has been linked to upstream moisture recycling (Tian et al., 2018), local raindrop re-evaporation (Gimenez et al., 2021; Landais et al., 2010), and convection tied to ENSO and regional monsoons (He et al., 2021). In snow-covered regions, sublimation can increase the $\Delta'^{17}$O of water vapor that is transported away from a snowpack, increasing the $\Delta'^{17}$O value of downstream precipitation (Pang et al., 2019; Surma et al., 2021). In polar regions, seasonal $\Delta'^{17}$O variations have been linked to the local precipitation rate at collection sites; relative humidity, sea surface temperatures, and the extent of sea ice at oceanic moisture sources; and kinetic fractionation during condensation under very cold, supersaturated conditions (Landais et al., 2012a, 2012b, 2008; Pang et al., 2019; Schoenemann et al., 2014; Schoenemann and Steig, 2016; Winkler et al., 2012).

The seasonal variation in $\Delta'^{17}$O that we observed in our dataset likely reflects a combination of the processes listed above. Some of the low $\Delta'^{17}$O values from summer-time precipitation may result from post-condensation evaporation (e.g., Eastoe and Dettman, 2016; Landais et al., 2010), whereas some of the higher winter $\Delta'^{17}$O values may reflect moisture recycling during continental-scale airmass transport (Li et al., 2015; Surma et al., 2021; Tian et al., 2019, 2018). Relative humidity above oceanic moisture sources and atmospheric mixing may be additional drivers of the seasonal $\Delta'^{17}$O signal (Li et al., 2015; Tian et al., 2018). While we cannot attribute seasonal variation in $\Delta'^{17}$O in U.S. precipitation to a single process, we use these data to highlight the seasonal pattern of higher winter $\Delta'^{17}$O values and lower summer $\Delta'^{17}$O values observed in this study and previous work.

### *5.4 Triple oxygen isotope meteoric water line*

The triple oxygen isotope meteoric water line was first defined in 2010 from Antarctic snow, Vostok ice (Landais et al., 2008), and a set of surface water, cave water, precipitation, and snow samples collected primarily from Asia and Europe (Luz and Barkan, 2010). This work laid the foundation for more than a decade of research by setting the $\delta'^{18}O$-$\delta'^{17}O$ regression slope through this sample set (0.528 ± 0.001) as the reference slope and establishing the intercept (0.033 ± 0.003) as the average $\Delta'^{17}O$ value of meteoric water on Earth. Since 2010, these values have provided a point of reference to evaluate isotopic variability and infer information about hydrology, paleoclimate, paleoaltimetry, and the rock cycle (e.g., Bindeman, 2021; Ibarra et al., 2021; Passey and Levin, 2021).

Since 2010 several studies have used water $\Delta'^{17}O$ data to re-evaluate the triple oxygen isotope meteoric water line (Table 1). These re-evaluations are motivated by an understanding that an accurate and representative meteoric water line is critical for applications of $\Delta'^{17}O$ in both modern and ancient systems and a growing number of meteoric water $\Delta'^{17}O$ datasets. Previously reported regression lines in Table 1 include surface waters that might be evaporated (Aron et al., 2021a; Sharp et al., 2018) or are biased toward polar precipitation (He et al., 2021). By including only precipitation data in this study, we minimize any effects of evaporation and focus on the $\delta'^{18}O$-$\delta'^{17}O$ relationship from non-polar regions.

Table 1. Slopes and intercepts of meteoric water $\delta'^{18}O$-$\delta'^{17}O$ regression lines.

| **Reference** | **Slope** | **Intercept (‰)** | **Observed or Defined** | **Notes** |
|---|---|---|---|---|
| Meijer and Li, 1998; Barkan and Luz, 2005 | 0.528 | 0 | Defined | Reference relationship |
| Luz and Barkan, 2010 | 0.528 | 0.033 | Observed | All available water data |
| Sharp et al., 2018 | 0.5265 | 0.014 | Observed | All water with $\delta^{18}O$ values > −20‰ |
| Aron et al., 2021a | 0.5268 | 0.015 | Observed | All integrated monthly precipitation and flowing rivers |

| | | | | |
|---|---|---|---|---|
| He et al., 2021 | 0.5279 | 0.021 | Observed | Tropical, mid-latitude, and polar precipitation and tap water |
| This study | 0.5264 | 0.014 | Observed | Precipitation data only [a] |
| [a] Precipitation data compiled from: Affolter et al., 2015; Aron et al., 2021b; Beverly er al., 2021; Gázquez et al., 2017; Gimenez et al., 2021; He et al., 2021; Landais et al., 2010; Luz and Barkan, 2010; Surma et al., 2018; Tian et al., 2019; 2021; Uechi and Uemura, 2019; this study. | | | | |

Similarities among the slopes and intercepts in Table 1 highlight two important points. First, all of the re-evaluated slopes are less than 0.528, which 1) means that the $\delta'^{18}O$ and $\delta'^{17}O$ values of non-polar precipitation record more than just Rayleigh distillation and 2) sets an expectation that $\Delta'^{17}O$ and $\delta'^{18}O$ values from precipitation and flowing surface water should be slightly anticorrelated (Beverly et al., 2021; Li et al., 2017; Passey and Ji, 2019; Surma et al., 2018, 2015; Voigt et al., 2021). Second, the re-evaluated $\delta'^{18}O$–$\delta'^{17}O$ relationships of most non-polar waters have intercepts less than 0.033‰. Although 33 per meg has been used as a 'typical' $\Delta'^{17}O$ value of meteoric water, our results show that this value does not represent either seasonal amount-weighted summer or winter precipitation $\Delta'^{17}O$ in the United States. Future studies should reconsider this assumed $\Delta'^{17}O$ value for meteoric waters in $\Delta'^{17}O$ interpretations and continue to probe the $\delta'^{18}O$–$\delta'^{17}O$ relationship as it may continue to vary with additional spatial and temporal coverage of samples (Putman et al., 2019).

*5.5 Utility of $\Delta'^{17}O$ in paleoclimate applications and directions of future work*

Isotopic techniques to quantify evaporation in modern waters are well established with d-excess (e.g., Gat 1996; Fiorella et al., 2015; Tappa et al. 2016; Bowen et al. 2018; Xia and Winnick, 2021), but the ability to isolate isotopic effects of evaporation has long been a challenge in oxygen isotope paleoclimatology. Reconstructing d-excess is challenging for paleoclimate applications because few geologic materials contain both hydrogen and oxygen, with the notable exceptions of fluid inclusions and gypsum where water itself is preserved (e.g., Evans et al. 2018; Wortham et al. 2022). However, given the consistent $\Delta'^{17}O$ response to evaporation, refined estimates of the

$\Delta'^{17}O$ values of precipitation make it possible to identify evaporation in oxygen-bearing geologic minerals and improve our understanding of paleoclimate and paleoaltimetry (e.g., Evans et al., 2018; Gázquez et al., 2018; Ibarra et al. 2021; Passey and Levin, 2021).

With additional work, seasonal variations of precipitation $\Delta'^{17}O$ may also add new information to interpret isotopic records. This could be particularly useful for paleoclimate archives that retain isotopic information about climate conditions but are susceptible to isotopic variations related to both seasonality and evaporative enrichment (e.g., Breecker et al., 2009; Kelson et al., 2020). In future hydrologic applications, precipitation $\Delta'^{17}O$ data may shed light on seasonal water use or $CO_2$ uptake by plants (Allen et al., 2019; Hofmann et al., 2017), distinguish water sources in seasonally snow-dominated watersheds (e.g., Jespersen et al., 2018; Tappa et al., 2016), track seasonal variations in evapotranspiration and boundary layer mixing (e.g., Fiorella et al., 2018; Welp et al., 2012), or monitor groundwater or surface water recharge (e.g., Jasechko et al., 2014; Voigt et al., 2021).

Before launching into new directions of paleoclimate triple oxygen isotope research, it is important to study the range and drivers of modern $\Delta'^{17}O$ variability. This is true of all paleoclimate proxies but is especially important for triple oxygen isotopes because $\Delta'^{17}O$ is defined as the deviation from a reference relationship and Table 1 shows that most waters follow a shallower slope and have a lower intercept than the canonical empirical $\delta'^{18}O$-$\delta'^{17}O$ relationship. This means that for most applications it will be critical to establish local amount-weighted precipitation $\Delta'^{17}O$ values.

Moving forward, additional $\Delta'^{17}O$ data from surface water, water vapor, and precipitation are still needed. Future event-scale and/or integrated monthly precipitation samples collected along elevation, latitudinal, and longitudinal transects will be useful to assess spatiotemporal triple oxygen isotope variability and improve interpretations of $\Delta'^{17}O$ in paleoclimate applications. Surface water samples, which are logistically easier to collect than rain and are often isotopically similar to annual amount-weighted precipitation, will also be useful to explore spatial $\Delta'^{17}O$ patterns and can provide information that is more relevant to the geologic community than individual precipitation samples (e.g., Bershaw et al. 2020).

## 6. Conclusion

This study presents new precipitation $\delta^{18}O$, d-excess, and $\Delta'^{17}O$ data from the western and central United States and stream $\delta^{18}O$, d-excess, and $\Delta'^{17}O$ data from the Willamette River Basin in western Oregon. The key findings are: 1) precipitation $\delta'^{18}O$-$\delta'^{17}O$ slopes often differ from the 0.528 reference value, 2) seasonal amount-weighted precipitation $\Delta'^{17}O$ values likely differ for summer and winter, 3) there are different controls on $\Delta'^{17}O$ and $\delta^{18}O$ such that $\Delta'^{17}O$ has the potential to bring additional information, and 4) it is critical to establish the local $\Delta^{17}O$ variation before using $\Delta^{17}O$ to characterize evaporation or derive other paleoclimate information.

Putting the $\Delta'^{17}O$ data into context with previous work, the most striking feature of precipitation $\Delta'^{17}O$ variability is the seasonal distinction in $\Delta'^{17}O$ values (higher in the winter, lower in the summer) that is consistent across the globe. These seasonal patterns likely reflect a combination of sub-cloud evaporation, atmospheric mixing, moisture recycling, sublimation, and/or variation in relative humidity at remote moisture sources, along moisture trajectories, and at local collection sites. Additional work is still needed to parse out the fractionating effects of each of these processes on precipitation $\Delta'^{17}O$. Still, it is clear that seasonal variation in $\Delta'^{17}O$ values differs from that of $\delta^{18}O$ and d-excess, indicating that $\Delta'^{17}O$ values provide new, complementary information.

Ultimately, controls on precipitation $\Delta'^{17}O$ are complex and comprehensive studies to understand the mechanisms driving its variation should be the focus of future work. Results presented here provide an overview of precipitation $\Delta'^{17}O$ variability, but do not have the spatial or temporal resolution to systematically understand the fractionating process responsible for the observed variation. Future studies with higher temporal and spatial resolution will help investigate synoptic processes responsible for seasonal variation in precipitation $\Delta'^{17}O$ values and to understand spatial variation in $\Delta'^{17}O$. In addition, future studies of water vapor and surface water $\Delta'^{17}O$ will be useful to assess the role of atmospheric mixing, evaluate whether $\Delta'^{17}O$ can be used to identify moisture source regions in North America, and help refine the slope and intercept of the triple oxygen isotope meteoric water line. Although there is still quite a bit left to understand about $\Delta'^{17}O$, initial results are clear that 33 per meg, which is inferred from the intercept of the original triple oxygen isotope line and assumed to represent the average meteoric water $\Delta'^{17}O$ value, can approximate average conditions in some circumstances but might not be appropriate in areas dominated by winter recharge or that have other seasonal dynamics. Future work that refines our understanding of $\Delta'^{17}O$ systematics will improve interpretations of triple oxygen isotope data for paleoclimate, paleoaltimetry, paleoecology, and paleo-atmospheric applications.

**Acknowledgments**

The authors thank the many individuals who supported this work over the years. We thank Rob Coulombe and Warren Evans for sample collection at the Environmental Protection Agency, National Atmospheric Deposition Network site operators for collecting samples that are part of the USNIP sample set, Huanting Hu and Haoyuan Ji for analytical assistance at Johns Hopkins University (JHU), Matt Rogers for analytical assistance at the UAA Stable Isotope Lab, and Ben Passey for useful discussions about the data. The authors also thank Jesse Nusbaumer and Patti Meeks for providing useful reviews of this manuscript. We are grateful for the constructive comments of three reviewers and the Associate Editor that improved this manuscript. Acknowledgement is made to the donors of the American Chemical Society Petroleum Research Fund for partial support of this research (ACS PRF# 52642-DNI2), in addition to funding support from Johns Hopkins University. Phoebe Aron received support from Chris Poulsen at the University of Michigan and funding from the Heising-Simons Foundation. Funding from NSF MRI to JMW (# 0953271) supported the USNIP sample analysis at the University of Alaska Anchorage. This manuscript has been subjected to Agency review and has been approved for publication. The views expressed in this paper are those of the author(s) and do not necessarily reflect the views or policies of the U.S. Environmental Protection Agency. Mention of trade names or commercial products does not constitute endorsement or recommendation for use.

**Open Research**

All isotope data from this study are available on the University of Utah Water Isotope Database under Project ID 00388 (Aron et al., 2023), 00011 (Brooks et al., 2012), and 00016 (Brooks, 2017).

**References**

Affolter, S., Häuselmann, A.D., Fleitmann, D., Häuselmann, P., Leuenberger, M., 2015. Triple isotope (δD, $\delta^{17}O$, $\delta^{18}O$) study on precipitation, drip water and speleothem fluid inclusions for a Western Central European cave (NW Switzerland). Quat. Sci. Rev. 127, 73–89. https://doi.org/10.1016/j.quascirev.2015.08.030

Alexandre, A., Landais, A., Vallet-Coulomb, C., Piel, C., Devidal, S., Pauchet, S., Sonzogni, C., Couapel, M., Pasturel, M., Cornuault, P., Xin, J., Mazur, J.C., Prié, F., Bentaleb, I., Webb, E., Chalié, F., Roy, J., 2018. The triple oxygen isotope composition of phytoliths as a proxy of continental atmospheric humidity: Insights from climate chamber and climate transect calibrations. Biogeosciences 15, 3223–3241. https://doi.org/10.5194/bg-15-3223-2018

Allen, S.T., Kirchner, J.W., Braun, S., Siegwolf, R.T.W., Goldsmith, G.R., 2019. Seasonal origins of soil water used by trees. Hydrol. Earth Syst. Sci. 23, 1199–1210. https://doi.org/10.5194/hess-23-1199-2019

Aron, P. G., Levin, N.E., Beverly, E.J., Huth, T.E., Passey, B.H., Pelletier, E.M., Poulsen, C.J., Winkelstern, I.Z., Yarian, D.A., 2021a. Triple oxygen isotopes in the water cycle. Chem. Geol. 565, 120026. https://doi.org/10.1016/j.chemgeo.2020.120026

Aron, P. G., Li, S., Brooks, J.R., Welker, J.M., Levin. N.E., 2023. Seasonal variations in triple oxygen isotope ratios of precipitation in the western and central United States - Final Data. [Dataset]. University of Utah Water Isotope Database. https://wateriso.utah.edu/waterisotopes/pages/spatial_db/SPATIAL_DB.html

Aron, P. G., Poulsen, C.J., Fiorella, R.P., Levin, N.E., Acosta, R.P., J, B., Yanites, Cassel, E.J., 2021b. Variability and controls on $\delta^{18}O$, d-excess, and $\Delta'^{17}O$ in southern Peruvian precipitation. J. Geophys. Res. Atmos. 126, 1–18. https://doi.org/10.1029/2020jd034009

Baker, L., Franchi, I.A., Maynard, J., Wright, I.P., Pillinger, C.T., 2002. A Technique for the Determination of $^{18}O/^{16}O$ and $^{17}O/^{16}O$ Isotopic Ratios in Water from Small Liquid and Solid Samples. Anal. Chem. 74, 1665–1673. https://doi.org/10.1021/ac010509s

Barkan, E., Luz, B., 2007. Diffusivity fractionations of $H_2{}^{16}O/H_2{}^{17}O$ and $H_2{}^{16}O/ H_2{}^{18}O$ in air and their implications for isotope hydrology. Rapid Commun. Mass Spectrom. 21, 2999–3005. https://doi.org/10.1002/rcm.3180

Barkan, E., Luz, B., 2005. High precision measurements of $^{17}O/^{16}O$ and $^{18}O/^{16}O$ ratios in $H_2O$. Rapid Commun. Mass Spectrom. 19, 3737–3742. https://doi.org/10.1002/rcm.2250

Benjamin, L., Knobel, L.L., Hall, L.F., Cecil, L.D., Green, J.R., 2004. Development of a Local Meteoric Water Line for Southeastern Idaho, Western Wyoming, and South-Central Montana. USGS 1–23.

Bergel, S. J., Barkan, E., Stein, M., & Affek, H. P. (2020). Carbonate $^{17}O$excess as a paleohydrology proxy: Triple oxygen isotope fractionation between $H_2O$ and biogenic aragonite, derived from freshwater mollusks. Geochim. Cosmochim. Acta 275, 36–47. https://doi.org/10.1016/j.gca.2020.02.005

Berman, E.S.F., Levin, N.E., Landais, A., Li, S., Owano, T., 2013. Measurement of $\delta^{18}O$, $\delta^{17}O$, and $^{17}O$-excess in Water by Off-Axis Integrated Cavity Output Spectroscopy and Isotope Ratio Mass Spectrometry. Anal. Chem. 85, 10,392–10,398. https://doi.org/10.1021/ac402366t

Bershaw, J., Hansen, D.D., Schauer, A.J., 2020. Deuterium excess and $^{17}O$-excess variability in meteoric water across the Pacific Northwest, USA. Tellus, Ser. B Chem. Phys. Meteorol. 72, 1–17. https://doi.org/10.1080/16000889.2020.1773722

Beverly, E.J., Levin, N.E., Passey, B.H., Aron, P.G., Yarian, D.A., Page, M., Pelletier, E.M., 2021. Triple oxygen and clumped isotopes in modern soil carbonate along an aridity gradient in the Serengeti, Tanzania. Earth Planet. Sci. Lett. 567, 116952. https://doi.org/10.1016/j.epsl.2021.116952

Bindeman, I.N., 2021. Triple Oxygen Isotopes in Evolving Continental Crust, Granites, and Clastic Sediments. Rev. Mineral. Geochemistry 86, 241–290. https://doi.org/10.2138/rmg.2021.86.08

Bowen, G. J., Putman, A., Brooks, J. R., Bowling, D. R., Oerter, E. J., Good, S. P. 2018. Inferring the source of evaporated waters using stable H and O isotopes. Oecologia, 187, 1025–1039. https://doi.org/10.1007/s00442-018-4192-5

Bowen, G. J., Cai, Z., Fiorella, R. P., & Putman, A. L. 2019. Isotopes in the Water Cycle: Regional- to Global-Scale Patterns and Applications. Ann. Rev. Earth Planet. Sci., 47, 453–479. https://doi.org/10.1146/annurev-earth-053018-060220

Brady, M. P., Hodell, D. A. 2021. Continuous and Simultaneous Measurement of Triple-oxygen and Hydrogen Isotopes of Liquid and Vapor during Evaporation Experiments. Rapid Commun Mass Spectrom 35 (10). https://doi.org/10.1002/rcm.9078.

Breecker, D.O., Sharp, Z.D., McFadden, L.D., 2009. Seasonal bias in the formation and stable isotopic composition of pedogenic carbonate in modern soils from central New Mexico, USA. Bull. Geol. Soc. Am. 121, 630–640. https://doi.org/10.1130/B26413.1

Brooks, J.R., Wigington, P.J., Phillips, D.L., Comeleo, R., Coulombe, R., 2012. Willamette River Basin surface water isoscape ($\delta^{18}O$ and $\delta^2H$): temporal changes of source water

within the river. Ecosphere 3, art39. https://doi.org/10.1890/es11-00338.1
Brooks, J.R., Wigington, P.J., Phillips, D.L., Comeleo, R., Coulombe, R., 2012. Willamette River Basin surface water isoscape ($\delta^{18}O$ and $\delta^{2}H$): Temporal changes of source water within the river. [Dataset]. University of Utah Water Isotope Database. https://wateriso.utah.edu/waterisotopes/pages/spatial_db/SPATIAL_DB.html
Brooks, J.R., 2017. OR Precipitation (EPA). [Dataset]. University of Utah Water Isotope Database. https://wateriso.utah.edu/waterisotopes/pages/spatial_db/SPATIAL_DB.html
Bryant, J.D., Froelich, P.N., 1995. A model of oxygen isotope fractionation in body water of large mammals. Geochim. Cosmochim. Acta 59, 4523–4537. https://doi.org/10.1016/0016-7037(95)00250-4
Chamberlain, C.P., Ibarra, D.E., Kukla, T., Methner, K.A., Gao, Y., 2021. Triple oxygen isotope paleoaltimetry of crystalline rocks. Front. Earth Sci. 9, 1–6. https://doi.org/10.3389/feart.2021.633687
Cooper, O.R., Gao, R.S., Tarasick, D., Leblanc, T., Sweeney, C., 2012. Long-term ozone trends at rural ozone monitoring sites across the United States, 1990-2010. J. Geophys. Res. Atmos. 117, 1990–2010. https://doi.org/10.1029/2012JD018261
Craig, H., 1961. Isotopic Variations in Meteoric Waters. Science. 133, 1702–1703. https://doi.org/10.1126/science.133.3465.1702
Craig, H., Gordon, L.I., 1965. Deuterium and oxygen 18 variations in the ocean and the marine atmosphere. In: Tongiorgi, E. (Ed.), Proceedings of a Conference on Stable Isotopes in Oceanographic Studies and Paleotemperatures. Spoleto, Italy, pp. 9–130.
Dansgaard, W., 1964. Stable isotopes in precipitation. Tellus 16, 436–468. https://doi.org/10.3402/tellusa.v16i4.8993
Dutton, A., Wilkinson, B.H., Welker, J.M., Bowen, G.J., Lohmann, K.C., 2005. Spatial distribution and seasonal variation in $^{18}O/^{16}O$ of modern precipitation and river water across the conterminous USA. Hydrol. Process. 19, 4121–4146. https://doi.org/10.1002/hyp.5876
Eastoe, C.J., Dettman, D.L., 2016. Isotope amount effects in hydrologic and climate reconstructions of monsoon climates: Implications of some long-term data sets for precipitation. Chem. Geol. 430, 78–89. https://doi.org/10.1016/j.chemgeo.2016.03.022
Evans, N.P., Bauska, T.K., Gázquez-Sánchez, F., Brenner, M., Curtis, J.H., Hodell, D.A., 2018.

Quantification of drought during the collapse of the classic Maya civilization. Science 361, 498–501. https://doi.org/10.1126/science.aas9871

Fiorella, R.P., Poulsen, C.J., Matheny, A.M., 2018. Seasonal patterns of water cycling in a deep, continental mountain valley inferred from stable water vapor isotopes. J. Geophys. Res. Atmos. 123, 7271–7291. https://doi.org/10.1029/2017JD028093

Fiorella, R.P., Poulsen, C.J., Pillco, R.S., Jeffery, M.L., Ehlers, T.A., 2015. Modern and long-term evaporation of central Andes surface waters suggests paleo archives underestimate Neogene elevations. Earth Planet. Sci. Lett. 432, 59–72. https://doi.org/10.1016/j.epsl.2015.09.045

Franz, P., Röckmann, T., 2005. High-precision isotope measurements of $H_2{}^{16}O$, $H_2{}^{17}O$, $H_2{}^{18}O$, and the $\Delta^{17}O$-anomaly of water vapor in the southern lowermost stratosphere. Atmos. Chem. Phys. 5, 5373–5403.

Friedman, I., Smith, G.I., Johnson, C.A., Moscati, R.J., 2002. Stable isotope compositions of waters in the Great Basin, United States 2. Modern precipitation. J. Geophys. Res. Atmos. 107, ACL 15-1-ACL 15-22. https://doi.org/10.1029/2001JD000566

Galewsky, J., Steen-Larsen, H. C., Field, R. D., Worden, J., Risi, C., & Schneider, M., 2016. Stable isotopes in atmospheric water vapor and applications to the hydrologic cycle: Isotopes in the Atmospheric Water Cycle. Reviews of Geophysics 54(4), 809–865. https://doi.org/10.1002/2015RG000512

Gat, J. R. 1996. Oxygen and hydrogen isotopes in the hydrologic cycle. Ann. Rev. Earth Planet. Sci., 24, 225–262. https://doi.org/10.1146/annurev.earth.24.1.225

Gázquez, F., Bauska, T.K., Comas-Bru, L., Ghaleb, B., Calaforra, J.M., Hodell, D.A., 2020. The potential of gypsum speleothems for paleoclimatology: application to the Iberian Roman Human Period. Sci. Rep. 10, 1–13. https://doi.org/10.1038/s41598-020-71679-3

Gázquez, F., Calaforra, J.M., Evans, N.P., Hodell, D.A., 2017. Using stable isotopes ($\delta^{17}O$, $\delta^{18}O$ and $\delta D$) of gypsum hydration water to ascertain the role of water condensation in the formation of subaerial gypsum speleothems. Chem. Geol. 452, 34–46. https://doi.org/10.1016/j.chemgeo.2017.01.021

Gázquez, F., Morellón, M., Bauska, T., Herwartz, D., Surma, J., Moreno, A., Staubwasser, M., Valero-garcés, B., Delgado-huertas, A., Hodell, D.A., 2018. Triple oxygen and hydrogen isotopes of gypsum hydration water for quantitative paleo-humidity reconstruction. Earth

Planet. Sci. Lett. 481, 177–188. https://doi.org/10.1016/j.epsl.2017.10.020

Gehler, A., Tütken, T., Pack, A., 2011. Triple oxygen isotope analysis of bioapatite as tracer for diagenetic alteration of bones and teeth. Palaeogeogr. Palaeoclimatol. Palaeoecol. 310, 84–91. https://doi.org/10.1016/j.palaeo.2011.04.014

Gimenez, R., Bartolome, M., Gazquez, F., Iglesias, M., Moreno, A., 2021. Underlying Climate Controls in Triple Oxygen ($^{16}O$, $^{17}O$, $^{18}O$) and Hydrogen ($^{1}H$, $^{2}H$) Isotopes Composition of Rainfall (Central Pyrenees). Front. Earth Sci. 9, 1–16. https://doi.org/10.3389/feart.2021.633698

Gonfiantini, R., Wassenaar, L.I., Araguas-Araguas, L., Aggarwal, P.K., 2018. A unified Craig-Gordon isotope model of stable hydrogen and oxygen isotope fractionation during fresh or saltwater evaporation. Geochim. Cosmochim. Acta 235, 224–236. https://doi.org/10.1016/j.gca.2018.05.020

He, S., Jackisch, D., Samanta, D., Yi, P.K.Y., Liu, G., Wang, X., Goodkin, N.F., 2021. Understanding tropical convection through triple oxygen isotopes of precipitation from the maritime continent. J. Geophys. Res. Atmos. 126, 1–14.

Hellmann, R., Harvey, A. H. 2020. First-principles diffusivity ratios for kinetic isotope fractionation of water in air. Geophys. Res. Let, 47. e2020GL089999. https://doi.org/10.1029/2020GL089999

Herwartz, D., Surma, J., Voigt, C., Assonov, S., Staubwasser, M., 2017. Triple oxygen isotope systematics of structurally bonded water in gypsum. Geochim. Cosmochim. Acta 209, 254–266. https://doi.org/10.1016/j.gca.2017.04.026

Hofmann, M.E.G., Horváth, B., Schneider, L., Peters, W., Schützenmeister, K., Pack, A., 2017. Atmospheric measurements of $\Delta^{17}O$ in $CO_2$ in Göttingen, Germany reveal a seasonal cycle driven by biospheric uptake. Geochim. Cosmochim. Acta 199, 143–163. https://doi.org/10.1016/j.gca.2016.11.019

Horita, J., Wesolowski, D.J., 1994. Liquid-vapor fractionation of oxygen and hydrogen isotopes of water from the freezing to the critical temperature. Geochim. Cosmochim. Acta 58, 3425–3437.

Ibarra, D.E., Kukla, T., Methner, K.A., Mulch, A., Chamberlain, C.P., 2021. Reconstructing past elevations from triple oxygen isotopes of lacustrine chert: application to the Eocene Nevadaplano, Elko Basin, Nevada, United States. Front. Earth Sci. 9, 1–19.

https://doi.org/10.3389/feart.2021.628868
Jasechko, S., Birks, S.J., Gleeson, T., Wada, Y., Fawcett, P.J., Sharp, Z.D., McDonnell, J.J., Welker, J.M., 2014. The pronounced seasonality of global groundwater recharge. Water Resour. Res. 50, 8845–8867. https://doi.org/10.1002/2014WR015809
Jespersen, R.G., Leffler, A.J., Oberbauer, S.F., Welker, J.M., 2018. Arctic plant ecophysiology and water source utilization in response to altered snow: isotopic ($\delta^{18}$O and $\delta^{2}$H) evidence for meltwater subsidies to deciduous shrubs. Oecologia 187, 1009–1023. https://doi.org/10.1007/s00442-018-4196-1
Kelson, J.R., Huntington, K.W., Breecker, D.O., Burgener, L.K., Gallagher, T.M., Hoke, G.D., Petersen, S. V., 2020. A proxy for all seasons? A synthesis of clumped isotope data from Holocene soil carbonates. Quat. Sci. Rev. 234, 106259. https://doi.org/10.1016/j.quascirev.2020.106259
Kelson, J. R., Petersen, S. V., Niemi, N. A., Passey, B. H., & Curley, A. N. 2022. Looking upstream with clumped and triple oxygen isotopes of estuarine oyster shells in the early Eocene of California, USA. Geology, 50, 755–759. https://doi.org/10.1130/G49634.1
Kendall, C., Coplen, T.B., 2001. Distribution of oxygen-18 and deuteriun in river waters across the United States. Hydrol. Process. 15, 1363–1393. https://doi.org/10.1002/hyp.217
Koch, P.L., 1998. Isotopic Reconstruction of past continental environments. Annu. Rev. Earth Planet. Sci. 26, 573–613. https://doi.org/10.1146/annurev.earth.26.1.573
Kohn, M.J., 1996. Predicting animal $\delta^{18}$O: Accounting for diet and physiological adaptation. Geochim. Cosmochim. Acta 60, 4811–4829. https://doi.org/10.1016/S0016-7037(96)00240-2
Landais, A., Barkan, E., Luz, B., 2008. Record of $\delta^{18}$O and $^{17}$O-excess in ice from Vostok Antarctica during the last 150,000 years. Geophys. Res. Lett. 35, 1–5. https://doi.org/10.1029/2007GL032096
Landais, A., Ekaykin, A., Barkan, E., Winkler, R., Luz, B., 2012a. Seasonal variations of $^{17}$O-excess and d-excess in snow precipitation at Vostok station, East Antarctica. J. Glaciol. 58, 725–733. https://doi.org/10.3189/2012JoG11J237
Landais, A., Risi, C., Bony, S., Vimeux, F., Descroix, L., Falourd, S., Bouygues, A., 2010. Combined measurements of $^{17}O_{excess}$ and d-excess in African monsoon precipitation: Implications for evaluating convective parameterizations. Earth Planet. Sci. Lett. 298,

104–112. https://doi.org/10.1016/j.epsl.2010.07.033

Landais, A., Steen-Larsen, H.C., Guillevic, M., Masson-Delmotte, V., Vinther, B., Winkler, R., 2012b. Triple isotopic composition of oxygen in surface snow and water vapor at NEEM (Greenland). Geochim. Cosmochim. Acta 77, 304–316. https://doi.org/10.1016/j.gca.2011.11.022

Lehmann, S. B., Levin, N. E., Passey, B. H., Hu, H., Cerling, T. E., Miller, J. H., Arppe, L., Beverly, E. J., Hoppe, K. A., Huth, T. E., Kelson, J. R., Luyt, J., & Sealy, J. 2022. Triple oxygen isotope distribution in modern mammal teeth and potential geologic applications. Geochim Cosmochim Acta 331, 105–122. https://doi.org/10.1016/j.gca.2022.04.033

Levin, N.E., Raub, T.D., Dauphas, N., Eiler, J.M., 2014. Triple oxygen isotope variations in sedimentary rocks. Geochim. Cosmochim. Acta 139, 173–189. https://doi.org/10.1016/j.gca.2014.04.034

Li, S., Levin, N.E., Chesson, L.A., 2015. Continental scale variation in $^{17}$O-excess of meteoric waters in the United States. Geochim. Cosmochim. Acta 164, 110–126. https://doi.org/10.1016/j.gca.2015.04.047

Li, S., Levin, N.E., Soderberg, K., Dennis, K.J., Caylor, K.K., 2017. Triple oxygen isotope composition of leaf waters in Mpala, central Kenya. Earth Planet. Sci. Lett. 468, 38–50. https://doi.org/10.1016/j.epsl.2017.02.015

Lin, M., Fiore, A.M., Horowitz, L.W., Langford, A.O., Oltmans, S.J., Tarasick, D., Rieder, H.E., 2015. Climate variability modulates western US ozone air quality in spring via deep stratospheric intrusions. Nat. Commun. 6, 1–11. https://doi.org/10.1038/ncomms8105

Lin, Y., Clayton, R.N., Huang, L., Nakamura, N., Lyons, J.R., 2013. Oxygen isotope anomaly observed in water vapor from Alert, Canada and the implication for the stratosphere. Proc. Natl. Acad. Sci. U. S. A. 110, 15608–15613. https://doi.org/10.1073/pnas.1313014110

Liu, Z., Tang, Y., Jian, Z., Poulsen, C.J., Welker, J.M., Bowen, G.J., 2017. Pacific North American circulation pattern links external forcing and North American hydroclimatic change over the past millennium. Proc. Natl. Acad. Sci. U. S. A. 114, 3340–3345. https://doi.org/10.1073/pnas.1618201114

Luz, B., Barkan, E., 2010. Variations of $^{17}O/^{16}O$ and $^{18}O/^{16}O$ in meteoric waters. Geochim. Cosmochim. Acta 74, 6276–6286. https://doi.org/10.1016/j.gca.2010.08.016

Lynch, J.A., Grimm, J.W., Bowersox, V.C., 1996. An analysis of the effects of precipitation chemistry of phase I of the Clean Air Act Amendments of 1990, Title IV. Atmos. Depos. to Gt. Waters 99–111.

Majoube, M., 1971. Fractionnement en oxygène 18 et en deutérium entre l'eau et sa vapeur. J. Chim. Phys. 68, 1432–1436.

Marchetti, D.W., Marchetti, S.B., 2019. Stable isotope compositions of precipitation from Gunnison, Colorado 2007–2016: implications for the climatology of a high-elevation valley. Heliyon 5, e02120. https://doi.org/10.1016/j.heliyon.2019.e02120

Meijer, H.A.J., Li, W.J., 1998. The Use of Electrolysis for Accurate $\delta^{18}$O and $\delta^{17}$O Isotope Measurements in Water. Isot. Evironmental Heal. Stud. 34, 349–369. https://doi.org/10.1080/10256019808234072

Miller, M.F., 2018. Precipitation regime influence on oxygen triple-isotope distributions in Antarctic precipitation and ice cores. Earth Planet. Sci. Lett. 481, 316–327. https://doi.org/10.1016/j.epsl.2017.10.035

Miller, M.F., 2013. Oxygen isotope anomaly not present in water vapor from Alert, Canada. Proc. Natl. Acad. Sci. U. S. A. 110, 4567. https://doi.org/10.1073/pnas.1318925110

Miller, M.F., 2002. Isotopic fractionation and the quantification of $^{17}$O anomalies in the oxygen three-isotope system: an appraisal and geochemical significance. Geochim. Cosmochim. Acta 66, 1881–1889.

Nava-Fernandez, C., Hartland, A., Gázquez, F., Kwiecien, O., Marwan, N., Fox, B., et al. (2020). Pacific climate reflected in Waipuna Cave drip water hydrochemistry. Hydrol. Earth Syst. 24(6), 3361–3380. https://doi.org/10.5194/hess-24-3361-2020

Pang, H., Hou, S., Landais, A., Delmotte, V.M., Jouzel, J., 2019. Influence of summer sublimation on δD , $\delta^{18}$O, and $\delta^{17}$O in precipitation, East Antarctica, and implications for climate reconstruction from ice cores. J. Geophys. Res. Atmos. 124, 7339–7358. https://doi.org/10.1029/2018JD030218

Passey, B.H., Hu, H., Ji, H., Montanari, S., Li, S., Henkes, G.A., Levin, N.E., 2014. Triple oxygen isotopes in biogenic and sedimentary carbonates. Geochim. Cosmochim. Acta 141, 1–25. https://doi.org/10.1016/j.gca.2014.06.006

Passey, B.H., Ji, H., 2019. Triple oxygen isotope signatures of evaporation in lake waters and carbonates: A case study from the western United States. Earth Planet. Sci. Lett. 518, 1–

12. https://doi.org/10.1016/j.epsl.2019.04.026

Passey, B.H., Levin, N.E., 2021. Triple oxygen isotopes in carbonates, biological apatites, and continental paleoclimate reconstruction. Rev. Mineral. Geochemistry 86, 429–462. https://doi.org/10.2138/rmg.2021.86.13

Pierchala, A., Rozanski, K., Dulinski, M., & Gorczyca, Z. 2022. Triple-isotope mass balance of mid-latitude, groundwater controlled lake. Science of The Total Environment 814, 151935. https://doi.org/10.1016/j.scitotenv.2021.151935

Putman, A.L., Bowen, G.J., 2019. Technical Note: A global database of the stable isotopic ratios of meteoric and terrestrial waters. Hydrol. Earth Syst. Sci. 23, 4389–4396. https://doi.org/10.5194/hess-23-4389-2019

Putman, A. L., Fiorella, R, Bowen, G.J., Cai, Z. 2019. A global perspective on local meteoric water lines: Metaanalytic insight into fundamental controls and practical constraints. Water Resour. Res., 55, 6896-6910 https://doi.org/10.1029/2019WR025181

Quade, J., Rech, J.A., Latorre, C., Betancourt, J.L., Gleeson, E., Kalin, M.T.K., 2007. Soils at the hyperarid margin: The isotopic composition of soil carbonate from the Atacama Desert, Northern Chile. Geochim. Cosmochim. Acta 71, 3772–3795. https://doi.org/10.1016/j.gca.2007.02.016

Rech, J.A., Currie, B.S., Jordan, T.E., Riquelme, R., Lehmann, S.B., Kirk-Lawlor, N.E., Li, S., Gooley, J.T., 2019. Massive middle Miocene gypsic paleosols in the Atacama Desert and the formation of the Central Andean rain-shadow. Earth Planet. Sci. Lett. 506, 184–194. https://doi.org/10.1016/j.epsl.2018.10.040

Rowley, D.B., 2007. Stable Isotope-Based Paleoaltimetry: Theory and Validation. Rev. Mineral. Geochemistry 66, 23–52. https://doi.org/10.2138/rmg.2007.66.2

Schoenemann, S.W., Schauer, A.J., Steig, E.J., 2013. Measurement of SLAP2 and GISP $\delta^{17}O$ and proposed VSMOW-SLAP normalization for $\delta^{17}O$ and $^{17}O$excess. Rapid Commun. Mass Spectrom. 27, 582–590. https://doi.org/10.1002/rcm.6486

Schoenemann, S.W., Steig, E.J., 2016. Seasonal and spatial variations of $^{17}O$excess and dexcess in Antarctic precipitation: Insights from an intermediate complexity isotope model. J. Geophys. Res. Atmos. 121, 11215–11247. https://doi.org/10.1002/2016JD025117.Received

Schoenemann, S.W., Steig, E.J., Ding, Q., Markle, B.R., Schauer, A.J., 2014. Triple waterisotopologue record from WAIS Divide, Antarctica: controls on glacial-interglacial changes in $^{17}$Oexcess of precipitation. J. Geophys. Res. Atmos. 119, 8741–8763. https://doi.org/10.1002/2014JD021770.Received

Sengupta, S., Pack, A., 2018. Triple oxygen isotope mass balance for the Earth's oceans with application to Archean cherts. Chem. Geol. 495, 18–26. https://doi.org/10.1016/j.chemgeo.2018.07.012

Sha, L., Mahata, S., Duan, P., Luz, B., Zhang, P., Baker, J., Zong, B., Ning, Y., Brahim, Y.A., Zhang, H., Edwards, R.L., Cheng, H., 2020. A novel application of triple oxygen isotope ratios of speleothems. Geochim. Cosmochim. Acta 270, 360–378. https://doi.org/10.1016/j.gca.2019.12.003

Sharp, Z.D., Wostbrock, J.A.G., Pack, A., 2018. Mass-dependent triple oxygen isotope variations in terrestrial materials. Geochemical Perspect. Lett. 7, 27–31. https://doi.org/10.7185/geochemlet.1815

Surma, J., Assonov, S., Bolourchi, M.J., Staubwasser, M., 2015. Triple oxygen isotope signatures in evaporated water bodies from the Sistan Oasis, Iran. Geophys. Res. Lett. 42, 8456–8462. https://doi.org/10.1002/2015GL066475

Surma, J., Assonov, S., Herwartz, D., Voigt, C., Staubwasser, M., 2018. The evolution of $^{17}$O-excess in surface water of the arid environment during recharge and evaporation. Sci. Rep. 8, 1–10. https://doi.org/10.1038/s41598-018-23151-6

Surma, J., Assonov, S., Staubwasser, M., 2021. Triple Oxygen Isotope Systematics in the Hydrologic Cycle. Rev. Mineral. Geochemistry 86, 401–428. https://doi.org/10.2138/rmg.2021.86.12

Tappa, D.J., Kohn, M.J., Mcnamara, J.P., Benner, S.G., Flores, A.N., 2016. Isotopic composition of precipitation in a topographically steep , seasonally snow-dominated watershed and implications of variations from the global meteoric water line 4592, 4582–4592. https://doi.org/10.1002/hyp.10940

Thompson, L.G., Mosley-Thompson, E., Henderson, K.A., 2000. Ice-core palaeoclimate records in tropical South America since the last glacial maximum. J. Quat. Sci. 15, 377–394. https://doi.org/10.1002/1099-1417(200005)15:4<377::AID-JQS542>3.0.CO;2-L

Tian, C., Jiao, W., Beysens, D., Farai Kaseke, K., Medici, M.G., Li, F., Wang, L., 2021. Investigating the role of evaporation in dew formation under different climates using $^{17}$O-excess. J. Hydrol. 592, 125847. https://doi.org/10.1016/j.jhydrol.2020.125847

Tian, C., Wang, L., 2019. Data Descriptor : Stable isotope variations of daily precipitation from 2014 – 2018 in the central United States. Sci. Data 6, 1–8. https://doi.org/10.1038/sdata.2019.18

Tian, C., Wang, L., Kaseke, K.F., Bird, B.W., 2018. Stable isotope compositions ($\delta^2$H, $\delta^{18}$O and $\delta^{17}$O) of rainfall and snowfall in the central United States. Sci. Rep. 8, 1–15. https://doi.org/10.1038/s41598-018-25102-7

Tian, C., Wang, L., Tian, F., Zhao, S., Jiao, W., 2019. Spatial and temporal variations of tap water $^{17}$O-excess in China. Geochim. Cosmochim. Acta 260, 1–14. https://doi.org/10.1016/j.gca.2019.06.015

Touzeau, A., Landais, A., Stenni, B., Uemura, R., Fukui, K., Fujita, S., Guilbaud, S., Ekaykin, A., Casado, M., Barkan, E., Luz, B., Magand, O., Teste, G., Le Meur, E., Baroni, M., Savarino, J., Bourgeois, I., Risi, C., 2016. Acquisition of isotopic composition for surface snow in East Antarctica and the links to climatic parameters. Cryosphere 10, 837–852. https://doi.org/10.5194/tc-10-837-2016

Uechi, Y., Uemura, R., 2019. Dominant influence of the humidity in the moisture source region on the $^{17}$O-excess in precipitation on a subtropical island. Earth Planet. Sci. Lett. 513, 20–28. https://doi.org/10.1016/j.epsl.2019.02.012

Voigt, C., Herwartz, D., Dorador, C., Staubwasser, M., 2021. Triple oxygen isotope systematics of evaporation and mixing processes in a dynamic desert lake system. Hydrol. Earth Syst. Sci. 25, 1211–1228. https://doi.org/10.5194/hess-25-1211-2021

Welker, J.M., 2012. ENSO effects on $\delta^{18}$O, $\delta^2$H and d-excess values in precipitation across the U.S. using a high-density, long-term network (USNIP). Rapid Commun. Mass Spectrom. 26, 1893–1898. https://doi.org/10.1002/rcm.6298

Welp, L.R., Lee, X., Griffis, T.J., Wen, X.F., Xiao, W., Li, S., Sun, X., Hu, Z., Val Martin, M., Huang, J., 2012. A meta-analysis of water vapor deuterium-excess in the midlatitude atmospheric surface layer. Global Biogeochem. Cycles 26, 1–12. https://doi.org/10.1029/2011GB004246

Winkler, R., Landais, A., Sodemann, H., Dümbgen, L., Prié, F., Masson-Delmotte, V., Stenni, B., Jouzel, J., 2012. Deglaciation records of $^{17}$O-excess in East Antarctica: Reliable reconstruction of oceanic normalized relative humidity from coastal sites. Clim. Past 8, 1–16. https://doi.org/10.5194/cp-8-1-2012

Wortham, B. E., Montañez, I. P., Swart, P. K., Vonhof, H., Tabor, C. 2022. Variability in effective moisture inferred from inclusion fluid $\delta^{18}O$ and $\delta^{2}H$ values in a central Sierra Nevada stalagmite (CA). Quat. Sci. Rev, 279, 107399. https://doi.org/10.1016/j.quascirev.2022.107399

Wostbrock, J.A.G., Brand, U., Coplen, T.B., Swart, P.K., Carlson, S.J., Brearley, A.J., Sharp, Z.D., 2020. Calibration of carbonate-water triple oxygen isotope fractionation: Seeing through diagenesis in ancient carbonates. Geochim. Cosmochim. Acta 288, 369–388. https://doi.org/10.1016/j.gca.2020.07.045

Wostbrock, J.A.G., Sharp, Z.D., 2021. Triple Oxygen Isotopes in Silica – Water and Carbonate – Water Systems. Rev. Mineral. Geochemistry 86, 367–400. https://doi.org/10.2138/rmg.2021.86.11

Xia, Z., Winnick, M.J., 2021. The competing effects of terrestrial evapotranspiration and raindrop re-evaporation on the deuterium excess of continental precipitation. Earth Planet. Sci. Lett. 572, 117120. https://doi.org/10.1016/j.epsl.2021.117120

Young, E.D., Galy, A., Nagahara, H., 2002. Kinetic and equilibrium mass-dependent isotope fractionation laws in nature and their geochemical and cosmochemical significance. Geochim. Cosmochim. Acta 66, 1095–1104. https://doi.org/10.1016/S0016-7037(01)00832-8

Zachos, J., 2001. Trends, Rhythms, and Aberrations in Global Climate 65 Ma to Present 292, 686–693. https://doi.org/10.1126/science.1059412

Figure 1. Spatial distribution of previously published (gray filled symbols) and new (black filled symbols) triple oxygen isotope water data from the United States.

Figure 2. Histograms of seasonal (A) and annual (B) distributions of precipitation samples from this study. Sites are listed longitudinally with western-most sites (Washington and Oregon) on the left and the eastern-most site (North Carolina) on the right. The latitude and longitude of each site is reported in Table S1.

Figure 3. Scatterplots of precipitation (filled circles) and stream (open squares) $\delta'^{18}O$ vs. $\delta'^{17}O$ (A) and $\delta^{18}O$ vs. $\delta^{2}H$ (B) from this study. The solid black lines show meteoric water reference lines with slopes of 0.528 and 8 and intercepts of 0 and 10, respectively.

Figure 4. Scatterplots of $\delta'^{18}O$ vs. $\Delta'^{17}O$ (A and D), $\delta^{18}O$ vs. d-excess (B and E), and d-excess vs. $\Delta'^{17}O$ (C and F). Error bars on $\Delta'^{17}O$ data show the standard deviation of $\Delta'^{17}O$ measurements. Shape differentiates water types and color differentiates seasons. From our study, summer data are in red and winter data are in blue. Among the published data, summer precipitation data are in pink and winter precipitation data are in teal. Precipitation data from spring or fall, or from tropical regions with no clear seasonal climate patterns, are in gray. New surface water data (red from summer, blue from winter) reported in this study are outlined in black. The dotted lines show regression lines through summer (red and pink) and winter (blue and teal) datasets. Panels A-C show all the available data points (published studies and this study); panels D-F only show data points with positive d-excess and positive $\Delta'^{17}O$ values. In each panel, new data reported in this study are shown with solid symbols and previously published data are shown with open symbols. Published precipitation data are from Affolter et al. (2015), Beverly et al. (2021), Gázquez et al. (2017), Gimenez et al. (2021), He et al. (2021) Landais et al. (2010), Luz and Barkan (2010), Surma et al. (2018), Tian et al. (2019), Tian et al. (2021), and Uechi and Uemura (2019). Published river or stream data are from Affolter et al. (2015), Aron et al. (2021a), Bergel et al. (2020), Bershaw et al. (2020), Beverly et al. (2021), Luz and Barkan (2010), Nava-Fernandez et al. (2020), Passey and Ji (2019), Surma et al. (2015), and Voigt et al. (2021). Published tap water are from Aron et al. (2021a), Li et al. (2015), Li et al. (2017), Luz and Barkan (2010), and Tian et al. (2019). Published lake data are from Aron et al. (2021a), Bershaw et al. (2020), Beverly et al. (2021), Li et al. (2017), Luz and Barkan (2010), Passey and Ji (2019), Surma et al. (2015), Surma et al. (2018), and Voigt et al. (2021).

Figure 5. Scatterplots of summer (red) and winter (blue) precipitation $\Delta'^{17}O$ vs. elevation (A), latitude (B), longitude (C), precipitation amount (D), local average weekly temperature (E), and local average weekly relative humidity (F). The dotted lines show linear regression lines between $\Delta'^{17}O$ and each x-axis variable for summer (red) and winter (blue) data.

Figure 6. Box plots of summer (red) and winter (blue) precipitation $\delta^{18}O$ (A), $\Delta'^{17}O$ (B), and d-excess (C). Sites are listed longitudinally with western-most sites (Washington and Oregon) on the left and the eastern-most site (North Carolina) on the right. The evaporated precipitation samples are excluded from this figure to highlight seasonal variation and reduce the isotopic ranges. A version of this figure that includes all the precipitation data is included in the Supplement (Figure S6).

Figure 7. Scatterplots of theoretical $\delta^{18}O$ (A), d-excess (B), and $\Delta'^{17}O$ (C) undergoing rainout Rayleigh Distillation (filled circles) and pan evaporation (filled squares) in winter (blue) and summer (red) seasons. Initial temperature and relative humidity were 7˚C and 83% in the winter and 17˚C and 65% in the summer. The pale symbols show observed summer (red) and winter (blue) precipitation data reported in this study. The observed data are plotted versus longitude, with the western-most sites on the left corresponding to coastal airmasses that have not lost much moisture and the eastern-most sites on the right corresponding to airmasses that have lost much of their moisture. Observations are included in these plots to help contextualize the outputs from these simple modeling exercises in general terms; they are not intended for direct comparison.

| Site | Site ID | Sample ID | Latitude | Longitude | Elevation (m) | Sample Type | Collection Date | Season | Quarter | Preciptation Amount (mm) | Local Average Weekly Temperature (C) | Local Average Weekly Relative Humidity (%) | $\delta^{18}O$ (‰) | $\delta^{2}H$ (‰) | d-excess (‰) | $\delta^{18}O$ and δ2H Reference | Average $\delta'^{18}O$ (‰, VSMOW-SLAP) | Average $\delta'^{17}O$ (‰, VSMOW-SLAP) | Average $\Delta'^{17}O$ (per meg) | $\Delta'^{17}O$ Std. Dev. (per meg) | n (triple oxygen analyses) | Notes |
|---|---|---|---|---|---|---|---|---|---|---|---|---|---|---|---|---|---|---|---|---|---|---|
| Yosemite National Park-Hodgdon Meadow | CA99 | NQ8115 | 37.8 | -119.9 | 1393 | Precipitation | 29-07-1997 | Summer | JJA | 5.08 | | | -5.3 | -31.3 | 11.1 | Welker, 2012 | -4.487 | -2.356 | 13 | | 1 | |
| Niwot Saddle | CO02 | NQ9129 | 40.1 | -105.6 | 3520 | Precipitation | 02-09-1997 | Fall | SON | 10.92 | | | -9 | -63 | 9 | Welker, 2012 | -4.813 | -2.519 | 22 | 13 | 2 | Outlier |
| Niwot Saddle | CO02 | 5-70-CO02-17JAN06 | 40.06 | -105.59 | 3520 | Precipitation | 10-01-2006 | Winter | DJF | 113.792 | -8.5 | 70.8 | -19.2 | -135.5 | 18.1 | Welker, 2012 | -19.454 | -10.245 | 27 | | 1 | |
| Niwot Saddle | CO02 | 5-52-CO02-17JAN06 | 40.06 | -105.59 | 3520 | Precipitation | 24-01-2006 | Winter | DJF | 17.018 | -11.4 | 80.5 | -21.7 | -159.4 | 14.2 | Welker, 2012 | -22.369 | -11.774 | 36 | | 1 | |
| Niwot Saddle | CO02 | 5-65-CO02-4JUL06 | 40.06 | -105.59 | 3520 | Precipitation | 11-07-2006 | Summer | JJA | 124.968 | 8.3 | 84.2 | -9.9 | -61.3 | 17.9 | Welker, 2012 | -9.969 | -5.226 | 38 | 10 | 2 | |
| Niwot Saddle | CO02 | 5-61-CO02-11JUL06 | 40.06 | -105.59 | 3520 | Precipitation | 18-07-2006 | Summer | JJA | 4.826 | 13.3 | 45.2 | -3.6 | -20.4 | 8.4 | Welker, 2012 | -3.860 | -2.020 | 18 | 5 | 3 | |
| Sand Spring | CO15 | 5-53-CO15-17JAN06 | 40.51 | -107.7 | 1998 | Precipitation | 24-01-2006 | Winter | DJF | 4.064 | -8.3 | 81.0 | -21.9 | -164.3 | 10.9 | Welker, 2012 | -22.162 | -11.663 | 39 | | 1 | |
| Sand Spring | CO15 | 5-64-CO15-28FEB06 | 40.51 | -107.7 | 1998 | Precipitation | 07-03-2006 | Spring | MAM | | 1.5 | 64.9 | | | | Welker, 2012 | -14.581 | -7.685 | 14 | | 1 | |
| Sand Spring | CO15 | 5-85-CO15-16MAY06 | 40.51 | -107.7 | 1998 | Precipitation | 23-05-2006 | Spring | MAM | 4.064 | 16.3 | 44.1 | -3.4 | -13.4 | 13.8 | Welker, 2012 | -4.015 | -2.118 | 2 | | 1 | |
| Sand Spring | CO15 | 5-63-CO15-5JUL06 | 40.51 | -107.7 | 1998 | Precipitation | 11-07-2006 | Summer | JJA | 8.382 | 18.5 | 66.5 | -3.9 | -30.6 | 0.6 | Welker, 2012 | -3.745 | -1.977 | 1 | | 1 | |
| Sand Spring | CO15 | 5-71-CO15-11JUL06 | 40.51 | -107.7 | 1998 | Precipitation | 20-07-2006 | Summer | JJA | 3.556 | 21.4 | 41.1 | -0.7 | 2.1 | 7.7 | Welker, 2012 | -1.721 | -0.908 | 1 | 13 | 2 | |
| Corvallis | Corvallis | NSW09-0020 | 44.5667 | -123.2833 | 95 | Precipitation | 17-02-2009 | Winter | DJF | 21.679 | 3.3 | 86.7 | -12.2 | -88.3 | 9.3 | Brooks et al., 2012 | -12.274 | -6.437 | 43 | | 1 | |
| Corvallis | Corvallis | NSW09-0074 | 44.5667 | -123.2833 | 95 | Precipitation | 09-03-2009 | Spring | MAM | 33.934 | 5.6 | 84.1 | -7.6 | -48.2 | 12.6 | Brooks et al., 2012 | -7.700 | -4.028 | 37 | | 1 | |
| Corvallis | Corvallis | NSW09-0103 | 44.5667 | -123.2833 | 95 | Precipitation | 30-03-2009 | Spring | MAM | 9.424 | 7.5 | 80.3 | -6 | -51.8 | -3.8 | Brooks et al., 2012 | -7.483 | -3.912 | 39 | | 1 | |
| Corvallis | Corvallis | NSW09-0115 | 44.5667 | -123.2833 | 95 | Precipitation | 20-04-2009 | Spring | MAM | 6.715 | 8.6 | 76.0 | -5.2 | -33.5 | 8.1 | Brooks et al., 2012 | -5.416 | -2.828 | 32 | | 1 | |
| Corvallis | Corvallis | NSW09-0147 | 44.5667 | -123.2833 | 95 | Precipitation | 11-05-2009 | Spring | MAM | 48.124 | 11.5 | 76.0 | -9.3 | -70.5 | 3.9 | Brooks et al., 2012 | -9.621 | -5.056 | 24 | | 1 | |
| Corvallis | Corvallis | NSW09-0198 | 44.5667 | -123.2833 | 95 | Precipitation | 15-06-2009 | Summer | JJA | 3.619 | 16.0 | 73.2 | -7.3 | -55.1 | 3.3 | Brooks et al., 2012 | -7.675 | -4.023 | 30 | | 1 | |
| Corvallis | Corvallis | NSW09-0199 | 44.5667 | -123.2833 | 95 | Precipitation | 13-07-2009 | Summer | JJA | 24.259 | 16.9 | 67.2 | -9.8 | -71.2 | 7.2 | Brooks et al., 2012 | -9.541 | -5.021 | 16 | 6 | 2 | |
| Corvallis | Corvallis | NSW09-0304 | 44.5667 | -123.2833 | 95 | Precipitation | 08-09-2009 | Fall | SON | 16.519 | 17.3 | 66.1 | -5 | -31.8 | 8.2 | Brooks et al., 2012 | -5.290 | -2.775 | 18 | | 1 | |
| Corvallis | Corvallis | NSW09-0330 | 44.5667 | -123.2833 | 95 | Precipitation | 05-10-2009 | Fall | SON | 2.587 | 11.7 | 71.5 | -2.2 | -15.7 | 1.9 | Brooks et al., 2012 | -2.159 | -1.132 | 8 | 2 | 2 | |
| Corvallis | Corvallis | NSW09-0379 | 44.5667 | -123.2833 | 95 | Precipitation | 26-10-2009 | Fall | SON | 17.035 | 12.8 | 78.4 | -4.2 | -25.3 | 8.3 | Brooks et al., 2012 | -4.522 | -2.362 | 26 | | 1 | |
| Corvallis | Corvallis | NSW09-0387 | 44.5667 | -123.2833 | 95 | Precipitation | 16-11-2009 | Fall | SON | 35.224 | 8.8 | 76.9 | -7.7 | -46.6 | 15 | Brooks et al., 2012 | -6.738 | -3.535 | 22 | | 1 | |
| Corvallis | Corvallis | NSW09-0390 | 44.5667 | -123.2833 | 95 | Precipitation | 14-12-2009 | Winter | DJF | 4.909 | | | -12.3 | -88.2 | 10.2 | Brooks et al., 2012 | -12.263 | -6.446 | 29 | | 1 | |
| Corvallis | Corvallis | NSW10-0017 | 44.5667 | -123.2833 | 95 | Precipitation | 25-01-2010 | Winter | DJF | 19.744 | 7.8 | 74.1 | -10.4 | -79.7 | 3.5 | Brooks et al., 2012 | -11.138 | -5.844 | 37 | 0 | 2 | |
| Corvallis | Corvallis | NSW10-0023 | 44.5667 | -123.2833 | 95 | Precipitation | 16-02-2010 | Winter | DJF | 35.869 | 9.2 | 79.1 | -7.7 | -57.1 | 4.5 | Brooks et al., 2012 | -8.917 | -4.679 | 29 | 4 | 2 | |
| Corvallis | Corvallis | NSW10-0024 | 44.5667 | -123.2833 | 95 | Precipitation | 08-03-2010 | Spring | MAM | 1.684 | 9.7 | 73.6 | -7.2 | -58 | -0.4 | Brooks et al., 2012 | -7.377 | -3.879 | 16 | | 1 | |
| Corvallis | Corvallis | NSW10-0031 | 44.5667 | -123.2833 | 95 | Precipitation | 19-04-2010 | Spring | MAM | 1.7 | 12.2 | 66.5 | -5.3 | -44.3 | -1.9 | Brooks et al., 2012 | -5.789 | -3.023 | 34 | | 1 | |
| Corvallis | Corvallis | NSW10-0126 | 44.5667 | -123.2833 | 95 | Precipitation | 10-05-2010 | Spring | MAM | 13.294 | 10.7 | 64.6 | -5.7 | -38.1 | 7.5 | Brooks et al., 2012 | -5.793 | -3.045 | 14 | 17 | 3 | |
| Corvallis | Corvallis | NSW10-0156 | 44.5667 | -123.2833 | 95 | Precipitation | 01-06-2010 | Summer | JJA | 16.519 | 13.7 | 69.6 | -8.7 | -68.5 | 1.1 | Brooks et al., 2012 | -8.434 | -4.436 | 17 | | 1 | |
| Corvallis | Corvallis | NSW10-0255 | 44.5667 | -123.2833 | 95 | Precipitation | 30-08-2010 | Summer | JJA | 15.229 | 18.9 | 51.3 | -11.1 | -82.8 | 6 | Brooks et al., 2012 | -11.155 | -5.856 | 34 | 8 | 2 | |
| Corvallis | Corvallis | NSW10-0257 | 44.5667 | -123.2833 | 95 | Precipitation | 20-09-2010 | Fall | SON | 37.933 | 17.7 | 76.4 | -9.5 | -71.8 | 4.2 | Brooks et al., 2012 | -9.301 | -4.894 | 17 | | 1 | |
| Corvallis | Corvallis | NSW10-0401 | 44.5667 | -123.2833 | 95 | Precipitation | 12-10-2010 | Fall | SON | 31.999 | 14.5 | 71.6 | -5.2 | -37.6 | 4 | Brooks et al., 2012 | -4.896 | -2.549 | 36 | | 1 | |
| Corvallis | Corvallis | NSW10-0426 | 44.5667 | -123.2833 | 95 | Precipitation | 01-11-2010 | Fall | SON | 48.124 | 9.5 | 84.9 | -7.9 | -50.8 | 12.4 | Brooks et al., 2012 | -8.047 | -4.217 | 32 | | 1 | |
| Corvallis | Corvallis | NSW10-0482 | 44.5667 | -123.2833 | 95 | Precipitation | 22-11-2010 | Fall | SON | 82.954 | 7.9 | 81.3 | -9.8 | -61.5 | 16.9 | Brooks et al., 2012 | -9.970 | -5.231 | 33 | | 1 | |
| Corvallis | Corvallis | NSW10-0485 | 44.5667 | -123.2833 | 95 | Precipitation | 13-12-2010 | Winter | DJF | 137.78 | 9.0 | 86.1 | -5.8 | -38.4 | 8 | Brooks et al., 2012 | -6.942 | -3.634 | 31 | | 1 | |
| Craters of the Moon National Monument | ID03 | 1-37-ID03-24JAN06 | 43.46 | -113.55 | 1807 | Precipitation | 31-01-2006 | Winter | DJF | 10.668 | -6.8 | 84.9 | -13.7 | -102.5 | 7.1 | Welker, 2012 | -14.611 | -7.656 | 58 | | 1 | |
| Craters of the Moon National Monument | ID03 | 2-28-ID03-31JAN06 | 43.46 | -113.55 | 1807 | Precipitation | 07-02-2006 | Winter | DJF | 3.81 | -5.7 | 82.9 | -12.9 | -94.6 | 8.6 | Welker, 2012 | -13.613 | -7.135 | 52 | | 1 | |
| Craters of the Moon National Monument | ID03 | 1-3-ID03-27JUL06 | 43.46 | -113.55 | 1807 | Precipitation | 05-07-2006 | Summer | JJA | 3.81 | 18.1 | 46.2 | 0.5 | -4.6 | -8.6 | Welker, 2012 | 0.314 | 0.146 | -19 | 2 | 2 | Evaporated summer rain |
| Craters of the Moon National Monument | ID03 | 2-73-ID03-18JUL06 | 43.46 | -113.55 | 1807 | Precipitation | 25-07-2006 | Summer | JJA | 3.048 | 21.8 | 37.4 | -6.7 | -51.7 | 1.9 | Welker, 2012 | -6.542 | -3.444 | 10 | | 1 | |
| Smith's Ferry | ID15 | 1-38-ID15-24JAN06 | 44.3 | -116.06 | 1442 | Precipitation | 31-01-2006 | Winter | DJF | 24.13 | -5.6 | 86.3 | -17.5 | -131.6 | 8.4 | Welker, 2012 | -18.096 | -9.528 | 26 | | 1 | |
| Smith's Ferry | ID15 | 1-22-ID15-31JAN06 | 44.3 | -116.06 | 1442 | Precipitation | 07-02-2006 | Winter | DJF | | -4.6 | 86.4 | -15.8 | -119.4 | 7 | Welker, 2012 | -16.849 | -8.886 | 10 | | 1 | |
| Smith's Ferry | ID15 | 2-76-ID15-6JUN06 | 44.3 | -116.06 | 1442 | Precipitation | 13-06-2006 | Summer | JJA | 7.62 | 12.4 | 75.9 | 0.5 | -33.7 | -37.7 | Welker, 2012 | -0.694 | -0.392 | -25 | 4 | 2 | Evaporated summer rain |
| Smith's Ferry | ID15 | 1-19-ID15-13JUN06 | 44.3 | -116.06 | 1442 | Precipitation | 20-06-2006 | Summer | JJA | 11.43 | 10.0 | 80.1 | 3.4 | -32 | -59.2 | Welker, 2012 | 3.039 | 1.563 | -42 | 1 | 2 | Evaporated summer rain |
| Konza Prairie | KS31 | NQ9015 | 39.1 | -96.6 | 350 | Precipitation | 02-09-1997 | Fall | SON | 6.6 | | | 0.8 | 10.1 | 3.7 | Welker, 2012 | 0.617 | 0.332 | 6 | 12 | 3 | |
| Lake Scott State Park | KS32 | 5-36-KS32-3JAN06 | 38.67 | -100.92 | 863 | Precipitation | 10-01-2006 | Winter | DJF | 3.302 | 5.5 | 51.8 | | | | Welker, 2012 | -19.432 | -10.212 | 48 | | 1 | |
| Lake Scott State Park | KS32 | 5-32-KS32-17JAN06 | 38.67 | -100.92 | 863 | Precipitation | 24-01-2006 | Winter | DJF | 3.81 | 1.3 | 59.9 | -19.1 | -141.7 | 11.1 | Welker, 2012 | -20.003 | -10.504 | 58 | | 1 | |
| Lake Scott State Park | KS32 | 5-40-KS32-27JUN06 | 38.67 | -100.92 | 863 | Precipitation | 04-07-2006 | Summer | JJA | 2.032 | 26.4 | 39.8 | -0.2 | -7.1 | -5.5 | Welker, 2012 | -0.425 | -0.232 | -7 | 0 | 2 | Evaporated summer rain |
| Lake Scott State Park | KS32 | 4-100-KS32-4JUL06 | 38.67 | -100.92 | 863 | Precipitation | 11-07-2006 | Summer | JJA | 13.208 | 23.5 | 68.7 | -6.3 | -38.4 | 12 | Welker, 2012 | -7.520 | -3.941 | 29 | | 1 | |
| Lake Scott State Park | KS32 | 5-25-KS32-11JUL06 | 38.67 | -100.92 | 863 | Precipitation | 18-07-2006 | Summer | JJA | 17.78 | 28.2 | 49.6 | -8 | -51.8 | 12.2 | Welker, 2012 | -8.631 | -4.539 | 18 | | 1 | |
| Little Bighorn Battlefield National Monumen | MT00 | 4-34-MT00-3JAN06 | 45.57 | -107.44 | 957 | Precipitation | 10-01-2006 | Winter | DJF | 5.588 | 3.0 | 62.0 | -20.4 | -149.5 | 13.7 | Welker, 2012 | -21.313 | -11.196 | 58 | 1 | 2 | |
| Little Bighorn Battlefield National Monumen | MT00 | 3-79-MT00-7FEB06 | 45.57 | -107.44 | 957 | Precipitation | 15-02-2006 | Winter | DJF | 7.366 | 0.8 | 51.5 | | | | Welker, 2012 | -16.987 | -8.908 | 62 | | 1 | |
| Little Bighorn Battlefield National Monumen | MT00 | 3-90-MT00-27JUL06 | 45.57 | -107.44 | 957 | Precipitation | 05-07-2006 | Summer | JJA | 3.048 | 23.2 | 45.8 | -2.1 | -24.4 | -7.6 | Welker, 2012 | -2.389 | -1.275 | -13 | | 1 | Evaporated summer rain |
| Little Bighorn Battlefield National Monumen | MT00 | 3-87-MT00-11JUL06 | 45.57 | -107.44 | 957 | Precipitation | 18-07-2006 | Summer | JJA | 4.064 | 26.9 | 28.7 | -1.7 | -15.3 | -1.7 | Welker, 2012 | -2.124 | -1.127 | -6 | 15 | 2 | Evaporated summer rain |
| Glacier National Park - Fire Weather Station | MT05 | 4-61-MT05-17JAN06 | 48.51 | -113.99 | 968 | Precipitation | 24-01-2006 | Winter | DJF | 22.606 | -0.7 | 62.0 | -18.5 | -136.9 | 11.1 | Welker, 2012 | -20.236 | -10.636 | 48 | | 1 | |
| Glacier National Park - Fire Weather Station | MT05 | 4-78-MT05-24JAN06 | 48.51 | -113.99 | 968 | Precipitation | 31-01-2006 | Winter | DJF | 23.37 | 1.9 | 52.0 | -18.7 | -142.9 | 6.7 | Welker, 2012 | -19.549 | -10.285 | 37 | | 1 | |
| Glacier National Park - Fire Weather Station | MT05 | 3-74-MT05-04JUL06 | 48.51 | -113.99 | 968 | Precipitation | 11-07-2006 | Summer | JJA | 17.78 | 20.8 | 49.5 | -8.3 | -62.2 | 4.2 | Welker, 2012 | -8.607 | -4.538 | 7 | 3 | 2 | |
| Glacier National Park - Fire Weather Station | MT05 | 3-35-MT05-8AUG06 | 48.51 | -113.99 | 968 | Precipitation | 15-08-2006 | Summer | JJA | 9.906 | 18.7 | 48.0 | -13.6 | -103.9 | 4.9 | Welker, 2012 | -13.643 | -7.198 | 6 | | 1 | |
| Lost Trail Pass | MT97 | 4-75-MT97-17JAN06 | 45.69 | -113.97 | 2414 | Precipitation | 24-01-2006 | Winter | DJF | 39.624 | -4.7 | 76.9 | -23.3 | -174.3 | 12.1 | Welker, 2012 | -23.965 | -12.602 | 51 | | 1 | |
| Lost Trail Pass | MT97 | 4-86-MT97-24JAN06 | 45.69 | -113.97 | 2414 | Precipitation | 31-01-2006 | Winter | DJF | 56.13 | -6.5 | 80.0 | -20.62 | -152.58 | 12.38 | Welker, 2012 | -21.490 | -11.287 | 60 | | 1 | |
| Lost Trail Pass | MT97 | 3-75-MT97-27JUN06 | 45.69 | -113.97 | 2414 | Precipitation | 04-07-2006 | Summer | JJA | 7.62 | 20.4 | 55.4 | -5.9 | -43.2 | 4 | Welker, 2012 | -6.600 | -3.462 | 23 | 13 | 2 | |
| Lost Trail Pass | MT97 | 4-69-MT97-04JUL06 | 45.69 | -113.97 | 2414 | Precipitation | 11-07-2006 | Summer | JJA | 3.81 | 20.4 | 51.8 | -5 | -29.7 | 10.3 | Welker, 2012 | -5.246 | -2.766 | 4 | 1 | 2 | |
| Lost Trail Pass | MT97 | 3-80-MT97-11JUL06 | 45.69 | -113.97 | 2414 | Precipitation | 18-07-2006 | Summer | JJA | 7.112 | 22.3 | 40.1 | -8.4 | -61.3 | 5.9 | Welker, 2012 | -9.130 | -4.816 | 5 | 8 | 2 | |
| Clinton Crops Research Station | NC35 | NQ8889 | 35 | -78.3 | 41 | Precipitation | 26-08-1997 | Summer | JJA | 50.29 | | | -6.5 | -37.6 | 14.4 | Welker, 2012 | -6.702 | -3.506 | 32 | | 1 | |
| Clinton Crops Research Station | NC35 | NQ9136 | 35 | -78.3 | 41 | Precipitation | 02-09-1997 | Fall | SON | 20.07 | | | -3.5 | -14.9 | 13.1 | Welker, 2012 | -4.325 | -2.235 | 48 | 30 | 2 | |
| Icelandic State Park | ND08 | 6-69-ND08-17JAN06 | 48.78 | -97.75 | 306 | Precipitation | 24-01-2006 | Winter | DJF | 14.478 | -11.8 | 82.6 | -24.2 | -184.6 | 9 | Welker, 2012 | -24.948 | -13.113 | 60 | | 1 | |
| Icelandic State Park | ND08 | 6-54-ND08-24JAN06 | 48.78 | -97.75 | 306 | Precipitation | 31-01-2006 | Winter | DJF | 6.096 | -4.0 | 86.8 | -18.3 | -133.3 | 13.1 | Welker, 2012 | -18.964 | -9.968 | 45 | | 1 | |
| Icelandic State Park | ND08 | 6-4-ND08-4JUL06 | 48.78 | -97.75 | 306 | Precipitation | 11-07-2006 | Summer | JJA | 8.382 | 20.7 | 68.8 | -10 | -71.5 | 8.5 | Welker, 2012 | -10.312 | -5.429 | 16 | | 1 | |
| Icelandic State Park | ND08 | 6-38-ND08-11JUL06 | 48.78 | -97.75 | 306 | Precipitation | 18-07-2006 | Summer | JJA | 6.35 | 24.8 | 65.7 | -4.6 | -38.9 | -2.1 | Welker, 2012 | -5.019 | -2.657 | -7 | | 1 | Evaporated summer rain |
| North Platte Agricultural Experimental Static | NE99 | 5-13-NE99-6JUN06 | 41.06 | -100.75 | 919 | Precipitation | 13-06-2006 | Summer | JJA | 28.448 | 22.3 | 61.8 | -7 | -45.9 | 10.1 | Welker, 2012 | -7.067 | -3.736 | -5 | | 1 | |
| North Platte Agricultural Experimental Static | NE99 | 5-23-NE99-13JUL06 | 41.06 | -100.75 | 919 | Precipitation | 20-06-2006 | Summer | JJA | 72.39 | 22.1 | 69.4 | -6 | -32.4 | 15.6 | Welker, 2012 | -6.127 | -3.210 | 25 | | 1 | |
| North Platte Agricultural Experimental Static | NE99 | 5-31-NE99-20JUN06 | 41.06 | -100.75 | 919 | Precipitation | 27-06-2006 | Summer | JJA | 18.228 | 20.4 | 65.0 | -7.8 | -52.8 | 9.6 | Welker, 2012 | -7.161 | -3.774 | 7 | | 1 | |
| North Platte Agricultural Experimental Static | NE99 | 5-21-NE99-4JUL06 | 41.06 | -100.75 | 919 | Precipitation | 11-07-2006 | Summer | JJA | 37.084 | 22.0 | 70.5 | -6.1 | -35.8 | 13 | Welker, 2012 | -6.400 | -3.354 | 25 | | 1 | |
| North Platte Agricultural Experimental Static | NE99 | 5-18-NE99-18JUL06 | 41.06 | -100.75 | 919 | Precipitation | 25-07-2006 | Summer | JJA | 2.286 | 24.6 | 61.2 | -1.7 | 0.4 | 14 | Welker, 2012 | -2.247 | -1.168 | 19 | | 1 | |
| North Platte Agricultural Experimental Static | NE99 | 5-24-NE99-25JUL06 | 41.06 | -100.75 | 919 | Precipitation | 01-08-2006 | Summer | JJA | 8.636 | 27.8 | 54.5 | -5.3 | -40.2 | 2.2 | Welker, 2012 | -5.883 | -3.089 | 18 | | 1 | |
| North Platte Agricultural Experimental Static | NE99 | 5-6-NE99-3OCT06 | 41.06 | -100.75 | 919 | Precipitation | 10-10-2006 | Fall | SON | 22.606 | 13.4 | 70.1 | -11.4 | -74.9 | 16.3 | Welker, 2012 | -11.342 | -5.977 | 11 | | 1 | |
| North Platte Agricultural Experimental Static | NE99 | 5-8-NE99-19DEC06 | 41.06 | -100.75 | 919 | Precipitation | 26-12-2006 | Winter | DJF | 50.292 | -3.0 | 83.9 | -13.7 | -99.6 | 10 | Welker, 2012 | -14.218 | -7.451 | 56 | 17 | 2 | |
| Kessler Farm Field Laboratory | OK17 | NQ7942 | 35 | -97.5 | 331 | Precipitation | 22-07-1997 | Summer | JJA | 4.06 | | | 0.6 | 12.3 | 7.5 | Welker, 2012 | 0.491 | 0.255 | -4 | 2 | 2 | |
| Alsea Guard Ranger Station | OR02 | NQ7169 | 44.4 | -123.6 | 104 | Precipitation | 01-07-1997 | Summer | JJA | 4.32 | | | -6.4 | -54.2 | -3 | Welker, 2012 | -7.155 | -3.764 | 13 | | 1 | |
| Alsea Guard Ranger Station | OR02 | NQ7613 | 44.4 | -123.6 | 104 | Precipitation | 15-07-1997 | Summer | JJA | 10.16 | | | -5.9 | -41.4 | 5.8 | Welker, 2012 | -6.578 | -3.460 | 13 | | 1 | |
| Alsea Guard Ranger Station | OR02 | NQ8815 | 44.4 | -123.6 | 104 | Precipitation | 26-08-1997 | Summer | JJA | 26.16 | | | -7.1 | -52.2 | 4.6 | Welker, 2012 | **-7.715** | **-4.033** | 40 | 9 | 3 | |
| Alsea Guard Ranger Station | OR02 | NQ9002 | 44.4 | -123.6 | 104 | Precipitation | 02-09-1997 | Fall | SON | 3.05 | | | -3.9 | -28.8 | 2.4 | Welker, 2012 | -4.512 | -2.382 | 0 | | 1 | |
| Alsea Guard Ranger Station | OR02 | 1-35-OR02-17JAN06 | 44.39 | -123.62 | 104 | Precipitation | 24-01-2006 | Winter | DJF | 65.786 | 8.1 | 80.0 | -10.6 | -75.4 | 9.4 | Welker, 2012 | -11.431 | -5.989 | 47 | | 1 | |
| Alsea Guard Ranger Station | OR02 | 1-33-OR02-24JAN06 | 44.39 | -123.62 | 104 | Precipitation | 31-01-2006 | Winter | DJF | 134.874 | 7.5 | 79.9 | -9.4 | -64.5 | 10.7 | Welker, 2012 | -10.041 | -5.238 | 64 | | 1 | |
| Alsea Guard Ranger Station | OR02 | 1-1-OR02-13JUN06 | 44.39 | -123.62 | 104 | Precipitation | 20-06-2006 | Summer | JJA | 6.604 | 17.6 | 61.0 | -5.2 | -38.3 | 3.3 | Welker, 2012 | -5.585 | -2.945 | 4 | | 1 | |
| Alsea Guard Ranger Station | OR02 | 2-90-OR02-11JUL06 | 44.39 | -123.62 | 104 | Precipitation | 18-07-2006 | Summer | JJA | 3.81 | 19.8 | 59.1 | -5.7 | -40.1 | 5.5 | Welker, 2012 | -6.120 | -3.214 | 17 | | 1 | |
| H.J. Andrews Experimental Forest | OR10 | NQ7295 | 44.2 | -122.3 | 443 | Precipitation | 01-07-1997 | Summer | JJA | 38.1 | | | -12.1 | -91.3 | 5.5 | Welker, 2012 | -12.146 | -6.403 | 10 | | 1 | |
| H.J. Andrews Experimental Forest | OR10 | NQ7749 | 44.2 | -122.3 | 443 | Precipitation | 15-07-1997 | Summer | JJA | 15.49 | | | -6.5 | -47.5 | 4.5 | Welker, 2012 | -7.251 | -3.802 | 27 | | 1 | |
| H.J. Andrews Experimental Forest | OR10 | NQ8966 | 44.2 | -122.3 | 443 | Precipitation | 26-08-1997 | Summer | JJA | 27.94 | | | -7.7 | -53.9 | 7.7 | Welker, 2012 | -9.586 | -5.037 | 24 | | 1 | |
| H.J. Andrews Experimental Forest | OR10 | 1-46-OR10-17JAN06 | 44.21 | -122.25 | 436 | Precipitation | 24-01-2006 | Winter | DJF | 93.98 | 8.1 | 80.0 | -14.9 | -107.7 | 11.5 | Welker, 2012 | -15.564 | -8.175 | 43 | | 1 | |
| H.J. Andrews Experimental Forest | OR10 | 1-40-OR10-24JAN06 | 44.21 | -122.25 | 436 | Precipitation | 31-01-2006 | Winter | DJF | 151.13 | 7.5 | 79.9 | -11.5 | -82.3 | 9.7 | Welker, 2012 | -12.322 | -6.453 | 53 | | 1 | |
| H.J. Andrews Experimental Forest | OR10 | 1-6-OR10-13JUN06 | 44.21 | -122.25 | 436 | Precipitation | 20-06-2006 | Summer | JJA | 6.096 | 17.6 | 61.0 | -5.9 | -46.4 | 0.8 | Welker, 2012 | -6.514 | -3.434 | 5 | | 1 | |
| H.J. Andrews Experimental Forest | OR10 | 1-18-OR10-27JUL06 | 44.21 | -122.25 | 436 | Precipitation | 05-07-2006 | Summer | JJA | 25.146 | 21.2 | 52.2 | -5.2 | -36.5 | 5.1 | Welker, 2012 | -5.839 | -3.064 | 19 | 1 | 2 | |
| H.J. Andrews Experimental Forest | OR10 | 2-68-OR10-1AUG06 | 44.21 | -122.25 | 436 | Precipitation | 08-08-2006 | Summer | JJA | 4.318 | 20.8 | 51.2 | -6.7 | -54 | -0.4 | Welker, 2012 | -7.326 | -3.839 | 30 | | 1 | |
| Starkey Experimental Forest | OR18 | 1-23-OR18-17JAN06 | 45.22 | -118.51 | 1253 | Precipitation | 24-01-2006 | Winter | DJF | 12.19 | -0.5 | 99.2 | -19.7 | -150.5 | 7.1 | Welker, 2012 | -20.306 | -10.651 | 71 | 9 | 2 | |
| Starkey Experimental Forest | OR18 | 1-47-OR18-24JAN06 | 45.22 | -118.51 | 1253 | Precipitation | 31-01-2006 | Winter | DJF | 11.176 | 0.6 | 85.4 | -21.1 | -162 | 6.8 | Welker, 2012 | -21.684 | -11.411 | 38 | | 1 | |
| Starkey Experimental Forest | OR18 | 1-15-OR18-27JUN06 | 45.22 | -118.51 | 1253 | Precipitation | 05-07-2006 | Summer | JJA | 8.382 | 23.6 | 48.5 | -4 | -34.5 | -2.5 | Welker, 2012 | -4.168 | -2.198 | 3 | | 1 | |
| Starkey Experimental Forest | OR18 | 1-7-OR18-5JUL06 | 45.22 | -118.51 | 1253 | Precipitation | 11-07-2006 | Summer | JJA | 15.24 | 21.3 | 50.9 | -8.2 | -58 | 7.6 | Welker, 2012 | -7.947 | -4.181 | 15 | | 1 | |
| Cottonwood | SD08 | 6-68-SD08-27JUN06 | 43.95 | -101.86 | 733 | Precipitation | 04-07-2006 | Summer | JJA | 9.398 | 25.8 | 42.9 | -5.6 | -42.7 | 2.1 | Welker, 2012 | -5.650 | -2.994 | -11 | | 1 | |
| Cottonwood | SD08 | 6-44-SD08-18JUL06 | 43.95 | -101.86 | 733 | Precipitation | 25-07-2006 | Summer | JJA | 8.382 | 26.1 | 44.3 | -3.2 | -31.9 | -6.3 | Welker, 2012 | -3.118 | -1.663 | -16 | | 1 | Evaporated summer rain |
| Cottonwood | SD08 | 6-49-SD08-21NOV06 | 43.95 | -101.86 | 733 | Precipitation | 14-11-2006 | Fall | SON | 7.874 | 4.6 | 71.5 | -18.6 | -135.6 | 13.2 | Welker, 2012 | -18.553 | -9.761 | 35 | | 1 | |
| Cottonwood | SD08 | 6-15-SD08-21NOV06 | 43.95 | -101.86 | 733 | Precipitation | 28-11-2006 | Fall | SON | 8.89 | 2.1 | 58.4 | -16.3 | -116.4 | 14 | Welker, 2012 | -15.899 | -8.342 | 53 | | 1 | |
| Huron Well Field | SD99 | NQ9001 | 44.4 | -98.3 | 398 | Precipitation | 02-09-1997 | Fall | SON | 2.54 | | | -0.8 | 4.4 | 10.8 | Welker, 2012 | -1.069 | -0.565 | 0 | 5 | 2 | |
| Huron Well Field | SD99 | 6-26-SD99-11JUL06 | 44.36 | -98.29 | 398 | Precipitation | 18-07-2006 | Summer | JJA | 9.906 | 26.9 | 53.6 | 3.2 | 8.2 | -17.4 | Welker, 2012 | 2.334 | 1.193 | -40 | 14 | 3 | Evaporated summer rain |
| Huron Well Field | SD99 | 6-22-SD99-18JUL06 | 44.36 | -98.29 | 398 | Precipitation | 25-07-2006 | Summer | JJA | 3.81 | 24.4 | 54.7 | -3.8 | -34.9 | -4.5 | Welker, 2012 | -3.867 | -2.052 | -10 | | 1 | Evaporated summer rain |
| Huron Well Field | SD99 | 6-30-SD99-25JUL06 | 44.36 | -98.29 | 398 | Precipitation | 01-08-2006 | Summer | JJA | 18.542 | 28.1 | 61.0 | 4.5 | -8 | -44 | Welker, 2012 | 4.205 | 2.166 | -54 | 6 | 2 | Evaporated summer rain |
| Huron Well Field | SD99 | 6-9-SD99-14NOV06 | 44.36 | -98.29 | 398 | Precipitation | 21-11-2006 | Fall | SON | 4.318 | -1.1 | 77.5 | -19.8 | -150.6 | 7.8 | Welker, 2012 | -20.248 | -10.660 | 31 | | 1 | |
| Huron Well Field | SD99 | 6-10-SD99-19DEC06 | 44.36 | -98.29 | 398 | Precipitation | 26-12-2006 | Winter | DJF | 4.064 | -1.7 | 75.3 | -18.1 | -142.7 | 2.1 | Welker, 2012 | -18.745 | -9.853 | 45 | | 1 | |
| Beeville | TX03 | NQ7917 | 28.5 | -97.7 | 82 | Precipitation | 22-07-1997 | Summer | JJA | 11.43 | | | -0.1 | 5.3 | 6.1 | Welker, 2012 | -0.183 | -0.101 | -4 | 5 | 2 | |
| Olympic National Park-Hoh Ranger Station | WA14 | NQ9171 | 47.9 | -123.9 | 182 | Precipitation | 02-09-1997 | Fall | SON | 41.91 | | | -3.9 | -25.5 | 5.7 | Welker, 2012 | -9.318 | -4.909 | 11 | 13 | 2 | Outlier |
| Olympic National Park - Hoh Ranger Station | WA14 | 1-36-WA14-23JAN06 | 47.86 | -123.92 | 176 | Precipitation | 23-01-2006 | Winter | DJF | 45.72 | 6.1 | 91.7 | -13.9 | -99.1 | 12.1 | Welker, 2012 | -14.007 | -7.388 | 8 | | 1 | |
| Olympic National Park - Hoh Ranger Station | WA14 | 1-21-WA14-23JAN06 | 47.86 | -123.92 | 176 | Precipitation | 28-01-2006 | Winter | DJF | 113.03 | 7.2 | 89.6 | -11.9 | -82.8 | 12.4 | Welker, 2012 | -12.475 | -6.557 | 30 | | 1 | |
| Olympic National Park - Hoh Ranger Station | WA14 | 3-12-WA14-11JUL06 | 47.86 | -123.92 | 176 | Precipitation | 18-07-2006 | Summer | JJA | 31.242 | 13.4 | 87.9 | -8 | -60.2 | 3.8 | Welker, 2012 | -8.206 | -4.314 | 19 | | 1 | |
| Olympic National Park - Hoh Ranger Station | WA14 | 2-89-WA14-25JUL06 | 47.86 | -123.92 | 176 | Precipitation | 01-08-2006 | Summer | JJA | 6.604 | 14.1 | 84.9 | -8.9 | -63.6 | 7.6 | Welker, 2012 | -8.614 | -4.534 | 15 | | 1 | |
| Palouse Conservation Farm | WA24 | 1-61-WA24-17JAN06 | 46.76 | -117.18 | 766 | Precipitation | 24-01-2006 | Winter | DJF | 20.828 | 2.8 | 80.3 | -17.6 | -131.3 | 9.5 | Welker, 2012 | -18.039 | -9.499 | 25 | | 1 | |
| Palouse Conservation Farm | WA24 | 1-31-WA24-24JAN06 | 46.76 | -117.18 | 766 | Precipitation | 31-01-2006 | Winter | DJF | 13.97 | 3.1 | 72.5 | -14 | -107.2 | 4.8 | Welker, 2012 | -14.311 | -7.529 | 27 | 33 | 2 | |
| Palouse Conservation Farm | WA24 | 1-20-WA24-13JUN06 | 46.76 | -117.18 | 766 | Precipitation | 20-06-2006 | Summer | JJA | 11.684 | 15.2 | 68.4 | -9 | -64.4 | 7.6 | Welker, 2012 | -8.575 | -4.513 | 15 | | 1 | |
| Palouse Conservation Farm | WA24 | 2-91-WA24-8AUG06 | 46.76 | -117.18 | 766 | Precipitation | 15-08-2006 | Summer | JJA | 3.302 | 19.3 | 47.1 | -5.4 | -55.4 | -12.2 | Welker, 2012 | -5.667 | -2.993 | -1 | | 1 | Evaporated summer rain |
| Pinedale | WY06 | NQ9057 | 42.9 | -109.8 | 2388 | Precipitation | 02-09-1997 | Fall | SON | | 15.1 | 46.2 | -5.5 | -41.1 | 2.9 | Welker, 2012 | -5.806 | -3.044 | 22 | 22 | 3 | |
| Pinedale | WY06 | 4-79-WY06-27DEC05 | 42.92 | -109.8 | 2388 | Precipitation | 10-01-2006 | Winter | DJF | | -5.8 | 82.3 | -20.9 | -161.7 | 5.5 | Welker, 2012 | -22.381 | -11.753 | 64 | | 1 | |
| Pinedale | WY06 | 3-62-WY06-31JAN06 | 42.92 | -109.8 | 2388 | Precipitation | 07-02-2006 | Winter | DJF | | -7.6 | 76.6 | -16.5 | -121.8 | 10.2 | Welker, 2012 | -17.373 | -9.121 | 52 | | 1 | |
| Pinedale | WY06 | 4-74-WY06-11JUL06 | 42.92 | -109.8 | 2388 | Precipitation | 18-07-2006 | Summer | JJA | 3.81 | 19.3 | 43.9 | -4.6 | -24.8 | 12 | Welker, 2012 | -5.143 | -2.700 | 16 | 1 | 2 | |
| Pinedale | WY06 | JHU-17O-1727 | 42.92 | -109.8 | 2388 | Precipitation | 01-08-2006 | Summer | JJA | 2.032 | 20.3 | 43.7 | -10.2 | -71.1 | 10.5 | Welker, 2012 | -10.471 | -5.530 | -2 | 11 | 2 | |

| | | | | | | | | | | | | | | | | | | | | | | |
|---|---|---|---|---|---|---|---|---|---|---|---|---|---|---|---|---|---|---|---|---|---|---|
| Brooklyn Lake | WY95 | NQ8961 | 41.4 | -106.2 | 3181 | Precipitation | 19-08-1997 | Summer | JJA | 23.62 | 15.8 | 55.8 | -9.1 | -58.9 | 13.9 | Welker, 2012 | -9.719 | -5.124 | 7 | 13 | 3 | |
| Brooklyn Lake | WY95 | NQ9119 | 41.4 | -106.2 | 3181 | Precipitation | 02-09-1997 | Fall | SON | 6.35 | 17.1 | 57.4 | -5 | -31.3 | 8.7 | Welker, 2012 | -5.311 | -2.798 | 7 | 7 | 3 | |
| Brooklyn Lake | WY95 | 4-76-WY95-17JAN06 | 41.36 | -106.24 | 3212 | Precipitation | 24-01-2006 | Winter | DJF | 26.924 | -7.1 | 66.3 | -19.7 | -143.4 | 14.2 | Welker, 2012 | -20.356 | -10.707 | 40 | | 1 | |
| Brooklyn Lake | WY95 | 4-56-WY95-24JAN06 | 41.36 | -106.24 | 3212 | Precipitation | 31-01-2006 | Winter | DJF | 63.5 | -4.1 | 54.7 | -19.9 | -145.6 | 13.6 | Welker, 2012 | -20.726 | -10.903 | 41 | | 1 | |
| Brooklyn Lake | WY95 | 3-88-WY95-27JUN06 | 41.36 | -106.24 | 3212 | Precipitation | 04-07-2006 | Summer | JJA | 11.176 | 18.6 | 41.0 | -5.8 | -37.4 | 9 | Welker, 2012 | -5.990 | -3.145 | 17 | | 1 | |
| Brooklyn Lake | WY95 | 4-94-WY95-4JUL06 | 41.36 | -106.24 | 3212 | Precipitation | 11-07-2006 | Summer | JJA | 54.61 | 15.5 | 70.6 | -9.6 | -59.9 | 16.9 | Welker, 2012 | -9.960 | -5.210 | 49 | 11 | 2 | |
| Brooklyn Lake | WY95 | 4-57-WY95-18JUL06 | 41.36 | -106.24 | 3212 | Precipitation | 25-07-2006 | Summer | JJA | 4.826 | 20.2 | 49.9 | -2.5 | -20.3 | -0.3 | Welker, 2012 | -2.673 | -1.418 | -6 | 4 | 2 | Evaporated summer rain |
| Newcastle | WY99 | 3-69-WY99-14FEB06 | 43.87 | -104.19 | 1466 | Precipitation | 21-02-2006 | Winter | DJF | 8.382 | -14.4 | 69.6 | -25.2 | -192.9 | 8.7 | Welker, 2012 | -25.927 | -13.661 | 28 | | 1 | |
| Newcastle | WY99 | 3-89-WY99-3JUL06 | 43.87 | -104.19 | 1466 | Precipitation | 11-07-2006 | Summer | JJA | 6.858 | 17.6 | 66.4 | -5.1 | -27.1 | 13.7 | Welker, 2012 | -5.074 | -2.661 | 18 | | 1 | |
| Newcastle | WY99 | 4-50-WY99-25JUL06 | 43.87 | -104.19 | 1466 | Precipitation | 01-08-2006 | Summer | JJA | 4.064 | 24.6 | 35.9 | -7.4 | -65.4 | -6.2 | Welker, 2012 | -7.551 | -3.983 | 5 | | 1 | |
| Newcastle | WY99 | 3-83-WY99-7NOV06 | 43.87 | -104.19 | 1466 | Precipitation | 14-11-2006 | Fall | SON | 17.272 | 0.7 | 69.8 | -17.7 | -129.6 | 12 | Welker, 2012 | -18.230 | -9.605 | 20 | | 1 | |
| Luckiamute | LK06 | DNSW09-0033 | 44.839 | -123.41 | 121 | River | 26-02-2009 | | | | | | -9 | -60.3 | 11.7 | Brooks et al., 2012 | -9.161 | -4.802 | 35 | | 1 | |
| Luckiamute | LK06 | DNSW09-0267 | 44.839 | -123.41 | 121 | River | 14-05-2009 | | | | | | -9.3 | -61.1 | 13.3 | Brooks et al., 2012 | -9.182 | -4.819 | 29 | 2 | 2 | |
| Luckiamute | LK06 | DNSW09-0488 | 44.839 | -123.41 | 121 | River | 13-10-2009 | | | | | | -9 | -60.8 | 11.2 | Brooks et al., 2012 | -8.942 | -4.697 | 25 | | 1 | |
| Luckiamute | LK06 | DNSW10-0074 | 44.83907 | -123.41 | 121 | River | 23-02-2010 | | | | | | -9.1 | -61.6 | 11.2 | Brooks et al., 2012 | -8.862 | -4.655 | 25 | | 1 | |
| Luckiamute | LK06 | DNSW10-0280 | 44.83907 | -123.41 | 121 | River | 24-05-2010 | | | | | | -9.1 | -61.2 | 11.6 | Brooks et al., 2012 | -8.919 | -4.681 | 28 | 17 | 3 | |
| Luckiamute | LK06 | DNSW10-0701 | 44.83918 | -123.41 | 121 | River | 14-10-2010 | | | | | | -8.4 | -59.9 | 7.3 | Brooks et al., 2012 | -9.118 | -4.793 | 21 | | 1 | |
| North Santiam | NS07 | DNSW09-0062 | 44.793 | -122.619 | 197 | River | 02-03-2009 | | | | | | -9.8 | -66.4 | 12 | Brooks et al., 2012 | -10.035 | -5.275 | 23 | | 1 | |
| North Santiam | NS07 | DNSW09-0439 | 44.793 | -122.619 | 197 | River | 27-08-2009 | | | | | | -9.2 | -63.2 | 10.4 | Brooks et al., 2012 | -9.845 | -5.161 | 37 | | 1 | |
| North Santiam | NS07 | DNSW09-0583 | 44.793 | -122.619 | 197 | River | 02-12-2009 | | | | | | -9.6 | -63.2 | 13.6 | Brooks et al., 2012 | -9.519 | -4.991 | 35 | | 1 | |
| North Santiam | NS07 | DNSW10-0158 | 44.79267 | -122.619 | 197 | River | 06-04-2010 | | | | | | -10 | -64.6 | 15.4 | Brooks et al., 2012 | -9.501 | -4.981 | 36 | 7 | 2 | |
| North Santiam | NS07 | DNSW10-0515 | 44.7926 | -122.619 | 197 | River | 26-08-2010 | | | | | | -9.3 | -63.3 | 11.1 | Brooks et al., 2012 | -9.320 | -4.894 | 27 | 3 | 3 | |
| North Santiam | NS07 | DNSW10-0855 | 44.79279 | -122.619 | 197 | River | 01-12-2010 | | | | | | -9.6 | -64.6 | 12.2 | Brooks et al., 2012 | -9.745 | -5.111 | 34 | | 1 | |
| North Santiam | NS19 | DNSW09-0243 | 44.66 | -121.918 | 838 | River | 12-05-2009 | | | | | | -12.4 | -86.9 | 12.3 | Brooks et al., 2012 | -13.102 | -6.881 | 37 | | 1 | |
| North Santiam | NS19 | DNSW09-0462 | 44.66 | -121.918 | 838 | River | 27-08-2009 | | | | | | -12.9 | -89.5 | 13.7 | Brooks et al., 2012 | -12.916 | -6.782 | 37 | 4 | 3 | |
| North Santiam | NS19 | DNSW09-0628 | 44.66 | -121.918 | 838 | River | 02-12-2009 | | | | | | -12.8 | -89.2 | 13.2 | Brooks et al., 2012 | -12.901 | -6.780 | 32 | | 1 | |
| North Santiam | NS19 | DNSW10-0314 | 44.66003 | -121.919 | 831 | River | 25-05-2010 | | | | | | -12.4 | -88.2 | 11 | Brooks et al., 2012 | -12.860 | -6.757 | 33 | | 1 | |
| North Santiam | NS19 | DNSW10-0521 | 44.65981 | -121.918 | 838 | River | 26-08-2010 | | | | | | -12.7 | -89.3 | 12.3 | Brooks et al., 2012 | -12.592 | -6.624 | 24 | | 1 | |
| North Santiam | NS19 | DNSW10-0866 | 44.66013 | -121.92 | 830 | River | 01-12-2010 | | | | | | -13 | -89.4 | 14.6 | Brooks et al., 2012 | -12.599 | -6.628 | 24 | 5 | 2 | |

| Analytical ID | Session | Sample ID | Sample Type | $\delta^{17}O$ (‰, vs O2 ref gas) | $\delta^{18}O$ (‰, vs O2 ref gas) | $\delta^{17}O$ (‰, VSMOW-SLAP) | $\delta^{18}O$ (‰, VSMOW-SLAP) |
|---|---|---|---|---|---|---|---|
| JHU-17O-693 | 680-847 | NQ7917 | precipitation | -18.343 | -35.017 | -0.017 | -0.018 |
| JHU-17O-695 | 680-847 | NQ7942 | precipitation | -17.985 | -34.358 | 0.354 | 0.675 |
| JHU-17O-697 | 680-847 | NQ9015 | precipitation | -17.881 | -34.158 | 0.456 | 0.875 |
| JHU-17O-698 | 680-847 | NQ9001 | precipitation | -18.703 | -35.692 | -0.416 | -0.781 |
| JHU-17O-699 | 680-847 | NQ9057 | precipitation | -21.098 | -40.157 | -2.953 | -5.589 |
| JHU-17O-701 | 680-847 | NQ9119 | precipitation | -21.011 | -40.011 | -2.868 | -5.446 |
| JHU-17O-724 | 680-847 | NQ9171 | precipitation | -22.718 | -43.190 | -4.759 | -9.033 |
| JHU-17O-725 | 680-847 | NQ9129 | precipitation | -20.704 | -39.438 | -2.634 | -5.007 |
| JHU-17O-726 | 680-847 | NQ8115 | precipitation | -20.435 | -38.938 | -2.353 | -4.477 |
| JHU-17O-729 | 680-847 | NQ9171 | precipitation | -22.960 | -43.606 | -5.034 | -9.517 |
| JHU-17O-834 | 680-847 | NQ8961 | precipitation | -24.444 | -46.314 | -6.995 | -13.193 |
| JHU-17O-835 | 680-847 | NQ8966 | precipitation | -22.576 | -42.906 | -5.025 | -9.540 |
| JHU-17O-836 | 680-847 | NQ8961 | precipitation | -21.663 | -41.201 | -4.063 | -7.716 |
| JHU-17O-837 | 680-847 | NQ9002 | precipitation | -20.066 | -38.202 | -2.379 | -4.502 |
| JHU-17O-838 | 680-847 | NQ7613 | precipitation | -21.079 | -40.108 | -3.454 | -6.556 |
| JHU-17O-839 | 680-847 | NQ7295 | precipitation | -23.846 | -45.237 | -6.382 | -12.072 |
| JHU-17O-841 | 680-847 | NQ8815 | precipitation | -21.884 | -41.667 | -4.316 | -8.253 |
| JHU-17O-842 | 680-847 | NQ7749 | precipitation | -21.388 | -40.703 | -3.795 | -7.225 |
| JHU-17O-843 | 680-847 | NQ7169 | precipitation | -21.349 | -40.607 | -3.757 | -7.129 |
| JHU-17O-844 | 680-847 | NQ8889 | precipitation | -21.102 | -40.182 | -3.500 | -6.680 |
| JHU-17O-845 | 680-847 | NQ9136 | precipitation | -20.295 | -38.748 | -2.651 | -5.147 |
| JHU-17O-858 | 848-880 | NSW09-0330 | precipitation | -19.136 | -36.531 | -1.187 | -2.266 |
| JHU-17O-859 | 848-880 | NQ9136 | precipitation | -19.735 | -37.675 | -1.814 | -3.484 |
| JHU-17O-861 | 848-880 | NSW09-0115 | precipitation | -20.701 | -39.481 | -2.824 | -5.402 |
| JHU-17O-862 | 848-880 | NSW09-0074 | precipitation | -21.841 | -41.607 | -4.020 | -7.670 |
| JHU-17O-863 | 848-880 | NSW09-0199 | precipitation | -22.754 | -43.258 | -4.978 | -9.431 |
| JHU-17O-864 | 848-880 | NSW09-0020 | precipitation | -24.124 | -45.851 | -6.417 | -12.199 |
| JHU-17O-865 | 848-880 | NSW09-0390 | precipitation | -24.136 | -45.848 | -6.425 | -12.188 |
| JHU-17O-867 | 848-880 | NSW09-0147 | precipitation | -22.831 | -43.420 | -5.044 | -9.575 |
| JHU-17O-868 | 848-880 | NSW09-0198 | precipitation | -21.857 | -41.624 | -4.015 | -7.646 |
| JHU-17O-869 | 848-880 | NSW09-0304 | precipitation | -20.679 | -39.416 | -2.771 | -5.276 |
| JHU-17O-871 | 848-880 | NQ9129 | precipitation | -20.331 | -38.793 | -2.397 | -4.595 |
| JHU-17O-872 | 848-880 | NQ8961 | precipitation | -22.117 | -42.071 | -4.274 | -8.097 |
| JHU-17O-876 | 848-880 | NSW09-0103 | precipitation | -21.781 | -41.497 | -3.904 | -7.455 |
| JHU-17O-877 | 848-880 | NSW09-0379 | precipitation | -20.316 | -38.755 | -2.359 | -4.512 |
| JHU-17O-879 | 848-880 | NSW09-0387 | precipitation | -21.435 | -40.826 | -3.529 | -6.715 |
| JHU-17O-880 | 848-880 | NQ9119 | precipitation | -20.595 | -39.225 | -2.641 | -4.995 |
| JHU-17O-888 | 881-980 | DNSW10-0866 | river | -24.447 | -46.417 | -6.712 | -12.712 |
| JHU-17O-889 | 881-980 | DNSW10-0314 | river | -24.468 | -46.479 | -6.735 | -12.778 |
| JHU-17O-891 | 881-980 | NSW10-0017 | precipitation | -23.701 | -45.063 | -5.929 | -11.269 |
| JHU-17O-892 | 881-980 | DNSW10-0701 | river | -22.606 | -43.004 | -4.782 | -9.077 |
| JHU-17O-898 | 881-980 | NSW10-0126 | precipitation | -20.966 | -39.912 | -3.061 | -5.782 |
| JHU-17O-899 | 881-980 | DNSW09-0488 | river | -22.517 | -42.842 | -4.686 | -8.902 |
| JHU-17O-901 | 881-980 | NSW10-0426 | precipitation | -22.061 | -42.010 | -4.208 | -8.015 |
| JHU-17O-902 | 881-980 | DNSW09-0062 | river | -23.067 | -43.860 | -5.261 | -9.985 |
| JHU-17O-904 | 881-980 | NSW10-0024 | precipitation | -21.741 | -41.387 | -3.871 | -7.350 |
| JHU-17O-906 | 881-980 | DNSW10-0074 | river | -22.479 | -42.771 | -4.644 | -8.823 |
| JHU-17O-911 | 881-980 | DNSW10-0521 | river | -24.349 | -46.238 | -6.602 | -12.513 |
| JHU-17O-913 | 881-980 | DNSW09-0243 | river | -24.593 | -46.713 | -6.857 | -13.017 |
| JHU-17O-914 | 881-980 | DNSW09-0439 | river | -22.962 | -43.688 | -5.148 | -9.796 |
| JHU-17O-922 | 881-980 | DNSW10-0515 | river | -22.920 | -43.584 | -5.100 | -9.682 |
| JHU-17O-925 | 881-980 | NSW10-0023 | precipitation | -23.018 | -43.780 | -5.203 | -9.890 |
| JHU-17O-927 | 881-980 | DNSW09-0583 | river | -22.805 | -43.390 | -4.978 | -9.473 |
| JHU-17O-928 | 881-980 | DNSW10-0855 | river | -22.920 | -43.601 | -5.098 | -9.698 |
| JHU-17O-930 | 881-980 | DNSW10-0280 | river | -22.264 | -42.338 | -4.411 | -8.353 |
| JHU-17O-931 | 881-980 | DNSW09-0033 | river | -22.627 | -43.059 | -4.791 | -9.119 |
| JHU-17O-940 | 881-980 | NSW10-0156 | precipitation | -22.282 | -42.385 | -4.426 | -8.398 |
| JHU-17O-942 | 881-980 | NSW10-0255 | precipitation | -23.539 | -44.756 | -5.743 | -10.922 |
| JHU-17O-943 | 881-980 | NSW10-0257 | precipitation | -22.718 | -43.194 | -4.882 | -9.258 |
| JHU-17O-946 | 881-980 | NSW10-0482 | precipitation | -23.039 | -43.817 | -5.217 | -9.921 |
| JHU-17O-947 | 881-980 | DNSW10-0515 | River? | -22.530 | -42.867 | -4.684 | -8.908 |
| JHU-17O-1159 | 1104-1208 | NSW09-0330 | precipitation | -19.073 | -36.396 | -1.075 | -2.048 |
| JHU-17O-1160 | 1104-1208 | NSW10-0031 | precipitation | -20.919 | -39.881 | -3.018 | -5.772 |
| JHU-17O-1161 | 1104-1208 | NSW10-0126 | precipitation | -20.921 | -39.875 | -3.018 | -5.762 |
| JHU-17O-1162 | 1104-1208 | NSW10-0485 | precipitation | -21.502 | -40.959 | -3.627 | -6.918 |
| JHU-17O-1163 | 1104-1208 | NSW10-0126 | precipitation | -20.949 | -39.904 | -3.042 | -5.784 |
| JHU-17O-1164 | 1104-1208 | NSW10-0023 | precipitation | -21.986 | -41.851 | -4.133 | -7.863 |
| JHU-17O-1165 | 1104-1208 | DNSW10-0280 | river | -22.583 | -42.973 | -4.760 | -9.060 |

| | | | | | | | |
|---|---|---|---|---|---|---|---|
| JHU-17O-1166 | 1104-1208 | DNSW10-0280 | river | -22.663 | -43.130 | -4.841 | -9.224 |
| JHU-17O-1167 | 1104-1208 | DNSW10-0515 | river | -22.683 | -43.147 | -4.860 | -9.238 |
| JHU-17O-1170 | 1104-1208 | DNSW09-0267 | river | -22.628 | -43.049 | -4.796 | -9.121 |
| JHU-17O-1171 | 1104-1208 | DNSW09-0267 | river | -22.652 | -43.088 | -4.818 | -9.158 |
| JHU-17O-1172 | 1104-1208 | NSW09-0199 | precipitation | -22.863 | -43.468 | -5.039 | -9.560 |
| JHU-17O-1173 | 1104-1208 | DNSW10-0158 | river | -22.793 | -43.375 | -4.963 | -9.456 |
| JHU-17O-1174 | 1104-1208 | DNSW10-0158 | river | -22.805 | -43.378 | -4.974 | -9.456 |
| JHU-17O-1175 | 1104-1208 | NSW10-0017 | precipitation | -23.520 | -44.715 | -5.724 | -10.883 |
| JHU-17O-1176 | 1104-1208 | DNSW09-0462 | river | -24.472 | -46.474 | -6.725 | -12.761 |
| JHU-17O-1176 | 1104-1208 | DNSW09-0462 | river | -24.478 | -46.499 | -6.731 | -12.788 |
| JHU-17O-1177 | 1104-1208 | DNSW09-0462 | river | -24.566 | -46.654 | -6.822 | -12.949 |
| JHU-17O-1178 | 1104-1208 | DNSW09-0628 | river | -24.507 | -46.536 | -6.757 | -12.818 |
| JHU-17O-1179 | 1104-1208 | NSW10-0255 | precipitation | -23.729 | -45.087 | -5.935 | -11.264 |
| JHU-17O-1180 | 1104-1208 | DNSW10-0866 | river | -24.268 | -46.086 | -6.501 | -12.328 |
| JHU-17O-1184 | 1104-1208 | 3-80-MT97-11JUL06 | precipitation | -22.790 | -43.315 | -4.935 | -9.346 |
| JHU-17O-1185 | 1104-1208 | 3-80-MT97-11JUL06 | precipitation | -22.544 | -42.838 | -4.673 | -8.831 |
| JHU-17O-1186 | 1104-1208 | 4-69-MT97-04JUL06 | precipitation | -20.744 | -39.500 | -2.775 | -5.255 |
| JHU-17O-1187 | 1104-1208 | 4-69-MT97-04JUL06 | precipitation | -20.722 | -39.462 | -2.750 | -5.210 |
| JHU-17O-1188 | 1104-1208 | 1-3-ID03-27JUL06 | precipitation | -17.970 | -34.294 | 0.152 | 0.327 |
| JHU-17O-1189 | 1104-1208 | 1-3-ID03-27JUL06 | precipitation | -17.983 | -34.322 | 0.140 | 0.300 |
| JHU-17O-1190 | 1104-1208 | 3-74-MT05-04JUL06 | precipitation | -22.437 | -42.656 | -4.549 | -8.615 |
| JHU-17O-1191 | 1104-1208 | 3-74-MT05-04JUL06 | precipitation | -22.397 | -42.576 | -4.505 | -8.525 |
| JHU-17O-1192 | 1104-1208 | 3-87-MT00-11JUL06 | precipitation | -19.142 | -36.523 | -1.074 | -2.042 |
| JHU-17O-1193 | 1104-1208 | 3-87-MT00-11JUL06 | precipitation | -19.243 | -36.675 | -1.179 | -2.201 |
| JHU-17O-1194 | 1104-1208 | 4-57-WY95-18JUL06 | precipitation | -19.437 | -37.048 | -1.380 | -2.596 |
| JHU-17O-1195 | 1104-1208 | 4-57-WY95-18JUL06 | precipitation | -19.508 | -37.190 | -1.453 | -2.743 |
| JHU-17O-1196 | 1104-1208 | 4-73-WY06-24JUL06 | precipitation | -23.248 | -44.130 | -5.391 | -10.167 |
| JHU-17O-1198 | 1104-1208 | 3-90-MT00-27JUL06 | precipitation | -19.344 | -36.868 | -1.274 | -2.386 |
| JHU-17O-1199 | 1104-1208 | 4-74-WY06-11JUL06 | precipitation | -20.580 | -39.221 | -2.574 | -4.900 |
| JHU-17O-1200 | 1104-1208 | 4-94-WY95-4JUL06 | precipitation | -23.099 | -43.943 | -5.225 | -9.951 |
| JHU-17O-1201 | 1104-1208 | 5-61-CO02-11JUL06 | precipitation | -20.110 | -38.338 | -2.073 | -3.946 |
| JHU-17O-1202 | 1104-1208 | 5-63-CO15-5JUL06 | precipitation | -20.019 | -38.148 | -1.975 | -3.738 |
| JHU-17O-1203 | 1104-1208 | 5-65-CO02-4JUL06 | precipitation | -22.992 | -43.725 | -5.105 | -9.704 |
| JHU-17O-1204 | 1104-1208 | 5-71-CO15-11JUL06 | precipitation | -18.864 | -35.982 | -0.754 | -1.412 |
| JHU-17O-1205 | 1104-1208 | 2-73-ID03-18JUL06 | precipitation | -21.414 | -40.759 | -3.438 | -6.520 |
| JHU-17O-1206 | 1104-1208 | 1-7-OR18-5JUL06 | precipitation | -22.112 | -42.066 | -4.172 | -7.915 |
| JHU-17O-1239 | 1209-1301 | 1-18-OR10-27JUL06 | precipitation | -20.910 | -39.828 | -3.032 | -5.769 |
| JHU-17O-1240 | 1209-1301 | 1-18-OR10-27JUL06 | precipitation | -20.961 | -39.925 | -3.087 | -5.875 |
| JHU-17O-1241 | 1209-1301 | 4-100-KS32-4JUL06 | precipitation | -21.764 | -41.435 | -3.934 | -7.491 |
| JHU-17O-1293 | 1209-1301 | 5-85-CO15-16MAY06 | precipitation | -19.970 | -38.061 | -2.116 | -4.007 |
| JHU-17O-1294 | 1209-1301 | 2-89-WA14-25JUL06 | precipitation | -22.256 | -42.334 | -4.523 | -8.577 |
| JHU-17O-1295 | 1209-1301 | 2-90-OR02-11JUL06 | precipitation | -21.006 | -40.015 | -3.209 | -6.101 |
| JHU-17O-1296 | 1209-1301 | 3-12-WA14-11JUL06 | precipitation | -22.046 | -41.951 | -4.304 | -8.172 |
| JHU-17O-1306 | 1302-1332 | 3-89-WY99-3JUL06 | precipitation | -20.714 | -39.457 | -2.658 | -5.061 |
| JHU-17O-1307 | 1302-1332 | 6-68-SD08-27JUN06 | precipitation | -21.020 | -39.976 | -2.989 | -5.634 |
| JHU-17O-1308 | 1302-1332 | 5-13-NE99-6JUN06 | precipitation | -21.711 | -41.272 | -3.729 | -7.042 |
| JHU-17O-1309 | 1302-1332 | 1-15-OR18-27JUN06 | precipitation | -20.260 | -38.585 | -2.196 | -4.160 |
| JHU-17O-1310 | 1302-1332 | 5-23-NE99-13JUL06 | precipitation | -21.204 | -40.382 | -3.205 | -6.108 |
| JHU-17O-1311 | 1302-1332 | 5-31-NE99-20JUN06 | precipitation | -21.728 | -41.323 | -3.767 | -7.135 |
| JHU-17O-1312 | 1302-1332 | 6-44-SD08-18JUL06 | precipitation | -19.738 | -37.579 | -1.661 | -3.113 |
| JHU-17O-1313 | 1302-1332 | 4-50-WY99-25JUL06 | precipitation | -21.911 | -41.659 | -3.975 | -7.523 |
| JHU-17O-1314 | 1302-1332 | 5-18-NE99-18JUL06 | precipitation | -19.259 | -36.750 | -1.167 | -2.244 |
| JHU-17O-1318 | 1302-1332 | 5-25-KS32-11JUL06 | precipitation | -22.402 | -42.595 | -4.529 | -8.594 |
| JHU-17O-1319 | 1302-1332 | 6-4-ND08-4JUL06 | precipitation | -23.229 | -44.129 | -5.414 | -10.259 |
| JHU-17O-1320 | 1302-1332 | 6-22-SD99-18JUL06 | precipitation | -20.053 | -38.179 | -2.050 | -3.860 |
| JHU-17O-1321 | 1302-1332 | 5-21-NE99-4JUL06 | precipitation | -21.270 | -40.506 | -3.348 | -6.380 |
| JHU-17O-1322 | 1302-1332 | 6-26-SD99-11JUL06 | precipitation | -16.993 | -32.445 | 1.185 | 2.294 |
| JHU-17O-1323 | 1302-1332 | 6-38-ND08-11JUL06 | precipitation | -20.603 | -39.208 | -2.654 | -5.006 |
| JHU-17O-1324 | 1302-1332 | 5-24-NE99-25JUL06 | precipitation | -21.002 | -39.994 | -3.084 | -5.866 |
| JHU-17O-1332 | 1302-1332 | 6-26-SD99-11JUL06 | precipitation | -17.103 | -32.603 | 1.002 | 1.996 |
| JHU-17O-1606 | 1586-1671 | NQ7917 | precipitation | -18.348 | -34.998 | -0.184 | -0.348 |
| JHU-17O-1607 | 1586-1671 | NQ7942 | precipitation | -18.026 | -34.388 | 0.156 | 0.306 |
| JHU-17O-1608 | 1586-1671 | NQ9001 | precipitation | -18.850 | -35.939 | -0.713 | -1.356 |
| JHU-17O-1609 | 1586-1671 | NQ9015 | precipitation | -18.093 | -34.554 | 0.087 | 0.129 |
| JHU-17O-1610 | 1586-1671 | 5-61-CO02-11JUL06 | precipitation | -20.115 | -38.322 | -2.047 | -3.911 |
| JHU-17O-1612 | 1586-1671 | NQ9057 | precipitation | -21.158 | -40.260 | -3.147 | -5.989 |
| JHU-17O-1613 | 1586-1671 | NQ9119 | precipitation | -20.897 | -39.758 | -2.871 | -5.451 |
| JHU-17O-1617 | 1586-1671 | 3-75-MT97-27JUN06 | precipitation | -21.540 | -40.989 | -3.548 | -6.770 |
| JHU-17O-1625 | 1586-1671 | 4-79-WY06-27DEC05 | precipitation | -29.253 | -55.314 | -11.684 | -22.132 |
| JHU-17O-1626 | 1586-1671 | 3-62-WY06-31JAN06 | precipitation | -26.784 | -50.738 | -9.079 | -17.223 |

| | | | | | | | |
|---|---|---|---|---|---|---|---|
| JHU-17O-1627 | 1586-1671 | 4-76-WY95-17JAN06 | precipitation | -28.273 | -53.467 | -10.650 | -20.150 |
| JHU-17O-1628 | 1586-1671 | 4-56-WY95-24JAN06 | precipitation | -28.457 | -53.806 | -10.844 | -20.513 |
| JHU-17O-1629 | 1586-1671 | 3-69-WY99-14FEB06 | precipitation | -31.039 | -58.543 | -13.568 | -25.593 |
| JHU-17O-1630 | 1586-1671 | 1-37-ID03-24JAN06 | precipitation | -25.410 | -48.205 | -7.627 | -14.505 |
| JHU-17O-1631 | 1586-1671 | 6-69-ND08-17JAN06 | precipitation | -30.527 | -57.654 | -13.027 | -24.639 |
| JHU-17O-1633 | 1586-1671 | 1-46-OR10-17JAN06 | precipitation | -25.898 | -49.081 | -8.141 | -15.444 |
| JHU-17O-1634 | 1586-1671 | 2-28-ID03-31JAN06 | precipitation | -24.921 | -47.289 | -7.110 | -13.521 |
| JHU-17O-1635 | 1586-1671 | 4-34-MT00-3JAN06 | precipitation | -28.551 | -54.008 | -10.940 | -20.727 |
| JHU-17O-1636 | 1586-1671 | 4-75-MT97-17JAN06 | precipitation | -30.052 | -56.761 | -12.523 | -23.680 |
| JHU-17O-1637 | 1586-1671 | 4-61-MT05-17JAN06 | precipitation | -28.210 | -53.361 | -10.580 | -20.032 |
| JHU-17O-1639 | 1586-1671 | 1-35-OR02-17JAN06 | precipitation | -23.843 | -45.281 | -5.971 | -11.366 |
| JHU-17O-1640 | 1586-1671 | 1-23-OR18-17JAN06 | precipitation | -28.444 | -53.843 | -10.826 | -20.548 |
| JHU-17O-1650 | 1586-1671 | NQ9015 | precipitation | -17.760 | -33.898 | 0.452 | 0.848 |
| JHU-17O-1651 | 1586-1671 | NQ9057 | precipitation | -21.048 | -40.088 | -3.017 | -5.790 |
| JHU-17O-1653 | 1586-1671 | 5-61-CO02-11JUL06 | precipitation | -20.022 | -38.140 | -1.934 | -3.701 |
| JHU-17O-1654 | 1586-1671 | NSW10-0401 | precipitation | -20.603 | -39.244 | -2.546 | -4.884 |
| JHU-17O-1655 | 1586-1671 | 5-40-KS32-27JUN06 | precipitation | -18.427 | -35.118 | -0.250 | -0.459 |
| JHU-17O-1656 | 1586-1671 | 6-30-SD99-25JUL06 | precipitation | -15.953 | -30.427 | 2.362 | 4.573 |
| JHU-17O-1657 | 1586-1671 | 1-20-WA24-13JUN06 | precipitation | -22.458 | -42.652 | -4.503 | -8.538 |
| JHU-17O-1658 | 1586-1671 | 2-91-WA24-8AUG06 | precipitation | -21.023 | -39.960 | -2.988 | -5.651 |
| JHU-17O-1663 | 1586-1671 | 1-23-OR18-17JAN06 | precipitation | -28.013 | -53.016 | -10.362 | -19.653 |
| JHU-17O-1664 | 1586-1671 | 2-76-ID15-6JUN06 | precipitation | -18.276 | -34.808 | -0.087 | -0.123 |
| JHU-17O-1665 | 1586-1671 | 5-8-NE99-19DEC06 | precipitation | -24.852 | -47.180 | -7.026 | -13.392 |
| JHU-17O-1666 | 1586-1671 | 1-33-OR02-24JAN06 | precipitation | -23.145 | -44.008 | -5.224 | -9.990 |
| JHU-17O-1671 | 1586-1671 | 2-76-ID15-6JUN06 | precipitation | -18.855 | -35.874 | -0.696 | -1.263 |
| JHU-17O-1686 | 1673-1768 | 6-26-SD99-11JUL06 | precipitation | -16.606 | -31.726 | 1.393 | 2.721 |
| JHU-17O-1687 | 1673-1768 | 6-30-SD99-25JUL06 | precipitation | -16.059 | -30.675 | 1.976 | 3.856 |
| JHU-17O-1688 | 1673-1768 | 1-19-ID15-13JUN06 | precipitation | -16.480 | -31.491 | 1.536 | 2.989 |
| JHU-17O-1689 | 1673-1768 | 3-35-MT05-8AUG06 | precipitation | -24.737 | -46.931 | -7.172 | -13.551 |
| JHU-17O-1691 | 1673-1768 | 1-1-OR02-13JUN06 | precipitation | -20.736 | -39.497 | -2.940 | -5.569 |
| JHU-17O-1692 | 1673-1768 | 1-6-OR10-13JUN06 | precipitation | -21.203 | -40.366 | -3.428 | -6.492 |
| JHU-17O-1693 | 1673-1768 | 3-88-WY95-27JUN06 | precipitation | -20.935 | -39.888 | -3.140 | -5.972 |
| JHU-17O-1694 | 1673-1768 | 5-52-CO02-17JAN06 | precipitation | -29.056 | -54.962 | -11.705 | -22.120 |
| JHU-17O-1695 | 1673-1768 | 5-70-CO02-17JAN06 | precipitation | -27.626 | -52.306 | -10.192 | -19.266 |
| JHU-17O-1696 | 1673-1768 | 5-53-CO15-17JAN06 | precipitation | -28.960 | -54.788 | -11.595 | -21.918 |
| JHU-17O-1697 | 1673-1768 | 5-64-CO15-28FEB06 | precipitation | -25.232 | -47.850 | -7.655 | -14.475 |
| JHU-17O-1702 | 1673-1768 | 1-22-ID15-31JAN06 | precipitation | -26.384 | -49.968 | -8.847 | -16.708 |
| JHU-17O-1703 | 1673-1768 | 1-38-ID15-24JAN06 | precipitation | -26.992 | -51.118 | -9.483 | -17.933 |
| JHU-17O-1704 | 1673-1768 | 5-32-KS32-17JAN06 | precipitation | -27.911 | -52.871 | -10.449 | -19.804 |
| JHU-17O-1707 | 1673-1768 | 4-78-MT05-24JAN06 | precipitation | -27.720 | -52.476 | -10.232 | -19.359 |
| JHU-17O-1709 | 1673-1768 | 6-54-ND08-24JAN06 | precipitation | -27.432 | -51.955 | -9.918 | -18.785 |
| JHU-17O-1712 | 1673-1768 | 1-47-OR18-24JAN06 | precipitation | -28.799 | -54.462 | -11.346 | -21.450 |
| JHU-17O-1713 | 1673-1768 | 6-10-SD99-19DEC06 | precipitation | -27.343 | -51.783 | -9.805 | -18.571 |
| JHU-17O-1714 | 1673-1768 | 6-9-SD99-14NOV06 | precipitation | -28.105 | -53.164 | -10.603 | -20.044 |
| JHU-17O-1715 | 1673-1768 | 1-21-WA14-23JAN06 | precipitation | -24.255 | -46.038 | -6.535 | -12.398 |
| JHU-17O-1716 | 1673-1768 | 1-36-WA14-23JAN06 | precipitation | -25.041 | -47.455 | -7.360 | -13.909 |
| JHU-17O-1717 | 1673-1768 | 1-31-WA24-24JAN06 | precipitation | -25.257 | -47.847 | -7.584 | -14.322 |
| JHU-17O-1718 | 1673-1768 | 1-61-WA24-17JAN06 | precipitation | -27.035 | -51.171 | -9.454 | -17.877 |
| JHU-17O-1719 | 1673-1768 | 3-83-WY99-7NOV06 | precipitation | -27.139 | -51.352 | -9.559 | -18.065 |
| JHU-17O-1720 | 1673-1768 | 4-74-WY06-11JUL06 | precipitation | -20.756 | -39.507 | -2.818 | -5.360 |
| JHU-17O-1721 | 1673-1768 | 5-71-CO15-11JUL06 | precipitation | -19.101 | -36.413 | -1.062 | -2.028 |
| JHU-17O-1725 | 1673-1768 | 3-75-MT97-27JUN06 | precipitation | -21.301 | -40.506 | -3.363 | -6.386 |
| JHU-17O-1726 | 1673-1768 | 5-6-NE99-3OCT06 | precipitation | -23.765 | -45.077 | -5.959 | -11.278 |
| JHU-17O-1727 | 1673-1768 | 4-73-WY06-24JUL06 | precipitation | -23.467 | -44.512 | -5.639 | -10.665 |
| JHU-17O-1730 | 1673-1768 | 5-40-KS32-27JUN06 | precipitation | -18.336 | -34.944 | -0.214 | -0.392 |
| JHU-17O-1734 | 1673-1768 | 4-34-MT00-3JAN06 | precipitation | -28.883 | -54.613 | -11.326 | -21.448 |
| JHU-17O-1735 | 1673-1768 | 5-8-NE99-19DEC06 | precipitation | -25.565 | -48.457 | -7.820 | -14.841 |
| JHU-17O-1736 | 1673-1768 | 6-49-SD08-21NOV06 | precipitation | -27.364 | -51.767 | -9.714 | -18.382 |
| JHU-17O-1737 | 1673-1768 | 5-65-CO02-4JUL06 | precipitation | -23.206 | -44.082 | -5.320 | -10.136 |
| JHU-17O-1738 | 1673-1768 | 2-68-OR10-1AUG06 | precipitation | -21.801 | -41.444 | -3.831 | -7.300 |
| JHU-17O-1739 | 1673-1768 | 6-15-SD08-21NOV06 | precipitation | -26.046 | -49.355 | -8.307 | -15.774 |
| JHU-17O-1741 | 1673-1768 | 1-31-WA24-24JAN06 | precipitation | -25.208 | -47.798 | -7.418 | -14.097 |
| JHU-17O-1742 | 1673-1768 | 4-94-WY95-4JUL06 | precipitation | -23.080 | -43.862 | -5.167 | -9.870 |
| JHU-17O-2009 | 1943-2041 | 1-19-ID15-13JUN06 | precipitation | -16.585 | -31.665 | 1.593 | 3.099 |
| JHU-17O-2010 | 1943-2041 | NQ8815 | precipitation | -21.603 | -41.151 | -3.771 | -7.194 |
| JHU-17O-2011 | 1943-2041 | NQ8815 | precipitation | -21.805 | -41.527 | -3.989 | -7.608 |
| JHU-17O-2012 | 1943-2041 | 1-40-OR10-24JAN06 | precipitation | -24.090 | -45.800 | -6.432 | -12.246 |
| JHU-17O-2013 | 1943-2041 | 3-79-MT00-7FEB06 | precipitation | -26.368 | -50.034 | -8.868 | -16.844 |
| JHU-17O-2014 | 1943-2041 | 5-36-KS32-3JAN06 | precipitation | -27.575 | -52.243 | -10.160 | -19.244 |
| JHU-17O-2015 | 1943-2041 | 4-86-MT97-24JAN06 | precipitation | -28.568 | -54.098 | -11.223 | -21.261 |

| | | | | | | | |
|---|---|---|---|---|---|---|---|
| JHU-17O-682 | 680-847 | SLAP-130116 | SLAP22 | -47.279 | -88.224 | -30.574 | -57.151 |
| JHU-17O-689 | 680-847 | VSMOW-2-201 | VVSMOW22 | -18.437 | -35.219 | -0.101 | -0.206 |
| JHU-17O-694 | 680-847 | VSMOW-2-201 | VSMOW2 | -18.298 | -34.937 | 0.027 | 0.060 |
| JHU-17O-696 | 680-847 | VSMOW-2-201 | VSMOW2 | -18.152 | -34.658 | 0.173 | 0.346 |
| JHU-17O-709 | 680-847 | SLAP-130116 | SLAP2 | -46.545 | -86.843 | -29.897 | -55.856 |
| JHU-17O-710 | 680-847 | SLAP-130116 | SLAP2 | -46.935 | -87.576 | -30.313 | -56.650 |
| JHU-17O-711 | 680-847 | SLAP-130116 | SLAP2 | -47.043 | -87.778 | -30.431 | -56.875 |
| JHU-17O-717 | 680-847 | VSMOW-2-201 | VSMOW2 | -18.207 | -34.777 | 0.036 | 0.062 |
| JHU-17O-718 | 680-847 | VSMOW-2-201 | VSMOW2 | -18.273 | -34.900 | -0.037 | -0.077 |
| JHU-17O-727 | 680-847 | SLAP-130116 | SLAP2 | -46.461 | -86.705 | -29.874 | -55.833 |
| JHU-17O-728 | 680-847 | SLAP-130116 | SLAP2 | -46.687 | -87.115 | -30.116 | -56.281 |
| JHU-17O-738 | 680-847 | VSMOW-2-201 | VSMOW2 | -18.169 | -34.699 | -0.003 | -0.008 |
| JHU-17O-739 | 680-847 | VSMOW-2-201 | VSMOW2 | -18.205 | -34.760 | -0.044 | -0.082 |
| JHU-17O-751 | 680-847 | SLAP 130116 | SLAP2 | -46.294 | -86.373 | -29.784 | -55.643 |
| JHU-17O-752 | 680-847 | SLAP 130116 | SLAP2 | -46.748 | -87.212 | -30.269 | -56.552 |
| JHU-17O-765 | 680-847 | VSMOW2-201 | VSMOW2 | -17.870 | -34.113 | 0.212 | 0.421 |
| JHU-17O-766 | 680-847 | VSMOW2-201 | VSMOW2 | -18.117 | -34.591 | -0.053 | -0.100 |
| JHU-17O-767 | 680-847 | VSMOW2-201 | VSMOW2 | -18.085 | -34.539 | -0.023 | -0.051 |
| JHU-17O-785 | 680-847 | SLAP-130116 | SLAP2 | -44.188 | -82.504 | -27.682 | -51.724 |
| JHU-17O-786 | 680-847 | SLAP-130116 | SLAP2 | -45.589 | -85.083 | -29.167 | -54.502 |
| JHU-17O-787 | 680-847 | SLAP-130116 | SLAP2 | -46.193 | -86.196 | -29.809 | -55.705 |
| JHU-17O-791 | 680-847 | VSMOW-2-201 | VSMOW2 | -18.586 | -35.485 | -0.643 | -1.245 |
| JHU-17O-792 | 680-847 | VSMOW-2-201 | VSMOW2 | -17.904 | -34.185 | 0.075 | 0.146 |
| JHU-17O-793 | 680-847 | VSMOW-2-201 | VSMOW2 | -18.012 | -34.388 | -0.044 | -0.080 |
| JHU-17O-813 | 680-847 | VSMOW2-201 | VSMOW2 | -17.806 | -33.998 | 0.100 | 0.191 |
| JHU-17O-815 | 680-847 | VSMOW2-201 | VSMOW2 | -17.587 | -33.582 | 0.323 | 0.624 |
| JHU-17O-831 | 680-847 | SLAP-130116 | SLAP2 | -45.299 | -84.546 | -29.025 | -54.239 |
| JHU-17O-832 | 680-847 | SLAP-130116 | SLAP2 | -45.561 | -85.018 | -29.306 | -54.754 |
| JHU-17O-833 | 680-847 | SLAP-130116 | SLAP2 | -45.776 | -85.460 | -29.537 | -55.236 |
| JHU-17O-860 | 848-880 | VSMOW-2-201 | VSMOW2 | -18.015 | -34.426 | 0.000 | 0.000 |
| JHU-17O-873 | 848-880 | SLAP-130116 | SLAP2 | -46.301 | -86.452 | -29.734 | -55.587 |
| JHU-17O-874 | 848-880 | SLAP-130116 | SLAP2 | -46.433 | -86.660 | -29.870 | -55.803 |
| JHU-17O-875 | 848-880 | SLAP-130116 | SLAP2 | -46.080 | -86.025 | -29.491 | -55.110 |
| JHU-17O-878 | 848-880 | VSMOW-2-201 | VSMOW2 | -18.080 | -34.545 | 0.000 | 0.000 |
| JHU-17O-883 | 881-980 | SLAP-130116 | SLAP2 | -46.708 | -87.208 | -30.044 | -56.146 |
| JHU-17O-884 | 881-980 | SLAP-130116 | SLAP2 | -46.654 | -87.109 | -29.987 | -56.040 |
| JHU-17O-885 | 881-980 | SLAP-130116 | SLAP2 | -46.514 | -86.870 | -29.841 | -55.785 |
| JHU-17O-894 | 881-980 | VSMOW-2-201 | VSMOW2 | -18.027 | -34.450 | 0.018 | 0.031 |
| JHU-17O-895 | 881-980 | VSMOW-2-201 | VSMOW2 | -18.116 | -34.611 | -0.075 | -0.139 |
| JHU-17O-896 | 881-980 | VSMOW-2-201 | VSMOW2 | -18.025 | -34.443 | 0.021 | 0.040 |
| JHU-17O-916 | 881-980 | SLAP2-130116 | SLAP2 | -46.558 | -86.917 | -29.876 | -55.823 |
| JHU-17O-917 | 881-980 | SLAP2-130116 | SLAP2 | -46.739 | -87.253 | -30.065 | -56.181 |
| JHU-17O-919 | 881-980 | SLAP2-051613-5 | SLAP2 | -46.890 | -87.523 | -30.223 | -56.468 |
| JHU-17O-920 | 881-980 | SLAP2-051613-5 | SLAP2 | -46.679 | -87.153 | -30.002 | -56.074 |
| JHU-17O-933 | 881-980 | VSMOW-2-201 | VSMOW2 | -18.089 | -34.561 | -0.034 | -0.070 |
| JHU-17O-934 | 881-980 | VSMOW-2-201 | VSMOW2 | -18.020 | -34.419 | 0.039 | 0.081 |
| JHU-17O-935 | 881-980 | VSMOW2-052013-4 | VSMOW2 | -18.020 | -34.426 | 0.040 | 0.074 |
| JHU-17O-936 | 881-980 | VSMOW2-052013-4 | VSMOW2 | -18.023 | -34.426 | 0.037 | 0.074 |
| JHU-17O-937 | 881-980 | VSMOW2-052013-4 | VSMOW2 | -18.062 | -34.512 | -0.005 | -0.016 |
| JHU-17O-967 | 881-980 | SLAP2-051613-5 | SLAP2 | -45.842 | -85.596 | -29.110 | -54.397 |
| JHU-17O-968 | 881-980 | SLAP2-051613-5 | SLAP2 | -46.334 | -86.499 | -29.625 | -55.358 |
| JHU-17O-972 | 881-980 | VSMOW2-052013-4 | VSMOW2 | -18.160 | -34.691 | -0.095 | -0.193 |
| JHU-17O-973 | 881-980 | VSMOW2-052013-4 | VSMOW2 | -17.919 | -34.209 | 0.158 | 0.320 |
| JHU-17O-974 | 881-980 | VSMOW2-052013-4 | VSMOW2 | -18.167 | -34.700 | -0.102 | -0.202 |
| JHU-17O-977 | 881-980 | SLAP2-051613-5 | SLAP2 | -45.852 | -85.604 | -29.117 | -54.402 |
| JHU-17O-978 | 881-980 | SLAP2-051613-5 | SLAP2 | -46.039 | -85.962 | -29.313 | -54.783 |
| JHU-17O-979 | 881-980 | SLAP2-051613-5 | SLAP2 | -46.180 | -86.223 | -29.460 | -55.060 |
| JHU-17O-980 | 881-980 | SLAP2-051613-5 | SLAP2 | -46.141 | -86.150 | -29.418 | -54.982 |
| JHU-17O-1106 | 1104-1208 | VSMOW2-052013-4 | VSMOW2 | -17.936 | -34.269 | 0.003 | 0.002 |
| JHU-17O-1107 | 1104-1208 | VSMOW2-052013-4 | VSMOW2 | -17.873 | -34.157 | 0.071 | 0.126 |
| JHU-17O-1127 | 1104-1208 | SLAP-2-51613 | SLAP2 | -46.591 | -86.969 | -30.132 | -56.299 |
| JHU-17O-1128 | 1104-1208 | SLAP-2-51613-5 | SLAP2 | -46.318 | -86.444 | -29.843 | -55.734 |
| JHU-17O-1156 | 1104-1208 | VSMOW2-052013-4 | VSMOW2 | -18.074 | -34.525 | -0.030 | -0.058 |
| JHU-17O-1157 | 1104-1208 | VSMOW2-052013-4 | VSMOW2 | -18.046 | -34.466 | 0.002 | 0.009 |
| JHU-17O-1158 | 1104-1208 | VSMOW2-052013-4 | VSMOW2 | -18.164 | -34.675 | -0.121 | -0.209 |
| JHU-17O-1181 | 1104-1208 | SLAP2-051613-5 | SLAP2 | -45.396 | -84.802 | -28.756 | -53.762 |
| JHU-17O-1182 | 1104-1208 | SLAP2-051613-5 | SLAP2 | -46.347 | -86.549 | -29.756 | -55.627 |
| JHU-17O-1183 | 1104-1208 | SLAP2-051613-5 | SLAP2 | -46.588 | -86.974 | -30.007 | -56.078 |
| JHU-17O-1207 | 1104-1208 | VSMOW2-052013-4 | VSMOW2 | -18.142 | -34.663 | 0.013 | 0.013 |
| JHU-17O-1208 | 1104-1208 | VSMOW2-052013-4 | VSMOW2 | -18.098 | -34.570 | 0.062 | 0.116 |

| | | | | | | | |
|---|---|---|---|---|---|---|---|
| JHU-17O-1211 | 1209-1301 | VSOMW2-052013 | VSMOW2 | -17.892 | -34.156 | 0.184 | 0.362 |
| JHU-17O-1218 | 1209-1301 | VSMOW2-052013-4 | VSMOW2 | -18.079 | -34.538 | -0.023 | -0.063 |
| JHU-17O-1219 | 1209-1301 | VSMOW2-052013-4 | VSMOW2 | -18.236 | -34.808 | -0.189 | -0.355 |
| JHU-17O-1236 | 1209-1301 | SLAP2-051613-5 | SLAP2 | -46.228 | -86.317 | -29.682 | -55.468 |
| JHU-17O-1237 | 1209-1301 | SLAP2-051613-5 | SLAP2 | -46.445 | -86.735 | -29.911 | -55.917 |
| JHU-17O-1238 | 1209-1301 | SLAP2-051613-5 | SLAP2 | -46.339 | -86.536 | -29.800 | -55.707 |
| JHU-17O-1269 | 1209-1301 | VSMOW-052013-4 | VSMOW2 | -17.996 | -34.376 | -0.005 | -0.011 |
| JHU-17O-1270 | 1209-1301 | VSMOW-052013-4 | VSMOW2 | -17.959 | -34.302 | 0.033 | 0.066 |
| JHU-17O-1297 | 1209-1301 | SLAP-051613-2 | SLAP2 | -46.089 | -86.064 | -29.615 | -55.334 |
| JHU-17O-1298 | 1209-1301 | SLAP-051613-2 | SLAP2 | -46.071 | -86.033 | -29.598 | -55.304 |
| JHU-17O-1299 | 1209-1301 | SLAP-051613-2 | SLAP2 | -46.059 | -85.999 | -29.587 | -55.269 |
| JHU-17O-1304 | 1302-1332 | VSMOW2-052113-4 | VSMOW2 | -18.253 | -34.850 | -0.032 | -0.071 |
| JHU-17O-1305 | 1302-1332 | VSMOW2-052113-4 | VSMOW2 | -18.183 | -34.700 | 0.036 | 0.078 |
| JHU-17O-1315 | 1302-1332 | SLAP2-051613-2 | SLAP2 | -45.762 | -85.481 | -29.306 | -54.774 |
| JHU-17O-1316 | 1302-1332 | SLAP2-051613-2 | SLAP2 | -46.199 | -86.274 | -29.777 | -55.640 |
| JHU-17O-1317 | 1302-1332 | SLAP2-051613-2 | SLAP2 | -46.416 | -86.678 | -30.014 | -56.087 |
| JHU-17O-1326 | 1302-1332 | VSMOW2-052013-4 | VSMOW2 | -18.130 | -34.607 | -0.049 | -0.086 |
| JHU-17O-1327 | 1302-1332 | VSMOW2-052013-4 | VSMOW2 | -18.035 | -34.441 | 0.045 | 0.079 |
| JHU-17O-1591 | 1586-1671 | VSMOW2-052113-1 | VSMOW2 | -18.199 | -34.696 | -0.032 | -0.029 |
| JHU-17O-1592 | 1586-1671 | VSMOW2-052113-1 | VSMOW2 | -18.179 | -34.703 | -0.011 | -0.037 |
| JHU-17O-1593 | 1586-1671 | VSMOW2-052113-1 | VSMOW2 | -18.127 | -34.605 | 0.044 | 0.069 |
| JHU-17O-1621 | 1586-1671 | SLAP2-051613 | SLAP2 | -46.579 | -86.861 | -29.969 | -55.970 |
| JHU-17O-1622 | 1586-1671 | SLAP2-051613 | SLAP2 | -46.646 | -86.975 | -30.040 | -56.092 |
| JHU-17O-1642 | 1586-1671 | VSMOW-052013-1 | VSMOW2 | -18.205 | -34.716 | -0.020 | -0.033 |
| JHU-17O-1643 | 1586-1671 | VSMOW-052013-1 | VSMOW2 | -18.170 | -34.658 | 0.018 | 0.030 |
| JHU-17O-1668 | 1586-1671 | SLAP2-051613-2 | SLAP2 | -45.922 | -85.693 | -29.260 | -54.700 |
| JHU-17O-1669 | 1586-1671 | SLAP2-051613-2 | SLAP2 | -46.189 | -86.201 | -29.541 | -55.245 |
| JHU-17O-1670 | 1586-1671 | SLAP2-051613-2 | SLAP2 | -46.324 | -86.433 | -29.683 | -55.494 |
| JHU-17O-1679 | 1673-1768 | VSMOW-2-052013-2a | VSMOW2 | -17.970 | -34.355 | -0.081 | -0.150 |
| JHU-17O-1681 | 1673-1768 | VSMOW-2-052013-2a | VSMOW2 | -17.815 | -34.060 | 0.093 | 0.181 |
| JHU-17O-1682 | 1673-1768 | VSMOW-2-052013-2a | VSMOW2 | -17.955 | -34.329 | -0.051 | -0.099 |
| JHU-17O-1698 | 1673-1768 | SLAP2-051613-1a | SLAP2 | -46.091 | -86.011 | -29.664 | -55.367 |
| JHU-17O-1699 | 1673-1768 | SLAP2-051613-1a | SLAP2 | -46.294 | -86.384 | -29.873 | -55.760 |
| JHU-17O-1701 | 1673-1768 | SLAP2-051613-1a | SLAP2 | -46.183 | -86.194 | -29.746 | -55.542 |
| JHU-17O-1722 | 1673-1768 | VSMOW2-052013-2a | VSMOW2 | -18.122 | -34.579 | -0.023 | -0.054 |
| JHU-17O-1723 | 1673-1768 | VSMOW2-052013-2a | VSMOW2 | -18.014 | -34.358 | 0.096 | 0.190 |
| JHU-17O-1724 | 1673-1768 | VSMOW2-052013-2a | VSMOW2 | -18.052 | -34.447 | 0.061 | 0.102 |
| JHU-17O-1731 | 1673-1768 | SLAP2-051613-1a | SLAP2 | -45.999 | -85.852 | -29.407 | -54.959 |
| JHU-17O-1732 | 1673-1768 | SLAP2-051613-1a | SLAP2 | -45.764 | -85.419 | -29.154 | -54.487 |
| JHU-17O-1733 | 1673-1768 | SLAP2-051613-1a | SLAP2 | -45.765 | -85.408 | -29.150 | -54.469 |
| JHU-17O-1743 | 1673-1768 | VSMOW-2-052013-2a | VSMOW2 | -18.264 | -34.824 | -0.078 | -0.172 |
| JHU-17O-1744 | 1673-1768 | VSMOW-2-052013-2a | VSMOW2 | -18.089 | -34.458 | 0.116 | 0.235 |
| JHU-17O-1745 | 1673-1768 | VSMOW-2-052013-2a | VSMOW2 | -18.329 | -34.902 | -0.132 | -0.233 |
| JHU-17O-1761 | 1673-1768 | SLAP2-051613-1a | SLAP2 | -46.601 | -86.958 | -29.898 | -55.929 |
| JHU-17O-1762 | 1673-1768 | SLAP2-051613-1a | SLAP2 | -46.586 | -86.925 | -29.878 | -55.885 |
| JHU-17O-1763 | 1673-1768 | SLAP2-051613-1a | SLAP2 | -47.196 | -88.067 | -30.516 | -57.103 |
| JHU-17O-1944 | 1943-2041 | SLAP2-051613-1a | SLAP2 | -45.463 | -85.019 | -29.089 | -54.438 |
| JHU-17O-1945 | 1943-2041 | SLAP2-051613-1a | SLAP2 | -45.560 | -85.143 | -29.196 | -54.578 |
| JHU-17O-1946 | 1943-2041 | SLAP2-051613-1a | SLAP2 | -45.629 | -85.272 | -29.272 | -54.722 |
| JHU-17O-1951 | 1943-2041 | VSMOW-2-052013-2b | VSMOW2 | -18.206 | -34.797 | 0.013 | 0.009 |
| JHU-17O-1952 | 1943-2041 | VSMOW-2-052013-2b | VSMOW2 | -18.249 | -34.849 | -0.035 | -0.053 |
| JHU-17O-1953 | 1943-2041 | VSMOW-2-052013-2b | VSMOW2 | -18.322 | -34.986 | -0.116 | -0.207 |
| JHU-17O-1963 | 1943-2041 | SLAP2-051613-1a | SLAP2 | -45.919 | -85.797 | -29.625 | -55.377 |
| JHU-17O-1964 | 1943-2041 | SLAP2-051613-1a | SLAP2 | -46.349 | -86.527 | -30.088 | -56.174 |
| JHU-17O-1965 | 1943-2041 | SLAP2-051613-1a | SLAP2 | -46.216 | -86.297 | -29.948 | -55.930 |
| JHU-17O-1974 | 1943-2041 | VSMOW-2-052013-2b | VSMOW2 | -18.042 | -34.475 | 0.128 | 0.236 |
| JHU-17O-1975 | 1943-2041 | VSMOW-2-052013-2b | VSMOW2 | -18.182 | -34.737 | -0.024 | -0.053 |
| JHU-17O-1976 | 1943-2041 | VSMOW-2-052013-2b | VSMOW2 | -18.303 | -34.946 | -0.158 | -0.290 |
| JHU-17O-1984 | 1943-2041 | SLAP2-051613-1a | SLAP2 | -46.063 | -86.040 | -29.833 | -55.746 |
| JHU-17O-1985 | 1943-2041 | SLAP2-051613-1a | SLAP2 | -45.998 | -85.926 | -29.766 | -55.627 |
| JHU-17O-1986 | 1943-2041 | SLAP2-051613-1a | SLAP2 | -46.105 | -86.108 | -29.883 | -55.830 |
| JHU-17O-1996 | 1943-2041 | VSMOW-2-052013-2b | VSMOW2 | -17.918 | -34.226 | 0.203 | 0.391 |
| JHU-17O-1997 | 1943-2041 | VSMOW-2-052013-2b | VSMOW2 | -18.022 | -34.439 | 0.088 | 0.154 |
| JHU-17O-1998 | 1943-2041 | VSMOW-2-052013-2b | VSMOW2 | -18.051 | -34.486 | 0.055 | 0.097 |
| JHU-17O-2016 | 1943-2041 | SLAP2-051613-1a | SLAP2 | -45.732 | -85.420 | -29.561 | -55.233 |
| JHU-17O-2017 | 1943-2041 | SLAP2-051613-1a | SLAP2 | -46.098 | -86.100 | -29.954 | -55.976 |
| JHU-17O-2018 | 1943-2041 | SLAP2-051613-1a | SLAP2 | -46.297 | -86.457 | -30.170 | -56.368 |
| JHU-17O-2039 | 1943-2041 | VSMOW2-052013-2B | VSMOW2 | -18.035 | -34.442 | -0.035 | -0.072 |
| JHU-17O-2040 | 1943-2041 | VSMOW2-052013-2B | VSMOW2 | -18.049 | -34.461 | -0.053 | -0.097 |
| JHU-17O-2041 | 1943-2041 | VSMOW2-052013-2B | VSMOW2 | -18.059 | -34.473 | -0.067 | -0.115 |

| | | | | | | | |
|---|---|---|---|---|---|---|---|
| JHU-17O-683 | 680-847 | USGS46-011713 | USGS46 | -33.701 | -63.490 | -16.220 | -30.562 |
| JHU-17O-684 | 680-847 | USGS46-011713 | USGS46 | -33.271 | -62.686 | -15.769 | -29.704 |
| JHU-17O-685 | 680-847 | USGS47-012113 | USGS47 | -28.433 | -53.796 | -10.657 | -20.153 |
| JHU-17O-686 | 680-847 | USGS47-012113 | USGS47 | -28.441 | -53.813 | -10.669 | -20.178 |
| JHU-17O-687 | 680-847 | USGS45-012113 | USGS45 | -19.711 | -37.606 | -1.441 | -2.758 |
| JHU-17O-688 | 680-847 | USGS45-012113 | USGS45 | -19.748 | -37.672 | -1.484 | -2.836 |
| JHU-17O-691 | 680-847 | USGS48-012113 | USGS48 | -19.360 | -36.966 | -1.085 | -2.100 |
| JHU-17O-692 | 680-847 | USGS48-012113 | USGS48 | -19.105 | -36.500 | -0.820 | -1.606 |
| JHU-17O-700 | 680-847 | USGS46-011713 | USGS46 | -33.426 | -62.947 | -15.988 | -30.093 |
| JHU-17O-706 | 680-847 | USGS45-012113 | USGS45 | -19.342 | -36.903 | -1.123 | -2.142 |
| JHU-17O-707 | 680-847 | USGS45-012513 | USGS45 | -19.309 | -36.845 | -1.092 | -2.087 |
| JHU-17O-708 | 680-847 | USGS45-012513 | USGS45 | -19.366 | -36.958 | -1.156 | -2.215 |
| JHU-17O-722 | 680-847 | USGS47-012113 | USGS47 | -28.226 | -53.412 | -10.575 | -20.008 |
| JHU-17O-734 | 680-847 | USGS45-012513 | USGS45 | -19.423 | -37.048 | -1.313 | -2.504 |
| JHU-17O-735 | 680-847 | USGS45-012513 | USGS45 | -19.449 | -37.087 | -1.344 | -2.554 |
| JHU-17O-782 | 680-847 | USGS45-012513 | USGS45 | -19.251 | -36.706 | -1.312 | -2.490 |
| JHU-17O-820 | 680-847 | USGS45-012113 | USGS45 | -18.772 | -35.815 | -0.948 | -1.813 |
| JHU-17O-821 | 680-847 | USGS45-012113 | USGS45 | -19.120 | -36.466 | -1.319 | -2.519 |
| JHU-17O-840 | 680-847 | USGS47-012113 | USGS47 | -27.722 | -52.474 | -10.482 | -19.854 |
| JHU-17O-866 | 848-880 | USGS47-012113 | USGS47 | -27.913 | -52.842 | -10.399 | -19.666 |
| JHU-17O-881 | 881-980 | USGS46-011713 | USGS46 | -33.278 | -62.715 | -15.970 | -30.068 |
| JHU-17O-882 | 881-980 | USGS46-011713 | USGS46 | -33.537 | -63.202 | -16.241 | -30.586 |
| JHU-17O-890 | 881-980 | USGS47-012113 | USGS47 | -28.209 | -53.419 | -10.655 | -20.167 |
| JHU-17O-903 | 881-980 | USGS48-012113 | USGS48 | -19.441 | -37.142 | -1.461 | -2.831 |
| JHU-17O-905 | 881-980 | USGS48-012113 | USGS48 | -19.104 | -36.503 | -1.108 | -2.149 |
| JHU-17O-926 | 881-980 | USGS45-012113 | USGS45 | -19.226 | -36.709 | -1.228 | -2.361 |
| JHU-17O-948 | 881-980 | USGS45-012113 | USGS45 | -19.114 | -36.484 | -1.104 | -2.111 |
| JHU-17O-957 | 881-980 | USGS47-012113 | USGS47 | -27.595 | -52.262 | -9.989 | -18.909 |
| JHU-17O-958 | 881-980 | USGS47-012113 | USGS47 | -27.741 | -52.537 | -10.142 | -19.201 |
| JHU-17O-1104 | 1104-1208 | USGS45-012113 | USGS45 | -19.162 | -36.597 | -1.293 | -2.497 |
| JHU-17O-1105 | 1104-1208 | USGS45-012113 | USGS45 | -19.072 | -36.418 | -1.196 | -2.302 |
| JHU-17O-1168 | 1104-1208 | USGS47-012113 | USGS47 | -28.199 | -53.381 | -10.668 | -20.187 |
| JHU-17O-1169 | 1104-1208 | USGS47-012113 | USGS47 | -28.132 | -53.248 | -10.596 | -20.040 |
| JHU-17O-1197 | 1104-1208 | USGS48-012113 | USGS48 | -19.244 | -36.745 | -1.170 | -2.259 |
| JHU-17O-1209 | 1209-1301 | USGS45-012113 | USGS45 | -19.105 | -36.465 | -1.091 | -2.102 |
| JHU-17O-1210 | 1209-1301 | USGS45-012113 | USGS45 | -19.086 | -36.411 | -1.072 | -2.047 |
| JHU-17O-1284 | 1209-1301 | USGS48-012113 | USGS48 | -19.168 | -36.602 | -1.259 | -2.426 |
| JHU-17O-1291 | 1209-1301 | USGS45-012113 | USGS45 | -19.081 | -36.413 | -1.176 | -2.241 |
| JHU-17O-1302 | 1302-1332 | USGS45-012113 | USGS45 | -19.145 | -36.587 | -0.965 | -1.918 |
| JHU-17O-1303 | 1302-1332 | USGS45-012113 | USGS45 | -19.128 | -36.518 | -0.954 | -1.856 |
| JHU-17O-1597 | 1586-1671 | USGS45-042414 | USGS45 | -19.404 | -36.995 | -1.301 | -2.494 |
| JHU-17O-1603 | 1586-1671 | USGS45-042414 | USGS45 | -19.666 | -37.536 | -1.575 | -3.072 |
| JHU-17O-1611 | 1586-1671 | USGS48-012113 | USGS48 | -19.503 | -37.234 | -1.400 | -2.744 |
| JHU-17O-1632 | 1586-1671 | USGS47-012113 | USGS45 | -28.307 | -53.542 | -10.684 | -20.228 |
| JHU-17O-1652 | 1586-1671 | USGS45-042414 | USGS45 | -19.526 | -37.227 | -1.411 | -2.722 |
| JHU-17O-1690 | 1673-1768 | USGS47-012113 | USGS47 | -28.001 | -52.993 | -10.612 | -20.040 |
| JHU-17O-1711 | 1673-1768 | USGS47-012113 | USGS47 | -28.143 | -53.274 | -10.658 | -20.184 |
| JHU-17O-1729 | 1673-1768 | USGS47-012113 | USGS47 | -27.900 | -52.777 | -10.314 | -19.517 |
| JHU-17O-1754 | 1673-1768 | USGS45-140815-1 | USGS45 | -19.316 | -36.768 | -1.130 | -2.165 |
| JHU-17O-1768 | 1673-1768 | USGS45-140815-1 | USGS45 | -21.439 | -40.801 | -3.301 | -6.383 |
| JHU-17O-2007 | 1943-2041 | USGS-45-140815-1 | USGS45 | -19.275 | -36.801 | -1.276 | -2.461 |

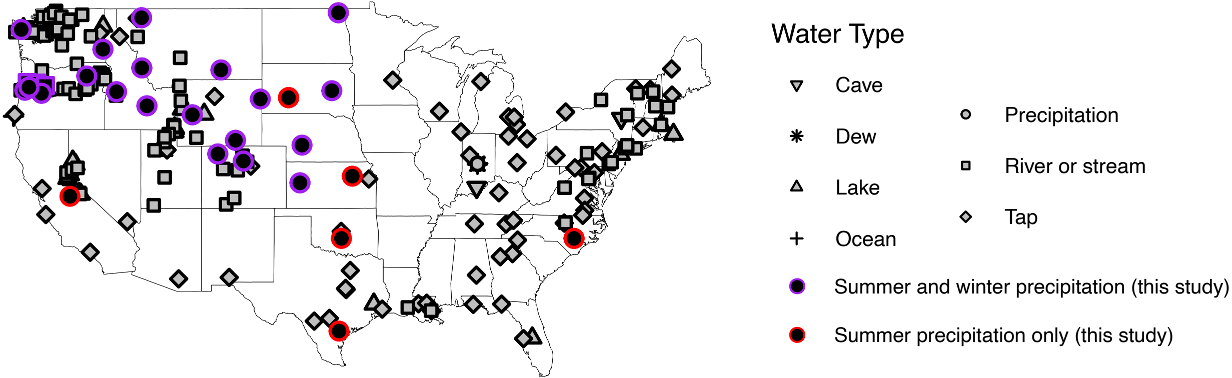
Water Type
Cave
Dew
Lake
Ocean
Precipitation
River or stream
Tap
Summer and winter precipitation (this study)
Summer precipitation only (this study)

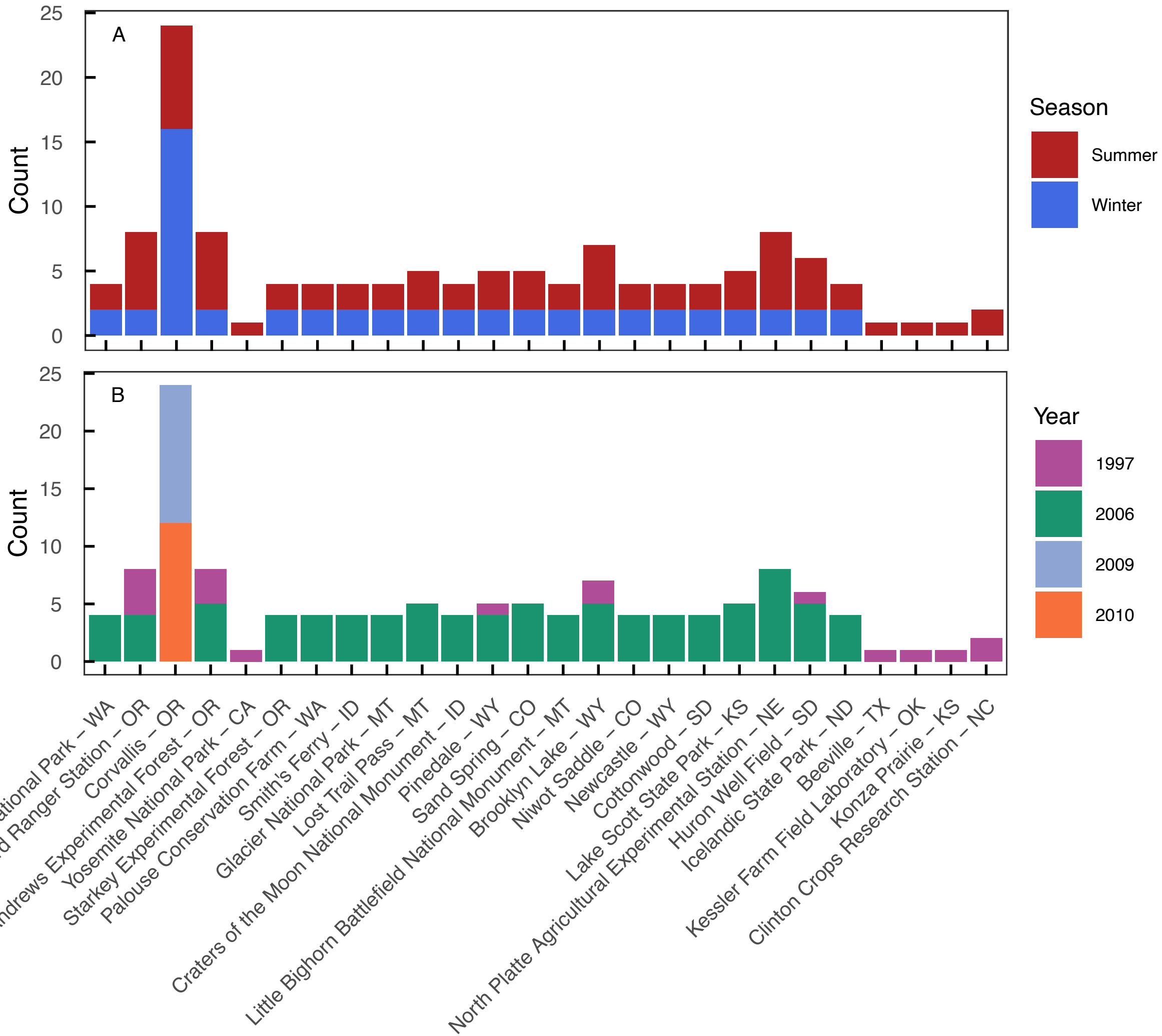

A
B
Count
Count
25
20
15
10
5
0
Season
Summer
Winter
Year
1997
2006
2009
2010
Olympic National Park – WA
Alsea Guard Ranger Station – OR
Corvallis – OR
H.J. Andrews Experimental Forest – OR
Yosemite National Park – CA
Starkey Experimental Forest – OR
Palouse Conservation Farm – WA
Smith's Ferry – ID
Glacier National Park – MT
Lost Trail Pass – MT
Craters of the Moon National Monument – ID
Pinedale – WY
Sand Spring – CO
Little Bighorn Battlefield National Monument – MT
Brooklyn Lake – WY
Niwot Saddle – CO
Newcastle – WY
Cottonwood – SD
Lake Scott State Park – KS
North Platte Agricultural Experimental Station – NE
Huron Well Field – SD
Icelandic State Park – ND
Beeville – TX
Kessler Farm Field Laboratory – OK
Konza Prairie – KS
Clinton Crops Research Station – NC

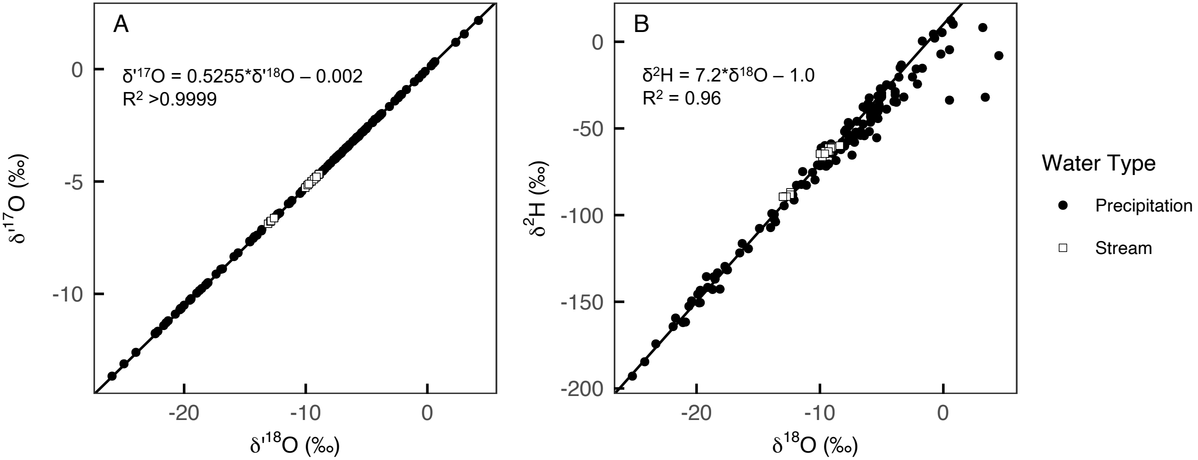
A
δ'17O = 0.5255*δ'18O – 0.002
R2 >0.9999
δ'17O (‰)
δ'18O (‰)
0
-5
-10
-20
-10
0
B
δ2H = 7.2*δ18O – 1.0
R2 = 0.96
δ2H (‰)
δ18O (‰)
0
-50
-100
-150
-200
-20
-10
0
Water Type
Precipitation
Stream

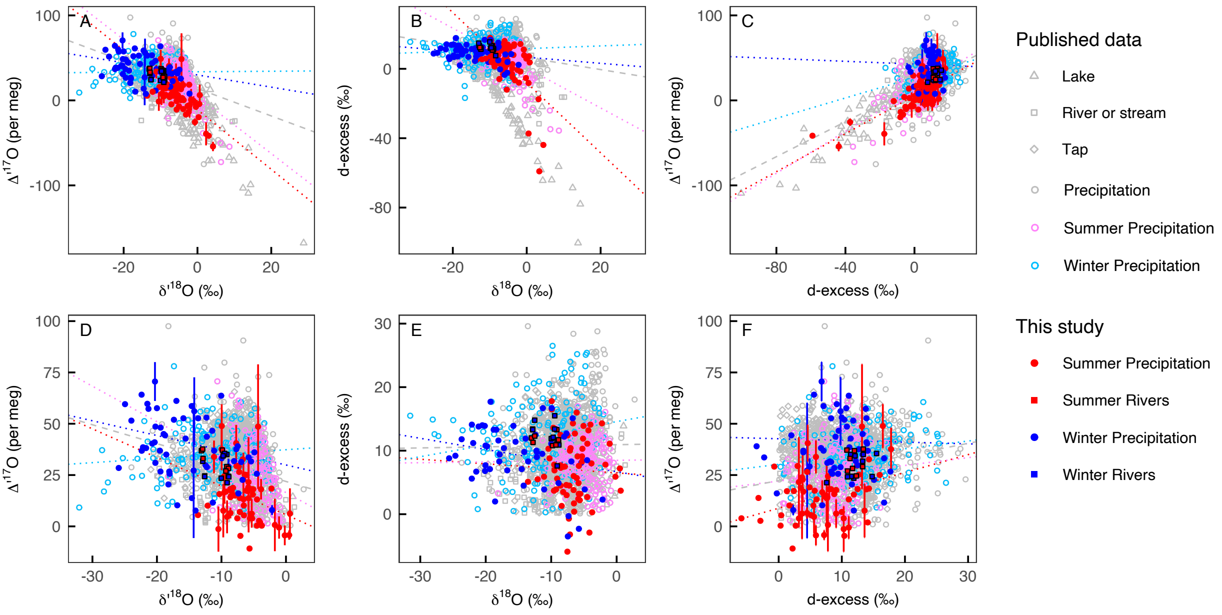
A
B
C
D
E
F
Δ'17O (per meg)
d-excess (‰)
δ'18O (‰)
δ18O (‰)
d-excess (‰)
Published data
Lake
River or stream
Tap
Precipitation
Summer Precipitation
Winter Precipitation
This study
Summer Precipitation
Summer Rivers
Winter Precipitation
Winter Rivers

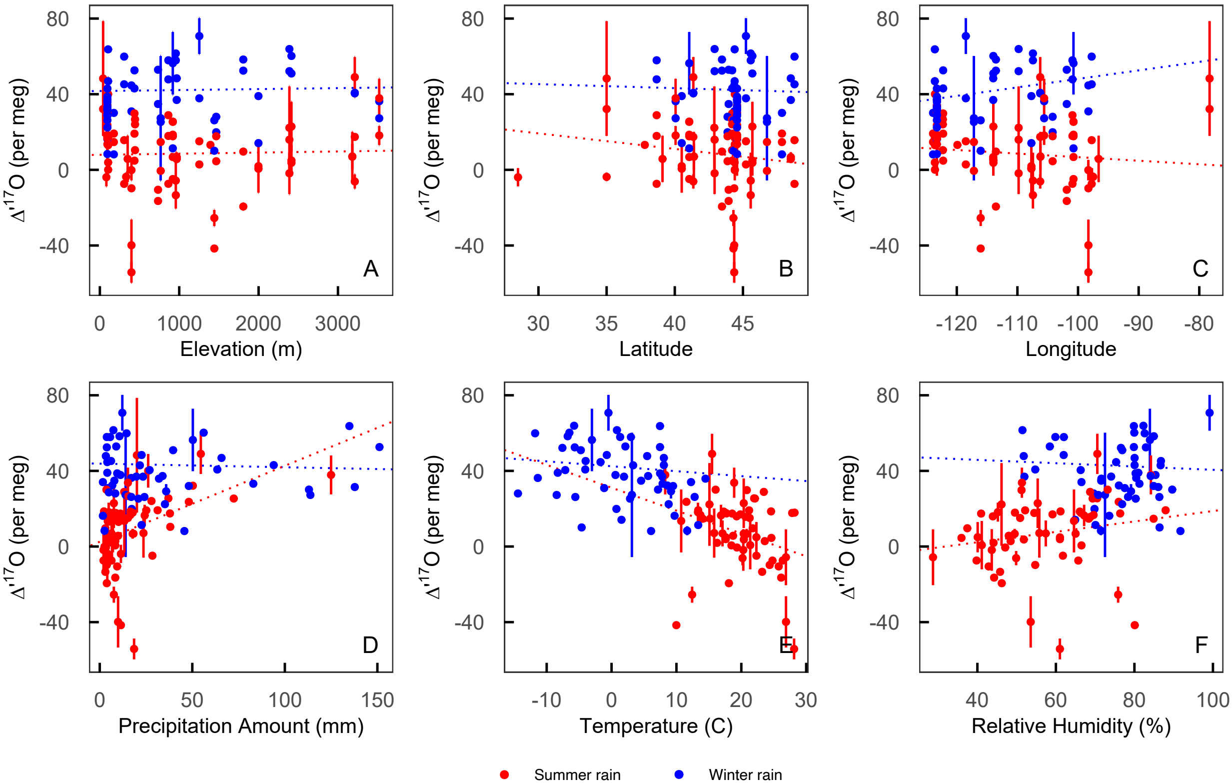

A
B
C
D
E
F
Δ''17O (per meg)
Elevation (m)
Latitude
Longitude
Precipitation Amount (mm)
Temperature (C)
Relative Humidity (%)
Summer rain
Winter rain

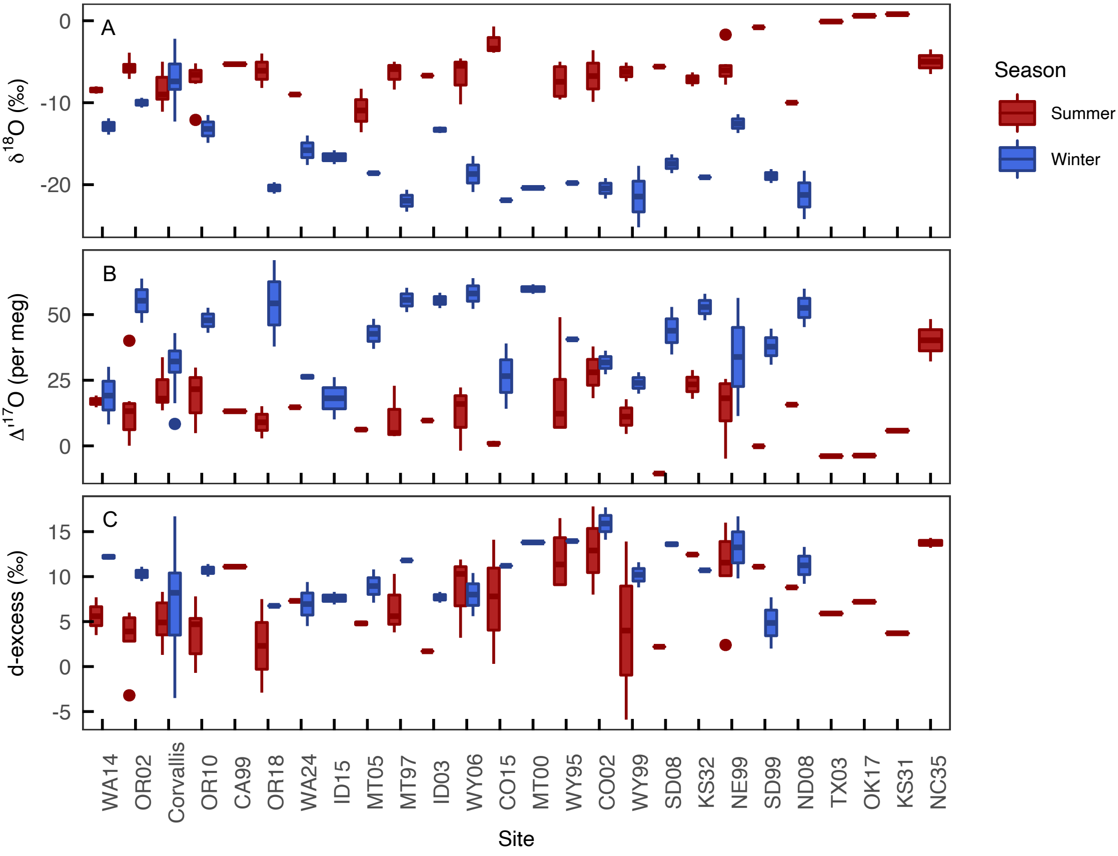

A
B
C
δ18O (‰)
Δ'17O (per meg)
d-excess (‰)
0
-10
-20
50
25
0
15
10
5
0
-5
Season
Summer
Winter
WA14
OR02
Corvallis
OR10
CA99
OR18
WA24
ID15
MT05
MT97
ID03
WY06
CO15
MT00
WY95
CO02
WY99
SD08
KS32
NE99
SD99
ND08
TX03
OK17
KS31
NC35
Site

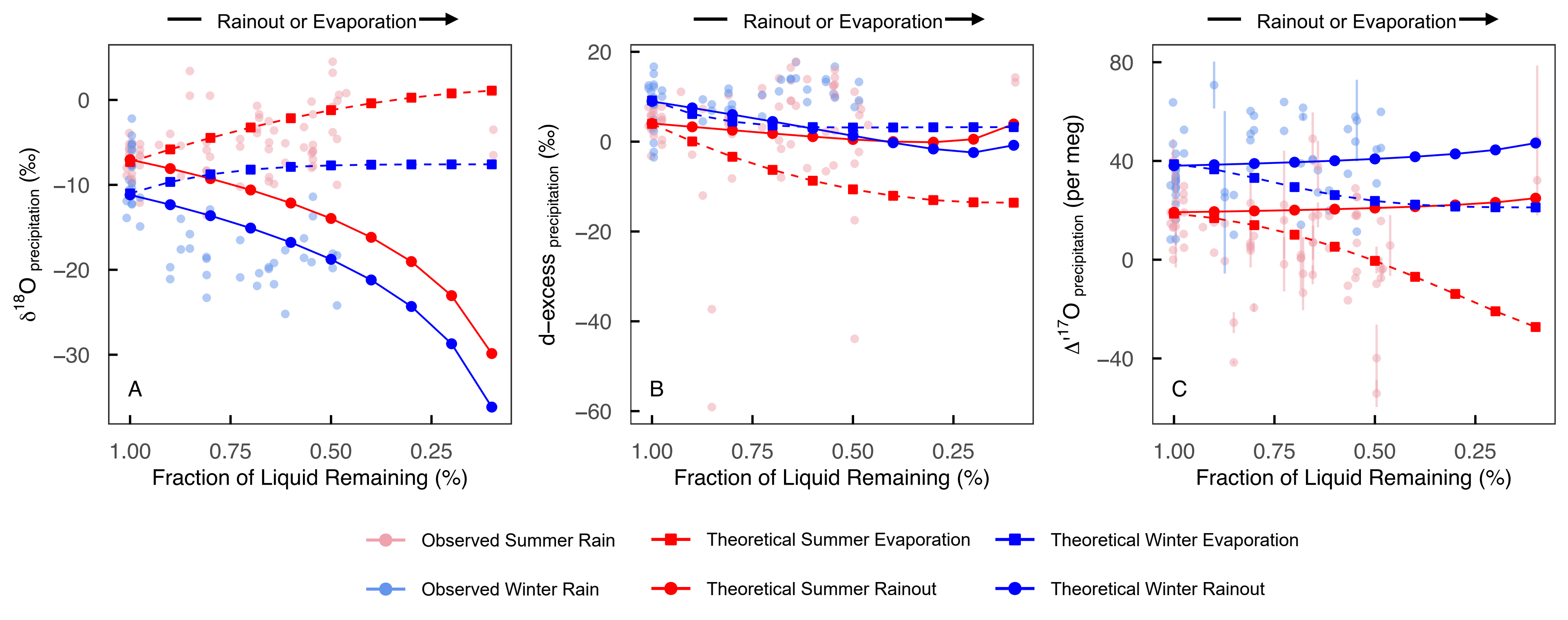

Rainout or Evaporation
δ18O precipitation (‰)
A
d−excess precipitation (‰)
B
Δ'17O precipitation (per meg)
C
Fraction of Liquid Remaining (%)
0
−10
−20
−30
20
0
−20
−40
−60
80
40
0
−40
1.00
0.75
0.50
0.25
Observed Summer Rain
Observed Winter Rain
Theoretical Summer Evaporation
Theoretical Summer Rainout
Theoretical Winter Evaporation
Theoretical Winter Rainout